

**GRINREY**



# **Efficient Engineering Systems**

**Volume 01**

Sandip A. Kale  
Editor

Engineering Research Transcripts



Engineering Research Transcripts

Volume 01

---

# **Efficient Engineering Systems: Volume 1**

---

## **Book Series by Grinrey Publications**

- Research Transcripts in Energy
- Research Transcripts in Engineering
- Research Transcripts in Materials
- Research Transcripts in Computer, Electrical and Electronics Engineering

**GRINREY**

[www.grinrey.com](http://www.grinrey.com)

Engineering Research Transcripts

Volume 01

---

# **Efficient Engineering Systems: Volume 1**

---

**Sandip A. Kale**

Editor

**GRINREY**

© 2021 Grinrey Publications



Creative Commons License CC-BY-NC-ND 4.0  
([www.creativecommons.org/licenses/by-nc-nd/4.0](http://www.creativecommons.org/licenses/by-nc-nd/4.0))

This work is published subject to a Creative Commons Attribution Noncommercial No Derivative License. For permission to publish commercial versions, please contact Grinrey Publications.

The publisher has taken a reasonable care in the preparation of this book. Publisher does not states or implied warranty of any content in this book and adopts no obligation for any errors or exclusions. The publisher shall not be responsible for any exceptional, resulting, or exemplary damages causing, in whole or in part, from the reader's use of, or dependence upon, this content.

Efficient Engineering Systems: Volume 1

Sandip A. Kale, editor (Technology Research and Innovation Centre, Pune, India)

Series: Engineering Research Transcripts

ISBN: 978-81-948951-8-3

Published by: Grinrey Publications

511, Ganesh Nakashtram, Dhayari, Pune, Maharashtra, India

[www.grinrey.com](http://www.grinrey.com)

Email: [contact@grinrey.com](mailto:contact@grinrey.com)

# Contents

	<b>Preface</b>	1
<b>Chapter 1</b>	<b>Effectiveness of Hydrogen Enrichment in CNG Fuelled SI Engine: A Review</b> <i>Kiran P. Pawar and Sanjay D. Yadav</i>	29
<b>Chapter 2</b>	<b>Entropy Generation Analysis of A Low-Temperature Waste Heat Power Generation System Integrated with the Agricultural Machinery</b> <i>Rupinder Pal Singh and R S Gill</i>	39
<b>Chapter 3</b>	<b>Modelling the Geometry of Wetted Zone in Soil Based Growing Media Under Drip Irrigation</b> <i>E. Sujitha, G. Thiyagarajan, A. Selvaperumal, S. Thangamani and K. Shanmugasundaram</i>	53
<b>Chapter 4</b>	<b>Feasibility of Waste Materials In High Strength Geopolymer Building Blocks</b> <i>Shamon K K and Deepa G Nair</i>	63
<b>Chapter 5</b>	<b>Pyrolysis of Tyre Waste: A Sustainable Waste Management Approach</b> <i>A. Sudharshan Reddy and Abhilash T. Nair</i>	75
<b>Chapter 6</b>	<b>Analysis of Strengthened Industrial Structure Under Seismic Loading</b> <i>Varsha Gokak, Swati Bekkeri, Tejas Doshi and R. V. Raikar</i>	91
<b>Chapter 7</b>	<b>Strategies for the Distribution of Uses, Occupation and Allocation of Land Explained with a Case Study of Paseo De Los Cañarís in the City of Cuenca</b> <i>Carla Sigüencia, Marco Avila and Yonimiler Castillo</i>	111
	<b>Index</b>	

# Effectiveness of Hydrogen Enrichment in CNG Fuelled SI Engine: A Review

Kiran P. Pawar<sup>a,\*</sup> and Sanjay D. Yadav<sup>a</sup>

<sup>a</sup>Department of Automobile Engineering, Rajarambapu Institute of Technology, Rajaramnagar (Sangli), India

\*Corresponding author: kppawar87@gmail.com

## ABSTRACT

Across the world, the demand for fossil fuel is growing notably because of the growth in vehicle populace and heavy use in energy generation plants. Vehicle exhaust dangerous emission is inflicting global warming and heavy health issues. To tackle this issue developing country like India opted to follow strict BS-VI emission norms. One of the viable solutions is to shift towards alternate fuel is the need of the hour. In recent years, predominant attention was to choose fuels that reducing fossil fuel consumption and pollutant emissions. Natural Gas vehicles are increasing but it has some disadvantages like low flame speed, low performance, low brake thermal efficiency, and high emission. Gaseous fuels like methane and hydrogen are the most interesting fuel that can be used in SI Engine vehicles as an alternative fuel. The burning fleetness of the mixture is appreciably high, the ignition energy is low, and the lean-burn potentiality is good. Antiknock property of Hydrogen fuel facilitates to enhance the compression ratio, which results in thermal efficiency. Hydrogen is a non-carbonaceous fuel therefore; it does not lead to carbon content emissions. This chapter offers reviews on HCNG blend compatibility with SI Engine and its Performance, Emission, and studies the combustion fundamentals of natural gas, hydrogen, and hydrogen-natural gas mixture.

**Keywords:** Alternative fuel, Combustion, Emission, Hydrogen, HCNG

## 1. INTRODUCTION

Automotive sector and power generation plant facing enormous challenges in fuel supply and demand chain and its cost in the past 2-4 decades. Fossil fuels like coal, diesel, natural gas facing a deficiency in various properties to meet the stricter emission norms and the economy of operations. Chimneys of the power plant and tailpipe of engines emit dangerous emission that pollutes the system and the environment. Oil price is very volatile and uncertain. It depends on the capacity of the originating source. Vehicles with Natural gas are increasing wherein it has many disadvantages like retarded flame speed, low performance, below average brake thermal efficiency, and high emission. Gaseous fuels like methane and hydrogen are the interesting fuel, which will be utilized in SI Engine vehicles as an alternate fuel. The burning fleetness of the mixture is interestingly high, the minimum ignition energy is low and the lean-burn potentiality is nice. Hydrogen's anti-knock characteristic enables it to reinforce the compression ratio, which ends up within the further enhancement of thermal efficiency.

To enhance the overall performance of the CNG engines at the lean-burn conditions, there need to increase its burning velocity, which may be consummated employing blending hydrogen (Hythane). Hythane has good flammability limits within the air with minimum ignition energy (0.02 mJ). Roopesh Kumar Mehra et al. [1] studied a mixture of Hythane 10% and 18%, and then compare it therewith of CNG. He concluded a 6% rise in thermal efficiency and a 4% reduction in engine emission. The single-cylinder CI engine is modified and fuelled by HCNG is studied by S. M.V. Sagar et al. [2]. The engine was tested at a speed of 1500 rpm at 250 BTDC; 30% Hythane blend confirmed the pleasant anti-knocking characteristics among all HCNG mixtures. Rohit Singh Lather, Changming Gong et al [3,4], investigated the relation of ignition timing on combustion and emissions of Hythane fuelled SI engine at constant engine speeds. They also dealt with the various parameters and concluded that the rise in IMEP, rise in-cylinder pressure, good heat loss rate, and increased combustion length at low engine speeds at numerous ignition timings and excess air ratio of 1.40. Selim Tangoz et al. [5] operated Hythane blend at 1500, 2000, and 2500 rpm underneath full load conditions on Isuzu three L engine, having a compression ratio of 12.5, the highest efficiency was usually obtained with Hythane 5 (five% Hydrogen in natural fuel) gasoline.

The HC and CO emissions usually not up to the Euro-5 and Euro-6 standards. Liu et al. [6], full-fledged the reduction of the heat loss and increase of indicated thermal efficiency of HCNG combination of the Atkinson cycle with high compression ratio and low heat rejection with a 55% hydrogen blend. Due to

---

prolonged and quicker flame propagation, wide flammability limits, and low minimum ignition energy of the gas, it's a perfect condition to mix hydrogen that enhances lean-burn capabilities [7]. Traditional, hybrid, electric, biofuel, fuel cell, and hydrogen-fueled ICE vehicles are relatively assessed supported their carbon dioxide and SO<sub>2</sub> emissions. Once the engine operates at partial load the throttle causes high pumping losses that decrease the engine efficiency, it is often overcome by lean mixture condition ends up in the misfiring of fuel. The combustion limits can be extended by the addition of hydrogen to the regular fuel [7, 8].

Spark ignition engine equipped with an indirect injection system with the result of Hythane addition for PFI and DI configurations was evaluated on an equivalent engine at 2000 rpm throttled condition [9]. Willian Cezar Nadaleti et al. [7, 8] experimented on the three cylinders naturally aspirated SI engine. Throughout the tests, the engine worked with a set speed of 1500 RPM. For all fuel mix, the engine output power has been 18% of most power (for 1500 RPM) reached by the engine for ratio combustion of HCNG fuel. Hydrogen Gas Enrichment is a promising and trending technology within which numerous researchers are working globally. Hydrogen gas will produce freely by the unconventional technique and with sustainable sources.

## **2. FUNDAMENTAL PHYSICOCHEMICAL PROPERTIES OF HCNG**

### **2.1. Lower heating value**

Heat Release rate after the combustion of the fuel when complete combustion is achieved. Natural gas like Methane, Ethanol, and hydrogen have a comparatively better value per unit mass than gasoline and diesel-fueled engine, Lower heating value per unit volume is lower as compared to gasoline which causes declination in the air-breathing capacity of the engine or volumetric efficiency. Although the volumetric efficiency of Hydrogen gas is low relative to methane of gasoline fuel, however, hydrogen requires very less air per unit volume. Fig.1 represents the volumetric lower heating value of fuel-air mixtures is compared with hydrogen fraction. For various mixtures and at various excess air-fuel ratios the hydrogen addition shows the declination in LHV after  $\lambda$  -1.6.

### **2.2. Adiabatic Flame Temperature and Auto-Ignition Temperature**

Adiabatic flame temperature (T<sub>ad</sub>) of the fuel/air mixture having strong influences on the combustion rates inside the combustion chamber. Elevated combustion temperature is helpful for more complete combustion and hence could reduce HC and CO emissions, but it adversely affects by increasing NO<sub>x</sub> emission. Theoretical calculation indicated that the T<sub>ad</sub> of Hythane and the air

mixture flame goes on increasing with an increasing fraction of Hydrogen. The upgrading trend of adiabatic flame temperature with hydrogen fractions similar in the least excess air ratios ( $\lambda$ ) as shown in Fig.2 Increase of excess air ratio  $\lambda$  leads to a drastic decrease in combustion temperature [10]. Although hydrogen addition can increase the peak flame temperature of Hythane mixtures from a theoretical point of view, in real engine applications, however, its effects on maximum in-cylinder gas temperature ( $T_{max}$ ) may depend upon other factors like charge efficiency, combustion phasing, heat loss, etc.

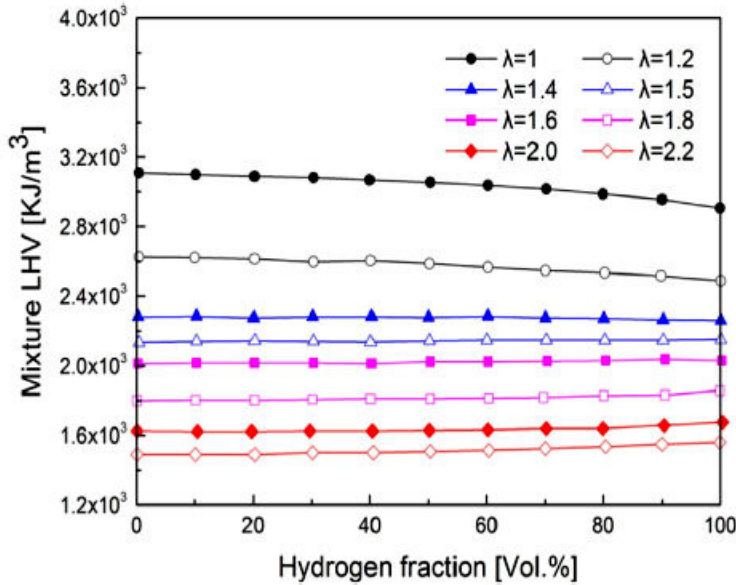


Fig. 1. Hydrogen fraction Versus the LHV value [5]

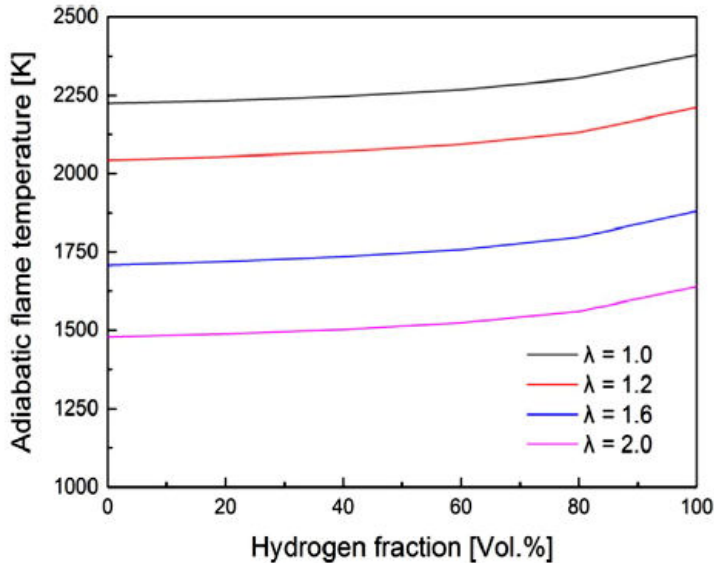
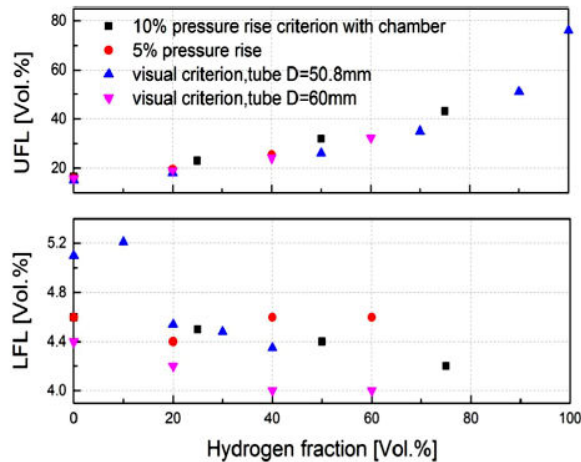


Fig. 2. Variation of adiabatic flame Temperature versus hydrogen fraction [5]

### 2.3. Minimum Ignition Energy and Flammability Limits

Spark plug supplies the spark to ignite and burn the air and fuel mixture in SI engines. The least initial energy required for burning and developing the flame of the fuel in the combustion chamber is termed as Minimum Ignition Energy. Explosion hazards are defined by this property, hence for designing the chamber and selects the source of burning is also verified with the property. The various properties of hydrogen are presented in Table No.1 by comparison with gasoline and natural gas methane fuel. Hydrogen has a good range of flame development limits compared to methane as shown in Fig.3. The addition of Hydrogen in Natural gas has a notable increase in the flame development limit. After burning and power stroke leftover flue gases are not getting expelled into the atmosphere even after exhaust stroke, low scavenging, and cylinder wall temperature also affect flame limit [21].



**Fig. 3.** Variation Hydrogen fraction and its effect on upper and lower flammability limits[5]

**Table1.**Hydrogen fuel Properties Compared to Diesel, Methane and Gasoline [1, 5, 7]

Properties of Fuel	Methane	Gasoline	Diesel	Hydrogen
Lower Heating Value (MJ/kg)	46.72	44.79	42.5	119.7
Volumetric Low Heating Value (MJ/m <sup>3</sup> )	32.97	216.38	-	10.22
LHV For Stoichiometric mixture (MJ/m <sup>3</sup> )	3.13	3.83	-	3.02
Density (kg/m <sup>3</sup> )	0.67	720-775	833-881	0.08
Molar Mass (kg/Mol)	16.04	100-105	204	2.02
Diffusion Coefficient (cm <sup>2</sup> /s)	0.189	-	-	0.61
Flammability Limits (Vol%)	5.3-15	1.2-6	0.7-5	4-75
Laminar Flame Speed (m/s)	0.38	0.37-0.43	-	2.65-3.25
Auto Ignition Temperature (K)	813	500-750	553	858
Adiabatic Flame Temperature (K)	2224	2470	2327	2379
Minimum Ignition Energy(mJ)	0.28	0.25	-	0.02
Quenching Distance (mm)	2.03	2	-	0.64

The lean burning ability of CNG or Natural Gas engine is very poor and leads to misfiring due to insufficient fuel, this can be overcome by adding the fast burning and highest lean-burn ability fuel, i.e. Hydrogen that can increase the thermal efficiency and emits low emission as plotted on the graph in Fig.4.

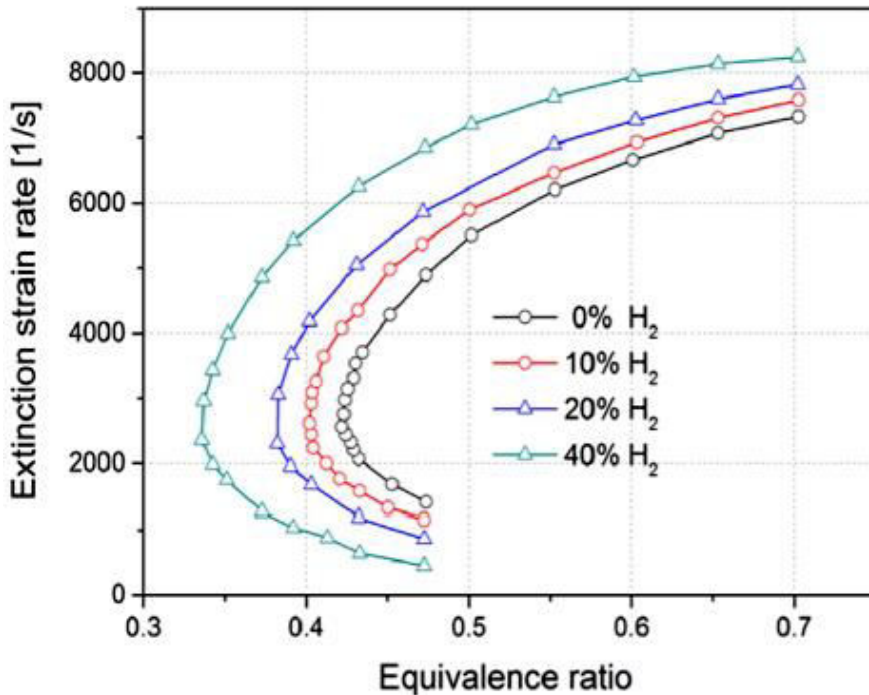


Fig. 4. Effects of hydrogen fraction on Equivalence ratio [5]

#### 2.4. Quenching Distance

During the combustion in SI engine fuel is atomized by injector or design of intake manifold, after burning which controls the motion of the flame propagation. Due to the intricate shape of the combustion chamber when the flame is reaching towards faraway space where relatively the cold surface is observed, it may shorten the length of the flame. This phenomenon is called Flame Quenching and it results in the heat loosed at those surfaces, which are the sources of incomplete combustion and finally produce the unburned HC and CO in the SI engine. As plotted in Fig. 5, in the fixed excess air ratio condition, as hydrogen fraction increases there is a decrease in the quenching distance. It also verified by various researchers as pointed out in the property Table no.1. Hydrogen has less quenching distance (0.64 mm) as compared to that of methane (2.03 mm).

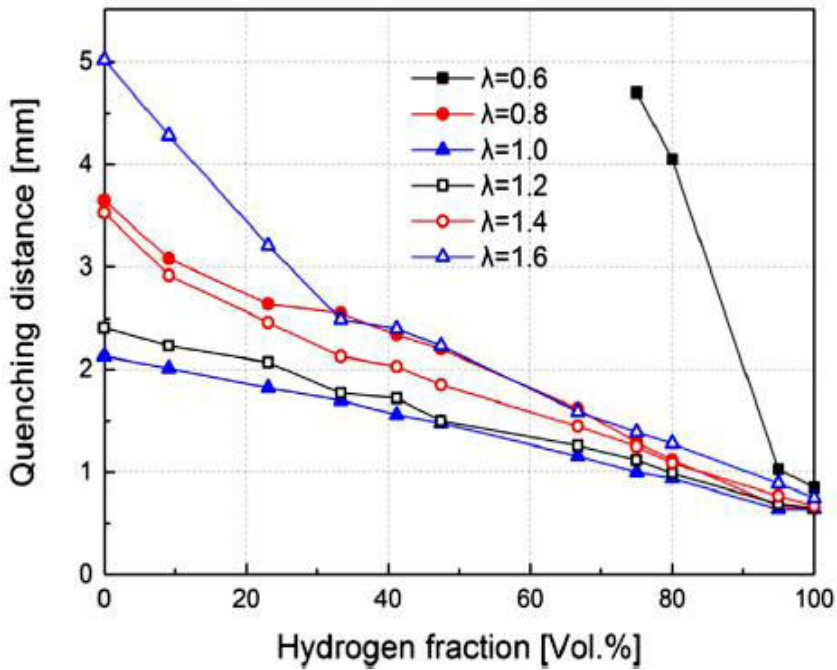


Fig. 5. Quenching Distances and its variation with Hydrogen Fraction [5]

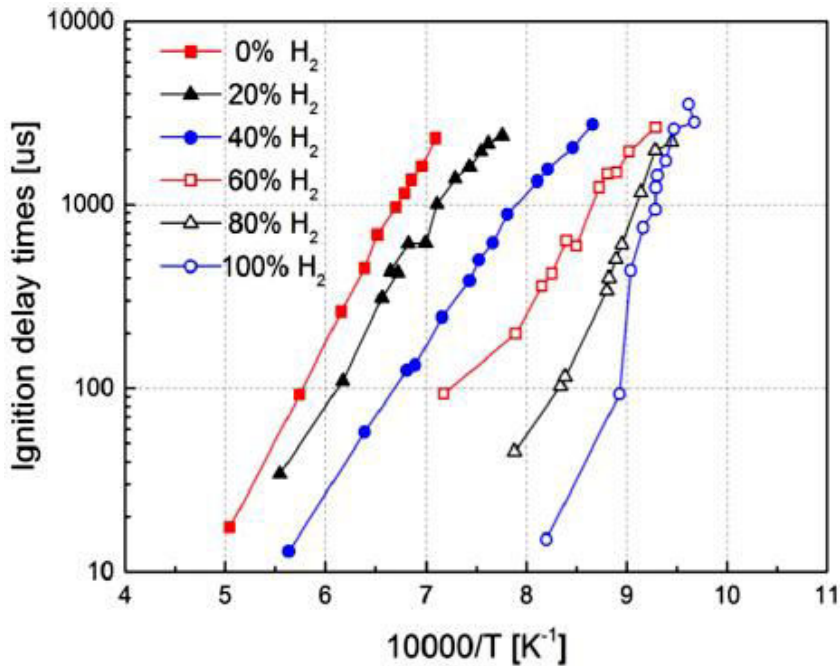


Fig. 6. Effect of hydrogen fraction on ignition delay at 0.5 Equivalence ratio [5]

## 2.5. Ignition Delay and Laminar Flame Speed

Inside SI Engine, the flame front compresses burnt gases, which results in the rise of pressure and temperature of the unburnt charge, which transfers the heat

to the remaining charge and auto-ignition takes place. This delay of flame reaches the farthest end where a charge is waiting for the flame that can be defined as ignition delay in the combustion chamber. To overcome this undesirable phenomenon laminar speed or streamline flame flow is necessary. Hydrogen addition in the CNG can increase the laminar speed of the flame propagation

## **2.6. Wobbe Index and Methane Number**

When utilizing gases in a thermal system, a parameter “Wobbe Index” can be defined, this indicates the interchangeability of gaseous fuels. If two gases have the same Wobbe Index, it is possible to directly substitute either of the gas, without any change in the fuel system [4]. The Wobbe Index of natural gas does not vary much when blended with small percentages of hydrogen, by volume. The knocking characteristics of gaseous fuels for internal combustion engines are measured using Methane Number (MN). The MN of Methane is 100, and of hydrogen, MN is 0. A higher value of MN indicates good anti-knocking characteristics [5]. Increasing the hydrogen percentage of methane, decrease the MN. Therefore, it is observed that hydrogen more than 20% by volume in CNG will not produce the desired performance in internal combustion engines [4].

## **3. FACTORS INFLUENCING PERFORMANCE AND EMISSION CHARACTERISTICS OF HCNG ENGINES**

### **3.1. Lean Burn Combustion**

It is the combustion process, in which the air percentage is more as compared to the standard stoichiometric value of the air and fuel mixture. Hythane SI engines work smoothly with a very less misfire. Ultra-lean and lean burning upper and lower limit of natural gas is elevated by the addition of hydrogen in natural gas. The Upper lean burn limit can achieve higher performance efficiency by reaching peak cylinder pressure and less coefficient of Variation.

### **3.2. Exhaust Gas Recirculation (EGR)**

The Addition of hydrogen increases the heat generation and subsequently increases the temperature, which results in the emission of NO<sub>x</sub> species in the tailpipe. To tackle the emission of NO<sub>x</sub> exhaust gas recirculation method is a viable solution.

### **3.3. Direct Fuel Injection System**

In the SI engine recently, direct injection system increases the fuel economy. Port fuel injection and direct fuel injection are the modern methods of fuel injection in IC engines, but the complexity in the process increases. Ignition

timing and injection timing are the key parameters on which the performance of the engine can be judged. Hythane-fuelled SI engine are very much depends on the direct fuel injection system from a homogeneous mixture of hydrogen and natural gas [10].

### **3.4. Stoichiometric A/F Mixture**

The theoretical air-fuel mixture is called a stoichiometric air-fuel ratio when the excess air-fuel ratio having value one. Exhaust emissions like CO and HC need to convert into CO<sub>2</sub> and water vapors by using a three-way catalytic converter in the exhaust tailpipe. However, the limitations to the use of a three-way catalytic converter for reduction of emission are that the engine should run at a stoichiometric air-fuel ratio. Overall, thermal efficiency depends on the conversion of these harmful products by the complete combustion of fresh charge or converting it into final less harmful products like CO<sub>2</sub> [6].

### **3.5. Ignition Timings**

If the ignition is extremely early, and therefore the combustion occurs before the compression stroke is ended, because of which the developed pressure opposes the piston motion and lowers the engine power. If the ignition is just too late, the piston would have already completed some a part of the expansion stroke before the pressure rise occurs, which resulted in a significant loss in engine power [3].

### **3.6. Engine Speed**

Brake thermal efficiency, indicated thermal efficiency, as well as the power output, is having a linear relation with engine speed. But we can run the engine at a higher speed because it will deteriorate the combustion process by producing very high unburnt charges. To get a higher speed without affecting the combustion process requires high quality of fuel, higher lean-burn ability, good scavenging, and precise ignition and injection timing [3].

## **4. PERFORMANCE AND EMISSION OF HCNG ENGINE**

Mechanical Power, thermal efficiency, power/torque output of the engine are the most important performance parameters of the engine.

### **4.1. Energy Consumption, Power Output, and Engine Torque**

The minimum ignition energy of hydrogen fuel is on the higher side than the gasoline and natural gas fuels, which results in a higher amount of energy consumption as hydrogen percentage increases in addition to natural gas. From Fig. 7 at different excess ratio variations in the energy consumption due to the availability of oxygen for complete combustion higher energy is required.

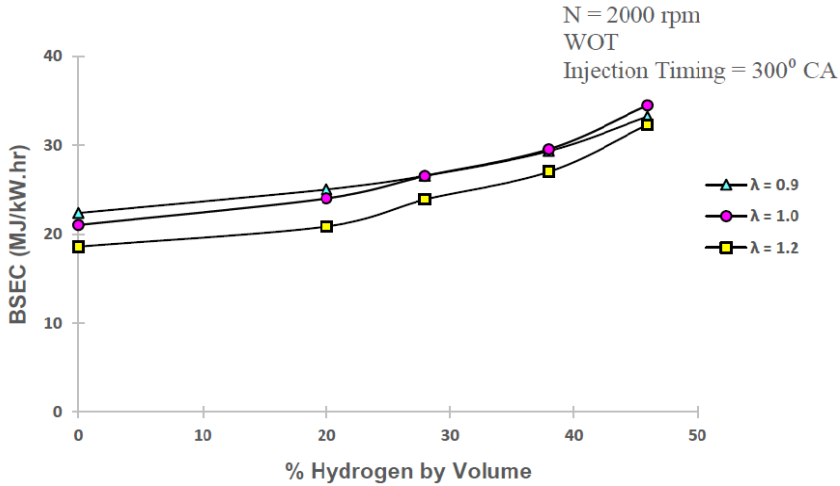


**Fig. 7.** Energy Consumption at different hydrogen fraction with different air-fuel ratio [26]

Hythane blend fuelled engines prominently signifies the better results compared to natural gas engines. The high heat dissipation rate from the cylinder compartment results in higher thermal efficiency and power output. Fig. 8. Shows the relation of the power output versus different hydrogen fractions at various RPM and it shows the increasing trend in power. The Power output at a different fraction of hydrogen from 0 to 50% at different excess ratios also shows an increasing trend with an increase in hydrogen percentage as shown in Fig. 9.

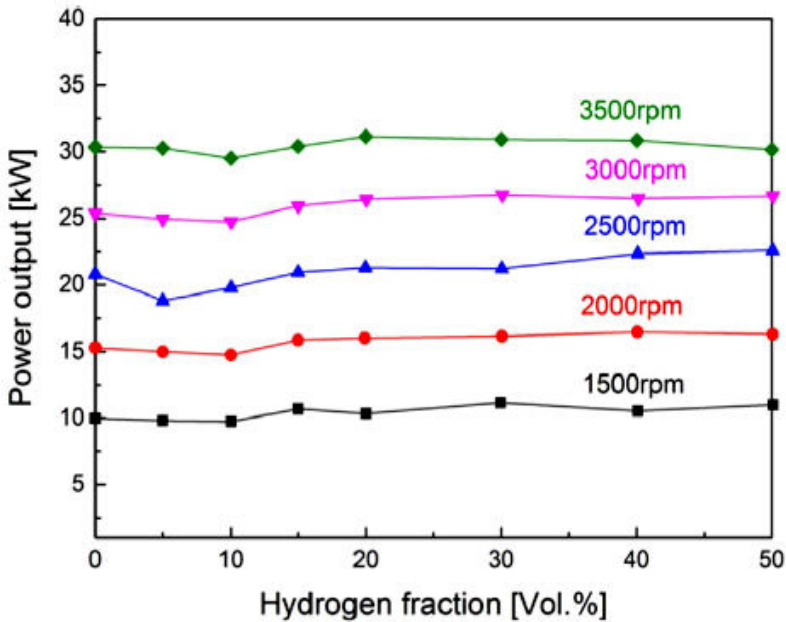


**Fig. 8.** Effect on the Hydrogen different percentage of power output [5]

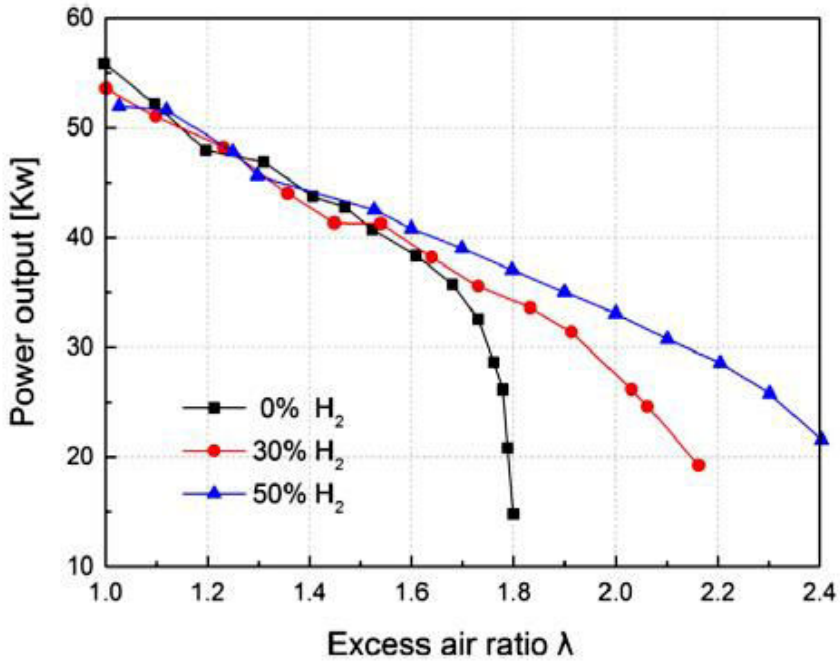


Fig. 9. Effect of the different Hydrogen percentage on power output with different excess air ratio[5]

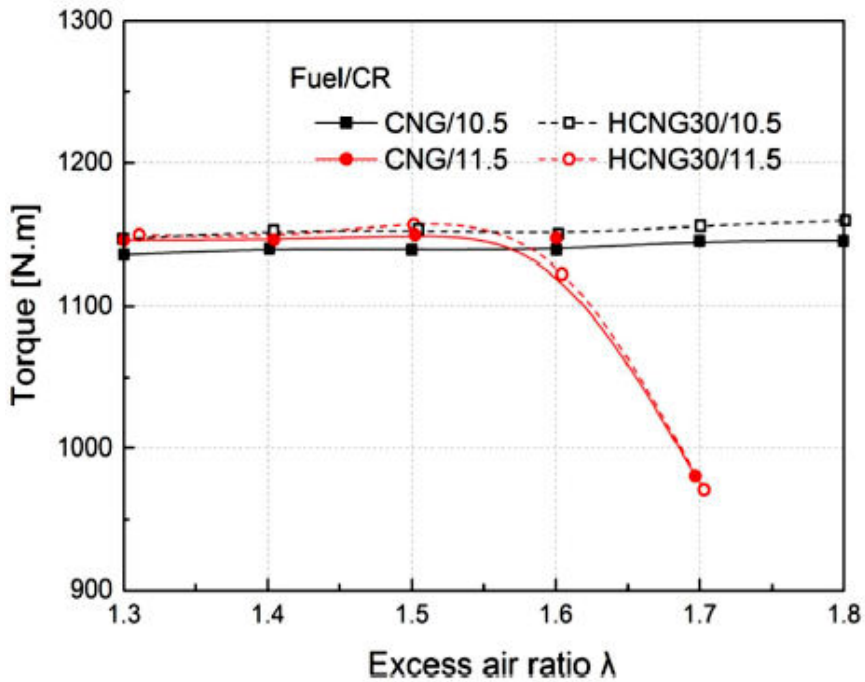
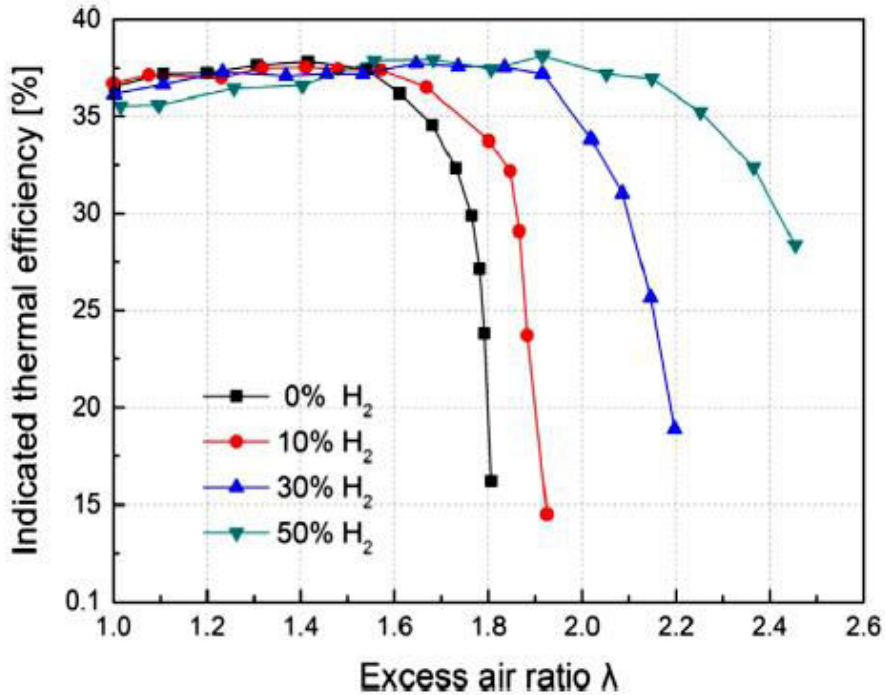


Fig. 10. Engine Torque variation at different excess air ratio at different hydrogen fraction[5]



**Fig. 11.** Indicated thermal efficiency at different excess air ratio at different hydrogen fraction [5]

Torque output defines the load levitating capacity as within the graph shown in Fig.10 Relation between excess air ratios, hydrogen fraction, compression ratio, and torque of the engines at the shaft. The lean-burn ability of the hydrogen fraction is nice and it can help to extend the compression ratio of the engine for better power output performance and thermal efficiency.

Fig.11 represents the relation between the surplus air ratios and indicated thermal efficiency at a different fraction of the hydrogen. As hydrogen percentage increases the indicated thermal efficiency increases with the good lean-burn ability [5].

#### 4.2. Emission Performances

The most fascinating and deserving property of the Hythane blend has the power to supply low levels of carbon monoxide, Hydrocarbon, CO<sub>2</sub>, and sulfur dioxide emissions as compared to Diesel, NG, and Gasoline engines. But there are chances of a rise within the level of the NO<sub>x</sub> because of high burning temperature. The graph is shown in Fig.12 ad 13 at 50% Hydrogen blends the best NO<sub>x</sub> emission. Ignition timing also plays a crucial role as an immediate relation with the retardation and NO<sub>x</sub> emission [5, 6].

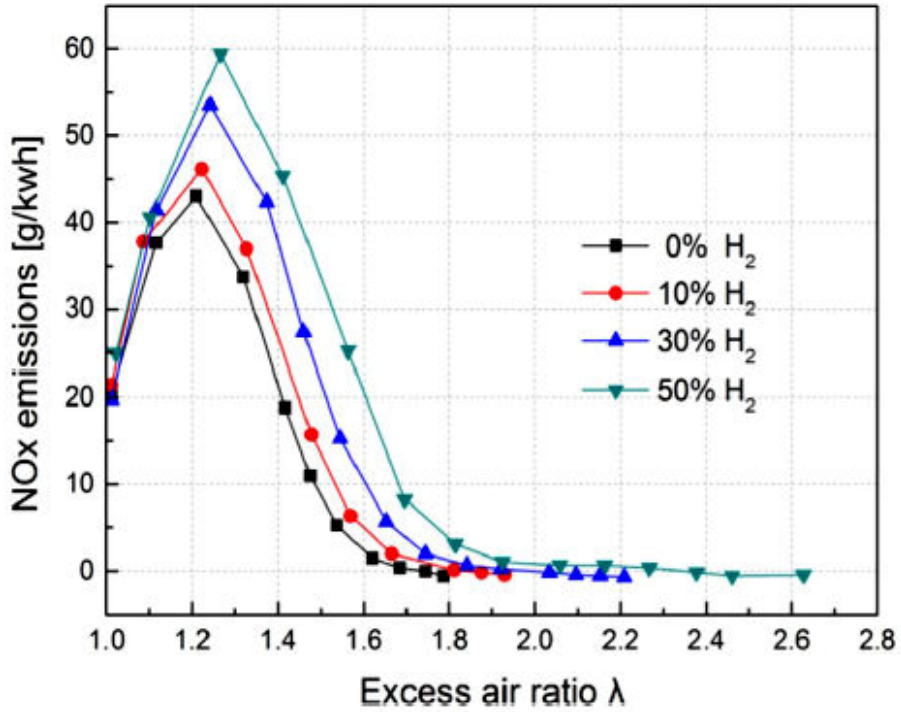


Fig. 12. NOx emission at different Excess Air Ratio and Hydrogen Fraction [5]

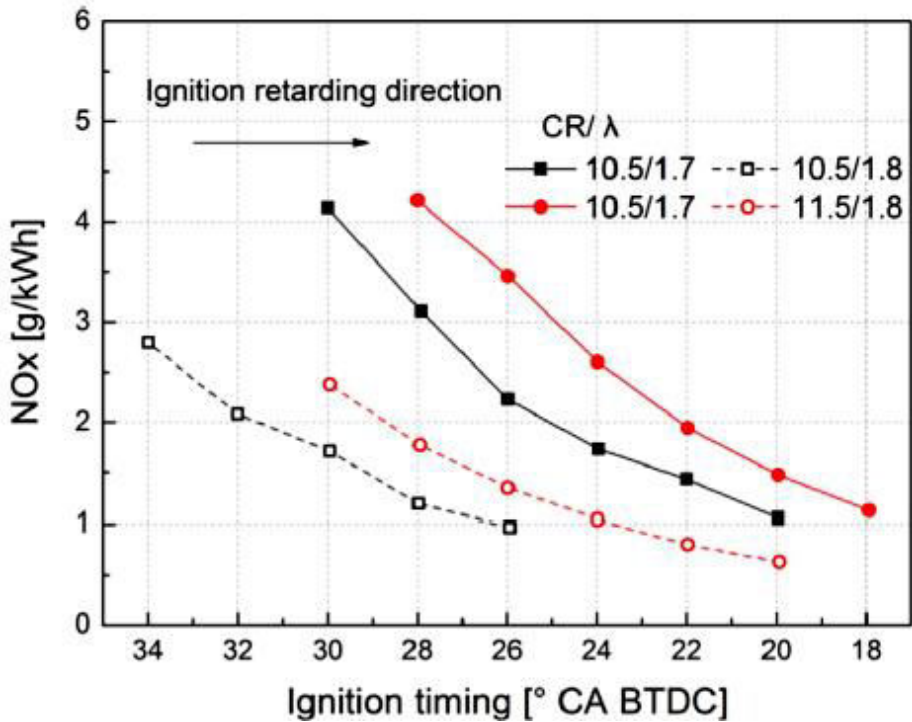


Fig. 13. NOx emission at different Excess Air Ratio and Hydrogen Fraction [5]

#### 4.2.1 Total HCs Emissions

The predominant causes of hydrocarbon emissions in S.I. engines are that the incompletely burned fuel trapped within the combustion chamber's intricate spaces where flame cannot reach. Incomplete burning of fuel by flame quenching within the vicinity of the cold combustion chamber wall or nearby spaces as well as air-fuel homogeneity is another source [53]. A mix of Hythane can effectively reduce the flame atomization distance and extend the flammability region.

#### 4.2.2 CO Emissions, Particulates, and Other Unregulated Emissions

The addition of hydrogen in natural gas reduces the emissions of carbon monoxide and it has a decreased trend if the continuous addition of increased hydrogen percentage [39]. Particulate matter emission is very less in the case of Hythane as compared to gasoline and natural gas engines. Fig.14 and 15 shows, emission trend compared with  $\lambda$  by adding a special fraction of hydrogen, it shows that the addition of hydrogen decreases the overall emission species.

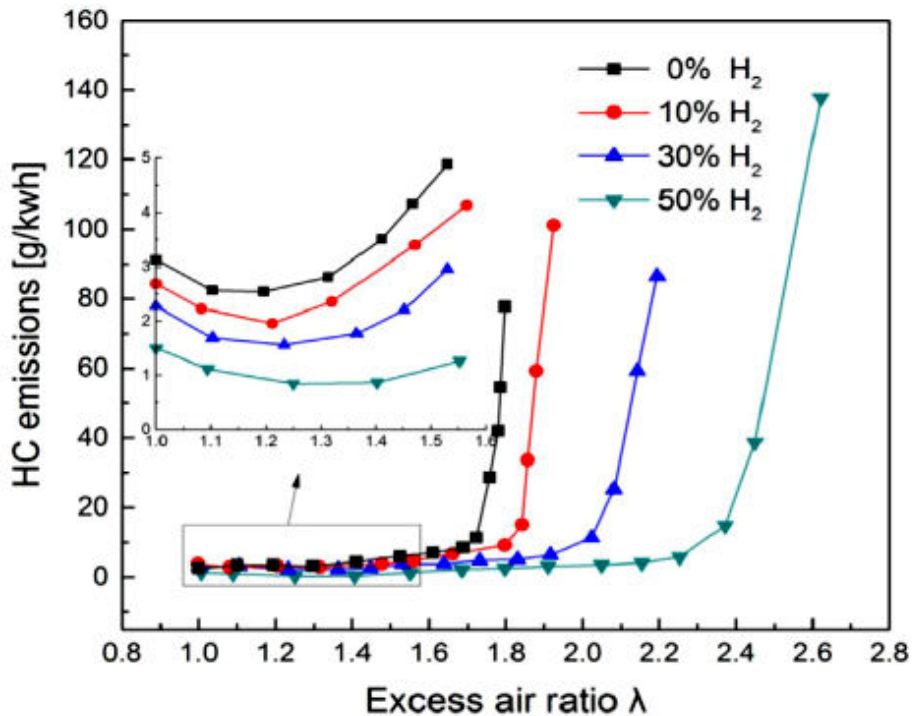


Fig. 14. Hydrocarbon emission at different excess ratio and different hydrogen fraction [5]

### 4.3. Lean Burn Limit

Hydrogen addition to natural gas is one of the key reasons to increase the lean-burn ability which signifies the rise of power output and a reduction in the engine emission. The fuel economy has also increased because of higher lean-burn ability, but it may result in frequent misfires.

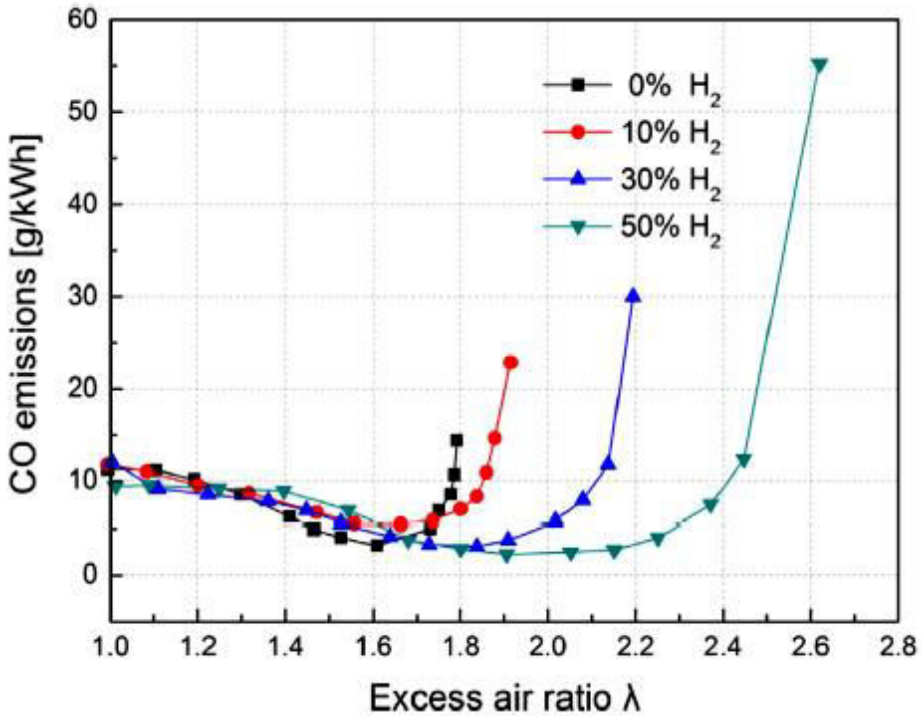


Fig. 15. Carbon Monoxide emission at different excess ratio and different hydrogen fraction [5]

### 4.4. Excess air ratio ( $\lambda$ )

It is the quotient of the actual air-fuel mixture to the standard stoichiometric air-fuel ratio, it is denoted by  $\lambda$ . When the value of  $\lambda$  is more than one, then it is the rich air-fuel mixture and if it is less than one, then the mixture of air and fuel is taken as lean. Stable engine combustion is the function of the variation of the various properties at peak cylinder pressure and effective pressure on indicated power.

Figure 16 shows the mass of the particulate size at different percentages of Hythane Fraction like 0, 10, 20, and 30Percent at various engine loads. Table 2, 3 & 4 gives detailed information about the parameters that need to consider while studying Hythane Blend.

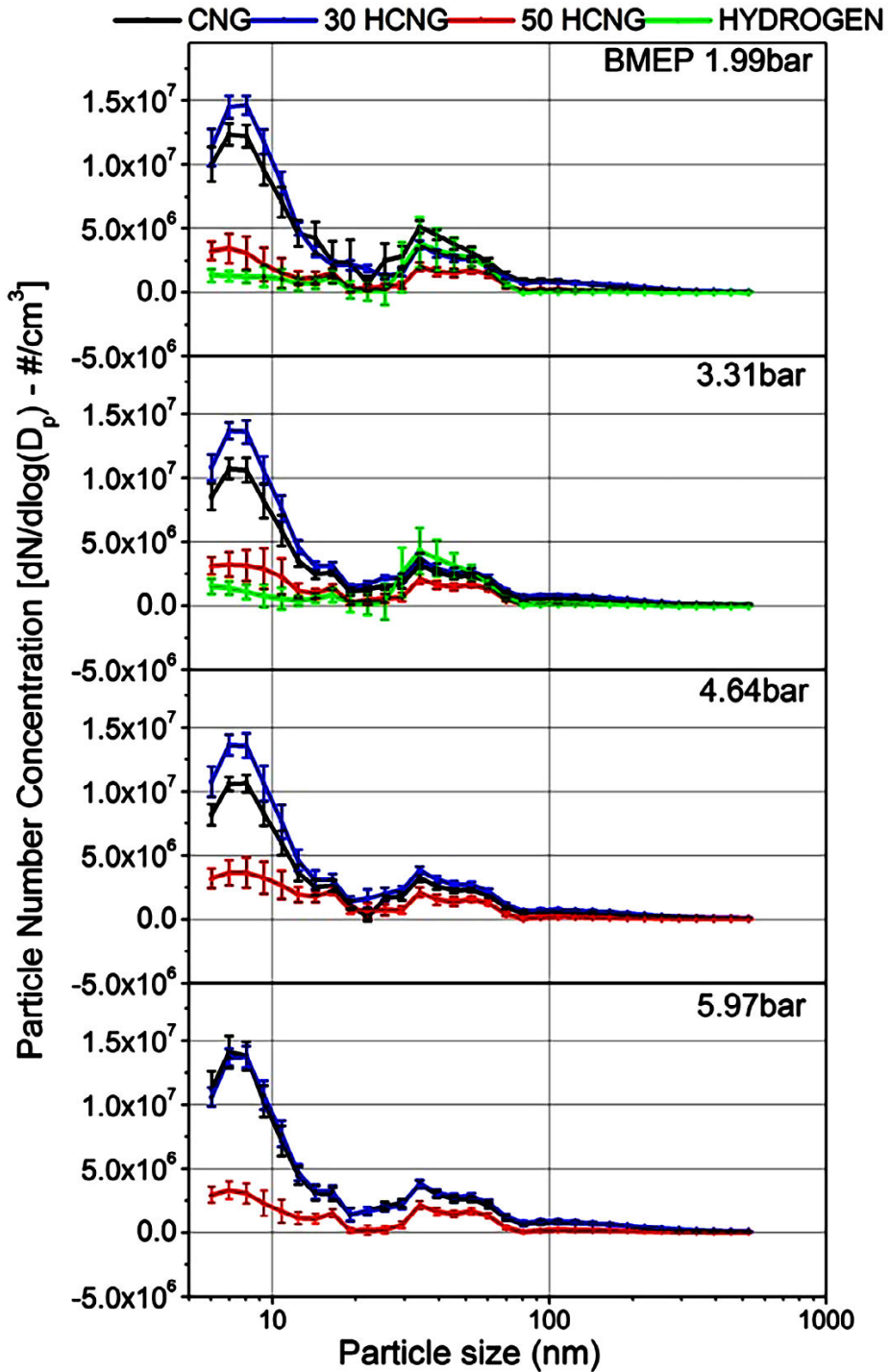


Fig. 16. Particle Size Versus Particle Mass Concentration at different fractions of Hythane fuel [2]

**Table2.**Engine Parameter needs to study

<b>Parameters of Engine to Control or Optimized</b>	<b>Parameters of study to meet objectives</b>	<b>Instrument for Measurement</b>
Equivalence ratio( $\lambda$ ), Air-fuel ratio	Maximum brake torque (MBT),	Suitable Lambda Sensor, customized high volume flow rate solenoid injectors
Brake torque, Fuel mass flow rate, Engine speed, Exhaust gas temperature, Calorific values of the test fuels, and volumetric energy density of the test fuel.	Indicated thermal efficiency (ITE)	Dynamometer
HCNG Vol %	Brake thermal efficiency (ITE), brake power	
Pressure-crank angle, Crank Angle Degree, Spark, and Injection Timing	Maximum in-cylinder pressure	Pressure Transducer, Data acquisition system, Flowmeter, Gas sensor
	Peak cylinder pressure	
Heat release rate (HRR), Rich A/F Ratio	Brake specific fuel consumption (BSFC), Brake mean Effective Pressure (BMEP), Brake Specific energy (BSEC), Volumetric efficiency	

**Table3.**Operating Parameters to be focused

<b>Parameters of Engine to Change or Optimized</b>	<b>Parameters of study to meet objectives</b>	<b>Instrument for Measurement</b>
Wide-open throttle, valve overlap timing, RAFR, port fuel injection, engine loads	Engine backfire, Research Octane Number	Precision shaft encoder
Port injection system, injection timing	Lean Burn Limits	
CR, crank angle position for various test fuels, shorter burning duration	Heat release rate	

Fuel injection pressure, fuel injection system, compression ratio	Peak pressure, coefficient of variation of indicated mean effective pressure	
Decreased Combustion Duration with an increase in BMEP	Mass fraction burned, Effective Pressure	
	Coefficient of variation knock's tendency	
Flame speed, adiabatic flame temperature	Peak cylinder temperature	Thermocouples

**Table 4.** Emission Parameters under consideration

Parameters of Engine to Change or Optimized	Parameters of study to meet objectives	Instrument for Measurement
Optimizing Compression ratio, Lean combustion. Excess-air ratio and Ignition timing, EGR rates, exhaust gas temperature	Reduce HC, NO <sub>x</sub> and CO Emissions, unburned hydrocarbons, CO <sub>2</sub> , particulate matter	Measurement and Plotting Graph by exhaust gas emission analyzer, Nitric Oxide sensor
Valve overlap angle, low carbon content	Total Hydrocarbon(THC)	
Hydrogen-to-carbon ratio	Greenhouse	
	gas emissions	
Incomplete combustion, misfire, insufficient oxygen	HC, CO, NO <sub>x</sub> ,	

**Table 5.** Summary of the Literature

Authors	Findings	Research Gap	Ref.
Roopesh Kumar Mehra [2017]	Hydrogen addition allows the engine to works on higher compression ratio without any combustion instability compared to CNG, which improves thermal efficiency.	Finding perfect mixture proportion is a major problem with implementing HCNG fuel  Optimum spark timing and A/F ratio for best performance  Delayed ignition timing	[1]

		and lean combustion are the area should be focused in future to regulate NOx emissions level.	
S.M.V. Sagar [2018]	Investigate particulate emissions from HCNG fueled prototype engine, for diverse test fuel mixture compositions	Very little research has been done on particulate emissions from gaseous fuels, especially HCNG mixtures	[2]
Rohit Singh Lather. [2018]	This paper is comprehensive overview of combustion fundamentals of hydrogen-natural gas mixture in SI Engine, The air-fuel ratio, the time of injection, the compression ratio and speed play a major role in blending HCNG in an SI engine	It is necessary to develop a strategy to control the NOx emissions under the promise of successful start of engine.	[3]
Changming Gong [2019]	Experimentally investigated the effects of ignition timing on combustion and emissions of an SI methanol engine with added hydrogen at different engine speeds	The relationship between NOX and soot emissions with added hydrogen needs to be clarified on future research work	[4]
Fuwu Yan [2017]	The physicochemical properties of hydrogen and its mixture with natural gas were firstly Analyzed	The hydrogen fractions need to be optimized and corresponding adjustments are required for various other engine operating and design parameters	[5]
Canan Acar [2018]	hydrogen-fueled internal combustion engines have the lowest GHG emissions, hydrogen fueled internal combustion engines have the lowest social cost of carbon	Hydrogen widespread use is still likely to be hindered by many practical difficulties of large scale hydrogen production, storage, fueling infrastructures as well as engine abnormal	[6]

		combustion.	
Willian C_azar Nadaleti [2017]	Experimental study of H-CNG fuel with partial load analysis of SI engine for road transport application.	The combustion duration had a significant effect on both performance and emission characteristics of the engine. It is another factor that should be designed carefully to achieve the best results from the engine's work	[7]
S.M.V. Sagar, [2017]	Experiment was conducted on SI using various % of HCNG mixtures having 0, 10, 20, 30, 50, 70 and 100%.The performance and combustion characteristics of these test fuels were compared with that of baseline CNG, versatile dynamic HCNG mixing System is used for correct composition	In order to conduct a comprehensive study and make sound conclusions, it is necessary to investigate entire span (0 to 100%) of hydrogen fraction in the HCNG mixtures.	[8]
F. Catapano [2016]	This paper is comparison between CH <sub>4</sub> and different CH <sub>4</sub> /H <sub>2</sub> mixtures in a single-cylinder Port Fuel/Direct Injection spark ignition (PFI/DISI) engine operating under steady state conditions.	Further improvement can be obtained reducing the duration of injection by using higher injection pressure.	[9]
G.M. Kosmadakis [2016]	This analysis considers engine load variation through a variable equivalence ratio, with the application of an in-house research, three-dimensional computational fluid dynamics code (3DCFD) for detailed in-cylinder simulations	Comprehensive study can be expanded to identify engine configurations and strategies for reducing pollutant emissions	[11]

BarisAcıkgoz [2015]	Decrement of fuel consumption by 14.04%. Taking into account the power costs, the fuel saving is 8.03%.	The operating parameter and design parameter such as spark timing and Compression ratio should be optimized.	[13]
Selim Tangoz [2017]	Isuzu 3.9 L engine having a 12.5 compression ratio at 1500, 2000 and 2500 rpm using ignition timings of 5, 10, 15 and 20 deg. CA BTDC fuelled by pure CNG, HCNG5, HCNG10, HCNG20. The HC values were generally obtained as lowest values at HCNG5 for given engine speeds and advance.	Optimization of Hydrogen CNG mixture need to select carefully and the selection of optimum ignition timing.	[14]
Silvana Di Iorio [2015]	Engine investigations were carried out at constant engine speed of 1500 rpm 42 for different H/C ratios, Spark timing and RAFR kept constant. It shows higher peak pressure, but lower maximum Brake torque (MBT), BTE was higher and NOx emissions also	HCNG engine fueled with a higher hydrogen fraction may cause abnormal combustion such as pre-ignition, knock and backfire  Numerical modeling and CFD analysis of combustion model and fuel injection timing are having big scope for the analysis of combustion performance.	[15]
Yang Liu [2019]	Combination of Atkinson cycle with high compression ratio and low heat rejection on the hydrogen-enriched Compressed natural gas prototype engine with 55% hydrogen blend	Validation by Software is need to study n depth	[16]
B.G. Agaie [2018]	Investigated the effects of hydrogen on the combustion stability and	Production and storage of hydrogen can be made completely sustainable	[18]

	thermal efficiency of a T-GDI engine in stoichiometric to lean conditions with low to high loads	which also could dramatically enhance the contribution of fuel cell and hydrogen internal combustion engines in the transportation sector.	
Deymi Dashtebayaz [2016]	Engine's work is important factor need to improve by using different mixtures of methane and hydrogen	Engine's work is important factor need to improve by using different mixtures of methane and hydrogen.	[21]
Tadveer Singh Hora [2015]	Experiments were performed to study the effect of varying content of hydrogen in HCNG. Effect of 0%, 10%, 20% and 30% (v/v) of HCNG was experimentally analyzed at constant engine speed 1500 rpm	Optimization HCNG blend composition	[23]
Saheed Wasii [2018]	An experimental study has been performed to study the brake specific energy consumption (BSEC) and exhaust emission characteristics of the direct injection hydrogen enriched compressed natural gas engine (DI-HCNG) at various air-fuel ratios., BSEC increases, BSCO decreases, BSNO <sub>x</sub> Decreases and BSUHC Decreases as H <sub>2</sub> % increases	Brake Specific Energy Consumption need to calculate accurately	[26]
Santiago Martinez [2018]	900 rpm and WOT, with methane as baseline fuel, 25%vol and 50%vol of hydrogen addition to methane, and finally two syngas equivalent Mixtures, with 50%vol and 75% vol hydrogen content	Spark timing re-calibration is required in order to fully take advantage of fuel properties such as higher laminar flame speed and increased stability	[32]

Rajesh Kumar Prasad [2016]	Investigated the effect of initial CVCC filling pressure, $k$ and H <sub>2</sub> percentage in the HCNG mixture on flame kernel evolution, peak cylinder pressure during combustion, and combustion duration, when laser ignition was used to initiate the combustion in the CVCC.	Addition of H <sub>2</sub> in the HCNG blends must be optimized to get superior engine combustion, depending on the application.	[34]
Javad Zareei [2018]	For stoichiometric operation, the addition of hydrogen to CNG has produced a brake-specific fuel combustion (bsfc) reduction ranging between 2% and 7% and a brake-specific total unburned hydrocarbons (bsTHCs) decrease up to 40%.	Engine characterization should not be made on the basis of one cylinder only	[38]

## 5. CONCLUSION

This study reviews the compatibility of the Hythane blend in SI Engines. Hydrogen has good characteristic sort of a lean mixture burning ability, minimum ignition energy, and a wide range of flammability and when blended with natural gas it elevates laminar and streamlines burning velocity of the combustion which caused high flame travel for complete combustion of fuel. Because of complete combustion and streamline flame velocity lower fuel combustion to brake power of the engine. Various studies concluded that overall thermal efficiency increases with compared natural gas-fueled SI engines, considering the parameters like lean mixture and different sparking timing. Variation in natural gas operations in the process is more and unstable operations of the engine. Hythane predominantly decreases this instability of vehicle performance. Due to high flame speed and more amount of energy produced during power strong results in temperature rise at the end which causes NO<sub>x</sub> emission. Other species of tailpipe emissions like HC, CO, CO<sub>2</sub>, and SO<sub>2</sub> significantly reduces due to carbon-free hydrogen gas. Due to the high auto-ignition temperature of the Hythane and air mixture compared to diesel and

gasoline fuel compression of the engines is often increased to urge the higher power output. The methane number of Hydrogen is zero as a Hydrogen fraction increases over 40%, then it's having limits to use as a fuel in engines. Currently, hydrogen generation and storage are facing huge challenging issues which are the scope for future studies. CNG infrastructure is insufficient for the extensive use of hydrogen.

## NOMENCLATURE

<i>BSEC</i>	: Brake Specific Energy Consumption
<i>BSECO</i>	: Brake Specific Emission Carbon Monoxide
<i>BSFC</i>	: Brake specific fuel consumption
<i>BTE</i>	: Brake thermal efficiency
<i>CFD</i>	: computational fluid dynamics
<i>CNG</i>	: Compressed natural gas
<i>CO</i>	: carbon monoxide
<i>CO<sub>2</sub></i>	: carbon dioxide
<i>EGR</i>	: Exhaust Gas Recirculation
<i>HC</i>	: hydrocarbon
<i>HCNG</i>	: Hydrogen and Compressed natural gas
<i>Hythane</i>	: Hydrogen and Compressed Natural Gas Blend
<i>IC</i>	: internal combustion
<i>NO<sub>x</sub></i>	: Nitrogen Oxides
<i>SI</i>	: spark ignition
<i>η<sub>bth</sub></i>	: Brake thermal efficiency

## REFERENCES

1. Roopesh Kumar Mehra, HaoDuan, RomualdasJuknelevičius, Fanhua Ma, Junyin Li, Progress in Hydrogen Enriched Compressed Natural Gas Internal Combustion Engines-A Comprehensive Review, *Renewable, and Sustainable Energy Reviews*, 80, 2017, 1458–1498.
2. S.M.V. Sagar, Avinash Kumar Agarwal, Knocking Behavior, and Emission Characteristics of a Port Fuel Injected Hydrogen Enriched Compressed Natural Gas-Fueled Spark Ignition Engine, *Applied Thermal Engineering*, 141, 2018, 42–50.
3. Rohit Singh Lather, L.M. Das, Performance and Emission Assessment of A Multicylinder S.I Engine Using CNG & HCNG as Fuels, *International Journal of Hydrogen Energy*, 44, 2019, 21181-21192.
4. Changming Gong, Zhaohui Li, YulinChend, Jiajun Liu, Fenghua Liu, Yongqiang Han, Influence of Ignition Timing on Combustion and Emissions of A Spark-Ignition Methanol Engine With Added Hydrogen Under Lean-Burn Conditions, *Fuel*, 235, 2019, 227–238.

5. Fuwa Yana, Lei Xua, Yu Wanga, Application of Hydrogen Enriched Natural Gas in Spark Ignition IC Engines: From Fundamental Fuel Properties to Engine Performances and Emissions, *Renewable And Sustainable Energy Reviews*, 82, 2017, 1125-1157.
6. CananAcar, Ibrahim Dincer, The Potential Role of Hydrogen as a Sustainable Transportation Fuel to Combat Global Warming, *International Journal of Hydrogen Energy*, 2018.
7. Willian, EzarNadaleti, Grzegorz Przybyla, Paulo Belli Filho, Samuel Souza, Methane-Hydrogen Fuel Blends For SI Engines in Brazilian Public Transport-Efficiency and Pollutant Emissions, *International Journal of Hydrogen Energy*, 20, 2018, 1-15.
8. S.M.V. Sagar, A. K. Agarwal, Experimental Investigation of Varying Composition of HCNG on Performance and Combustion Characteristics of a SI Engine, *International Journal of Hydrogen Energy*, 20, 2017.
9. F. Catapano, S. Di Iorio, P. Sementa, B.M. Vaglieco, Analysis of Energy Efficiency of Methane and Hydrogen-Methane Blends In a PFI/DI SI Research Engine, *Energy*, 2016, 1-20.
10. Changming Gong, Dong Li, Zhaohui Li, Fenghua Liu, Numerical Study on Combustion and Emission in a DISI Methanol Engine With Hydrogen Addition, *International Journal of Hydrogen Energy*, 45, 2015.
11. G.M. Kosmadakis, D.C. Rakopoulos, C.D. Rakopoulos, Methane/Hydrogen Fueling A Spark-Ignition Engine For Studying NO<sub>x</sub>, CO And HC Emissions With a Research CFD Code, *Fuel*, 2016, 185, 903–915.
12. G.M. Kosmadakis, D.C. Rakopoulos, C.D. Rakopoulos, Investigation of Nitric Oxide Emission Mechanisms in a SI Engine Fueled With Methane/Hydrogen Blends Using a Research CFD Code, *International Journal of Hydrogen Energy*, 40, 2015, 15088-15104.
13. BarisAcikgoz, CenkCelik, Hakan S. Soyhan, BurakGokalp, Bilal Karabag, Emission Characteristics of a Hydrogen–CH<sub>4</sub>Fuelled Spark Ignition Engine, *Fuel*, 159, 2015, 298–307.
14. SelimTangeoz, NafizKahraman, SelahaddinOrhanAkansu, The Effect of Hydrogen on The Performance and Emissions of an SI Engine Having a High Compression Ratio Fuelled By Compressed Natural Gas, *International Journal of Hydrogen Energy*, 2017.
15. Silvana Di Iorio, Paolo Sementa, Bianca Maria Vaglieco, Analysis of Combustion of Methane and Hydrogen Methane Blends In Small DISI (Direct Injection Spark Ignition) Engine Using Advanced Diagnostics, *Energy*, 2015, 1-20.

16. Yang Liu, Yuan He, Cuijie Han And Chenheng Yuan, Combustion And Energy Distribution of Hydrogen-Enriched Compressed Natural Gas Engines With Low Heat Rejection Based on Atkinson Cycle, *Advances In Mechanical Engineering*, 11, 2019, 1-12.
17. Tanveer Singh Hora, Avinash Kumar Agarwal, Experimental Study of The Composition of Hydrogen Enriched Compressed Natural Gas on Engine Performance, Combustion and Emission Characteristics, *Fuel*, 160, 2015, 470–478.
18. B.G. Agaie, I. Khan, Z. Yacoob, I. Tlili, A Novel Technique of Reduce Order Modelling Without Static Correction for Transient Flow of Non-Isothermal Hydrogen-Natural Gas Mixture, *Results In Physics*, 10, 2018, 532–540.
19. Roopesh Kumar Mehra, Fanhua Ma, DuanHao, Study of Turbulent Entrainment Quasi-Dimensional Combustion Model for HCNG Engines With Variable Ignition Timings, *SAE International*, 21, 2018, 1-12.
20. J. Pradeep Bhasker, E. Porpatham, Effects of Compression Ratio and Hydrogen Addition on Lean Combustion Characteristics and Emission Formation in a Compressed Natural Gas Fuelled Spark Ignition Engine, *Fuel*, 208, 2017, 260–270.
21. [21] DeymiDashtebayaz M, EbrahimiMoghadam A, Pishbin Si, Pourramezan M, Investigating the Effect of Hydrogen Injection on Natural Gas Thermo-Physical Properties with Various Compositions, *Energy*, 2018, Doi:10.1016/J.Energy.2018.10.186.
22. HaoDuan, Yue Huang, Roopesh Kumar Mehra, Panpan Song, Fanhua Ma, Study on Influencing Factors of Prediction Accuracy of Support Vector Machine (SVM) Model for NO<sub>x</sub> Emission of a Hydrogen Enriched Compressed Natural Gas Engine, *Fuel*, 234, 2018, 954–964.
23. Tadveer Singh Hora, Pravesh Chandra Shukla, Avinash Kumar Agarwal, Particulate Emissions from Hydrogen Enriched Compressed Natural Gas Engine, *Fuel*, 166, 2016, 574–580.
24. Hora, T.S., Agarwal, A.K., Effect of Varying Compression Ratio on Combustion, Performance, and Emissions of a Hydrogen Enriched Compressed Natural Gas Fuelled Engine, *Journal of Natural Gas Science & Engineering*, 2016, Doi: 10.1016/J.Jngse.2016.03.041.
25. Yue Huang, Fanhua Ma, Intelligent Regression Algorithm Study Based on Performance and NO<sub>x</sub> Emission Experimental Data of a Hydrogen Enriched Natural Gas Engine, *International Journal of Hydrogen Energy*, 2016.
26. SaheedWasiu, Rashid Abdul Aziz And PuteriMegat, Brake Specific Energy Consumption (BSEC) and Emission Characteristics of the Direct Injection Spark Ignition Engine Fuelled by Hydrogen Enriched

- Compressed Natural Gas at Various Air- Fuel Ratios, *International Journal of Applied Engineering Research*, 13, 2018, 677-683.
27. SaheedWasiu, Rashid Abdul Aziz And MuazamGhozali, Engine Performance Characteristics Fuelled by In-Situ Mixing of Small Amount of Hydrogen and Compressed Natural Gas at Various Relative Air-Fuel Ratios, *International Journal of Applied Engineering Research*, 13, 2018, 714-719.
  28. Adrian Irimescu, Francesco Catapano, Silvana Di Iorio, Paolo Sementa, Influence of Combustion Efficiency on the Operation of Spark Ignition Engines Fueled With Methane and Hydrogen Investigated in a Quasi-Dimensional Simulation Framework, *SAE International*, 15, 2018, 1-15.
  29. RomualdasJuknelevičius, R. Kumar Mehra, Fanhua Ma, In-Cylinder Combustion Analysis of a SI Engine Fuelled With Hydrogen Enriched Compressed Natural Gas (HCNG): Engine Performance, Efficiency and Emissions, *Journal of Kones Powertrain and Transport*, 2018,
  30. Sunyoup Lee, Changgi Kim, Young Choi, Gihun Lim, Cheolwoong Park, Emissions, and Fuel Consumption Characteristics of an HCNG-Fueled Heavy-Duty Engine at Idle, *International Journal of Hydrogen Energy*, 39, 2014, 8078-8086.
  31. J. Zareei, A.Rohani, Wan Mohd, Combined Effect of Ignition and Injection Timing along with Hydrogen Enrichment to Natural Gas in a Direct Injection Engine on Performance and Exhaust Emission, *International Journal of Automotive Engineering*, 8, 2018, 2614-2631.
  32. Santiago Martinez, Pedro Lacava Pedro Luis Curto, Adrian Irimescu, Simona Silvia Merola, Effect of Hydrogen Enrichment on Flame Morphology and Combustion Evolution in a SI Engine under Lean Burn Conditions, *SAE International*, 2018.
  33. Simona Silvia Merola, Silvana Di Iorio, Adrian Irimescu, Paolo Sementa, Bianca Maria Vaglieco, Spectroscopic Characterization of Energy Transfer and Thermal Conditions of The Flame Kernel in a Spark-Ignition Engine Fueled with Methane and Hydrogen, *International Journal of Hydrogen Energy*, 39, 2017, 8078-8086.
  34. Rajesh Kumar Prasad, Siddhant Jain, Gaurav Verma, Avinash Kumar Agarwal, Laser Ignition and Flame Kernel Characterization of HCNG in a Constant Volume Combustion Chamber, *Fuel*, 208, 2016, 260–270.
  35. Anas Rao, Roopesh Kumar Mehra, HaoDuan, Fanhua Ma, Comparative Study of the NO<sub>x</sub> Prediction Model of HCNG Engine, *International Journal of Hydrogen Energy*, 31, 2017, 1021-1034.
  36. S. M. V. Sagar, Avinash Kumar Agarwal, Experimental Validation of Accuracy of Dynamic Hydrogen-Compressed Natural Gas Mixing

- System using a Single Cylinder Spark Ignition Engine, *International Journal of Hydrogen Energy*, 20, 2016, 1201-1213.
37. Gaurav Verma, R. Kumar Prasad, R. A. Agarwal, S. Jain, A. Kumar Agarwal, Experimental Investigations of Combustion, Performance and Emission Characteristics of a Hydrogen Enriched Natural Gas Fuelled Prototype Spark Ignition Engine, *Fuel*, 208, 2016, 297–298.
  38. JavadZareei, Abbas Rohani, Wan Mohd, Simulation of a Hydrogen/Natural Gas Engine, and Modelling of Engine Operating Parameters, *International Journal of Hydrogen Energy*, 39, 2018, 8078-8086.
  39. Bo Zhang, Changwei Ji, Shuofeng Wang, Combustion Analysis and Emissions Characteristics of a Hydrogen-Blended Methanol Engine at Various Spark Timings, *International Journal of Hydrogen Energy*, 40, 2015, 4707-4716.
  40. S. D. Yadav, Bimlesh Kumar, S. S. Thipse, Characteristics of Biogas Operated Automotive SI Engine to Reduce Exhaust Emission for Green Development, *SAE Technical Papers*, 5 2013.

#### **Cite this article**

---

Kiran P. Pawar and Sanjay D. Yadav, Effectiveness of Hydrogen Enrichment in CNG Fuelled SI Engine: A Review, In: Sandip A. Kale editor, *Efficient Engineering Systems: Volume 1*, Pune: Grinrey Publications, 2021, pp. 1-28.

# Entropy Generation Analysis of A Low-Temperature Waste Heat Power Generation System Integrated with the Agricultural Machinery

Rupinder Pal Singh<sup>a,\*</sup> and R S Gill<sup>a</sup>

<sup>a</sup>Department of Mechanical Engineering, Punjab Agricultural University, Ludhiana, Punjab, India

\*Corresponding author: rupinderpal@pau.edu

## ABSTRACT

The heavy-duty diesel engines play a significant role in agricultural production. However, the lower efficiency, higher fuel consumption, and environmental pollution put a barrier to their effective utilization in the farmland. Hence, there is an urgent need to effectively enhance efficiency by tapping the rejected heat, which is otherwise directly expelled into the atmosphere. The present work proposes an entropy generation analysis of the heat recovery system. The conventional energy analysis is not sufficient to detect the sources/components for maximum exergy destruction. Hence, entropy generation analysis based on the second law is implemented to obtain the exergetic efficiency. The organic Rankine cycle using R-245fa as working fluid is used to recover the rejected heat discharged from coolant, lubricating oil and intercooler. The total exergy input to ORC system is calculated as 545 kW. The maximum irreversibilities are found in the evaporator (137kW) which is approximately 25% of the total exergy input followed by turbine, condenser and pump. The total exergy loss is higher in condenser as compared to turbine whereas irreversibilities are more in turbine than condenser. It means that a huge available work is lost in the cooling water.

**Keywords:** Entropy, Exergy, Organic Rankine cycle, Thermodynamics, rejected heat

## 1. INTRODUCTION

The continuous depletion of fossil fuels, high-energy cost, and energy dependent society along with stringent environment legislations demands for highly efficient systems/ technologies. The agriculture sector is heavily relying upon the high-grade energy in the form of heavy-duty diesel engine (HDDE) [1]. These engines produce a lot of environmental pollution and possess lower efficiencies. There is a huge amount of rejected heat is being discharged directly into the atmosphere. Broadly, the rejected heat is categorized as high temperature and low-temperature heat sources [2-3]. The exhaust gas from the HDDE is a high temperature heat source whereas heat recovered from the lubricating oil, coolant, etc. are low temperature heat sources. There is a need to tap the rejected heat by implementing various thermodynamic technologies like organic Rankine cycle (ORC), supercritical CO<sub>2</sub> cycle, Kalina cycle, trigeneration cycle, thermo-acoustic power generators, etc. [4-5]. The waste heat can be further utilized for district heating, heat pumps, and power generation, etc. [6]. The rejected heat has a huge work potential, which further reduces the system operating cost by using heat recovery technologies.

The technologies for recovering the high temperature heat have already been commercialized. However, there is much less information on the low temperature waste heat recovery integrated with HDDE. Sayedkavoosi et al.[7] presented an exergy optimization of ORC for recovering rejected heat from IC engine. It was concluded that R-123 is the best working fluid under the set conditions and generated 468 kW power. Kumar and Shukla [8] presented the ORC for solar thermal power plant using Benzene as working fluid. Li et al. [9] studied the thermal performance of the ORC using R-245fa and carbon dioxide. Kaska [10] presented a rejected heat recovery system from a steel industry using an ORC. It was concluded that boiler pressure has a great impact on the exergy and energy performance. The literature suggests that R-245fa has excellent thermos-physical properties, which makes it suitable for low temperature applications.

In order to evaluate the work potential of the rejected heat, second law analysis is required based on energy and irreversibility rate. For a real process, entropy is generated due to internal and external irreversibilities. An effort has been made to evaluate the thermodynamic efficiency of the recovery system for the heavy-duty agricultural engines. The ORC system was installed driven by rejected heat of recover the low-temperature waste heat discharged from coolant, lubricating oil, and intercooler.

## 2. METHODOLOGY

The line diagram of the ORC is shown in Fig. 1. Hot heat transfer fluid (Therminol 66) was obtained after circulating through the engine compartment. The properties of R-245fa is given in the Table 1 [11]. An easy step-by-step general procedure to study the performance of a heat recovery system is also presented.

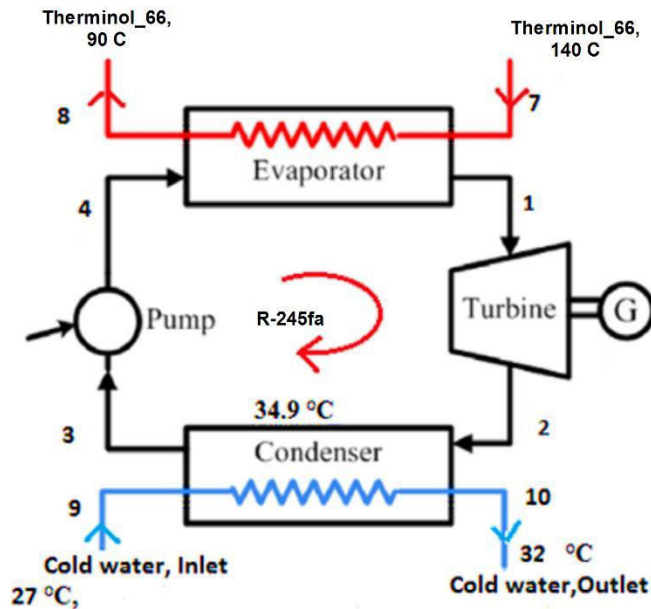


**Fig. 1.** Organic Rankine cycle system [10]

**Table 1.** Properties of working fluids

Refrigerant	Critical Temp. (°C)	Critical Pressure (bar)	Boiling Temp (°C)	Molecular mass (g/mol)	ODP	GWP
R-245fa	154.2	36.4	15.05	134.05	0	950

### Input Conditions

1. Ambient conditions are assumed as 25°C; 1 bar.
2. The working fluid R-245fa is dry saturated at the inlet of turbine.
3. The efficiency of turbine and pump is 75 %.
4. Condenser temperature is 34.9°C and the corresponding pressure is 3.28 bar.
5. Therminol-66 is used as heat transfer fluid flowing at 25 kg/s.

The first step is to evaluate the optimum evaporator pressure based on the constant PPTD of 6.8°C.

Pinch Point temperature,

$$T_{PP} = \frac{(T_{h,in} - T_{h,out})}{\Delta H_{14}} \Delta H_{54} + T_{h,out} \quad (1)$$

Pinch point temperature difference,

$$\Delta T_p = T_{PP} - T_5 \quad (2)$$

Second step is to use the energy balance in condenser.

$$\dot{m}_c C_p (T_{c,out} - T_{c,in}) = \dot{m}_{fl} (h_2 - h_3) \quad (3)$$

where,  $\dot{m}_c$  and  $\dot{m}_{fl}$  are the flow rate of cold water and working fluid respectively,  $T_{c,out}$  and  $T_{c,in}$  are the outlet and inlet of cold water,  $h_2$  and  $h_3$  are the inlet and outlet enthalpies in the condenser. Third step is to evaluate the waste heat flow rate into the evaporator.

$$\dot{m}_{fl} (h_1 - h_4) = \dot{m}_h C_p (T_{h,in} - T_{h,out}) \quad (4)$$

where,  $\dot{m}_h$  is the mass flow rate of waste steam,  $T_{h,in}$  and  $T_{h,out}$  are the inlet & outlet temperature of steam.

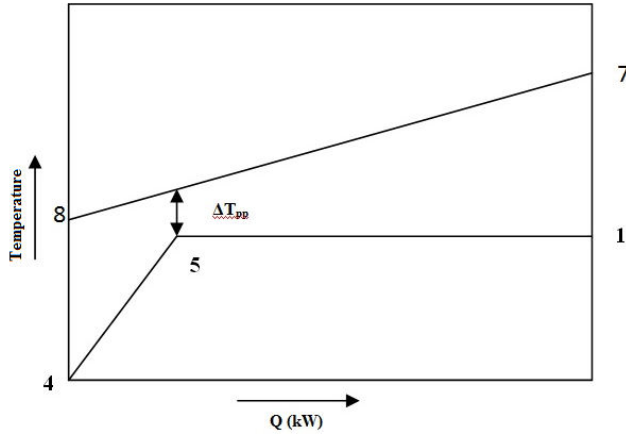


**Fig. 2.** Temperature-Heat Transfer Diagram for Evaporator

Fourth step is to evaluate the exergy rate at all the state points using the basic equation given by second law of thermodynamics

Exergy rate,

$$\dot{E} = \dot{m} e = \dot{m} \times [h - h_o - T_o (s - s_o)] \quad (5)$$

where,  $e$  is specific flow exergy,

Fifth step is to calculate the rate of exergy destruction

For an unsteady control volume system with single inlet and outlet irreversibility rate is given as,

$$\dot{I} = \dot{m}_{fl} T_o \left[ (s_{out} - s_{in}) + \frac{q}{T} + \frac{ds_{sys}}{dt} \right] \quad (6)$$

For steady flow,

$$\frac{ds_{sys}}{dt} = 0 \quad (7)$$

Each component in ORC is described with the following equations Process 3-4 (Pump)

$$\eta_p = \frac{W_{p,ideal}}{W_{p,act}} = \frac{h_3 - h_{4a}}{h_3 - h_4} \quad (8)$$

$$\dot{I}_{34} = \dot{m}_{fl} T_o (s_4 - s_3) \quad (9)$$

Process 1-2 (Turbine),

$$\eta_t = \frac{W_{t,act}}{W_{t,ideal}} \quad (10)$$

$$\dot{I}_{12} = \dot{m}_{fl} T_o (s_2 - s_1) \quad (11)$$

$$\dot{W}_{12} = \dot{m}_{fl} T_o (h_2 - h_1) \quad (12)$$

Process 4-1 (Evaporator),

Exergy balance in evaporator,

$$\dot{I}_{41} + \left( \dot{E}_8 + \dot{E}_1 \right) = \dot{E}_7 + \dot{E}_1 \quad (13)$$

Exergetic Efficiency, Evaporator,

$$\eta_{ex,evap} = \left( \frac{\dot{E}_1 - \dot{E}_4}{\dot{E}_7 - \dot{E}_8} \right) \quad (14)$$

Heat transfer in the evaporator,

$$\dot{Q}_e = \dot{m}_f (h_1 - h_4) \quad (15)$$

Process 2-3 (Condenser)

Exergy balance in Condenser,

$$\dot{I}_{23} + \left( \dot{E}_3 + \dot{E}_{10} \right) = \dot{E}_9 + \dot{E}_2 \quad (16)$$

Exergetic Efficiency, Condenser,

$$\eta_{ex,cond} = \left( \frac{E_{10} - E_9}{E_2 - E_3} \right) \quad (17)$$

Total Irreversibility,

$$\dot{I}_{total} = \dot{I}_{34} + \dot{I}_{41} + \dot{I}_{12} + \dot{I}_{23} \quad (18)$$

Net Work done,

$$\dot{W}_{net} = \dot{W}_t - \dot{W}_p = E_{in} - E_{loss} \quad (19)$$

Exergy Input to the evaporator by the furnace cooling water,

$$\dot{E}_{in} = \dot{E}_7 - \dot{E}_8 \quad (20)$$

Energy Efficiency of ORC,

$$\eta_{en} = \frac{W_t - W_p}{Q_{in}} \quad (21)$$

Exergetic Efficiency of ORC,

$$\eta_{exerg} = \frac{W_{net}}{\dot{E}_{in}} \quad (22)$$

### 3. RESULTS AND DISCUSSION

The mathematical model is solved to evaluate the exergy efficiency of the combined system. The heat transfer fluid supplied 2359 kW of heat to the ORC which generates a gross power of 222 kW at turbine shaft. The pump work is negligibly small (11 kW) as compared to turbine output. The net first law efficiency of the ORC system is 9 % at a fixed pinch point temperature of 6.8°C using R-245fa as a working fluid. The total exergy input to ORC system is calculated as 545.2 kW. The maximum irreversibilities are found in the evaporator (137kW) which is approximately 25% of the total exergy input followed by condenser, turbine, and pump. The total exergy loss is higher in condenser as compared to turbine where irreversibilities are more. It means that a huge work potential is lost in the condenser cooling water.

The effect of waste heat source temperature on the energy and exergy efficiency is given in Fig. 3. The energy efficiency decreases from 44 % to 23 % at the heat source temperature of 135 °C and 165 °C, respectively. Also, the exergy efficiency also decreases with the rise in heat source temperature. The maximum exergetic efficiency of 85% is obtained at 135°C. The higher temperature of the heat source reflects the large destruction of exergy. The effect of evaporator pressure on energy and exergy efficiency is shown in Fig. 4.

The energy and exergy efficiency of the ORC rises with an increase in evaporator pressure. The increased pressure at the evaporator inlet produces more turbine work and hence gives the higher potential for the available work. The exergy efficiency rises from 36% to 49% when the evaporator pressure increases from 750 kPa to 1200 kPa.

**Table 2.** Thermal performance data based on Energy and Exergy analysis

Component	Process	Irreversibility (kW)	Exergy Efficiency	Heat transfer /Work (kW)	Exergy Losses <sup>a</sup>
Turbine	Isentropic(ideally)	4.5	80.67 %	222.4	1.8 %
Condenser	Isobaric	107.4	23.7%	2219	42.97 %
Evaporator	Isobaric	137	74.9%	2359	55 %
Pump	Isentropic(ideally)	0.26	72%	11	0.1 %
Total (Cycle)	-	249	<b>Energy Efficiency----- 9.1%</b>		
			<b>Exergy Efficiency -----38.7%</b>		

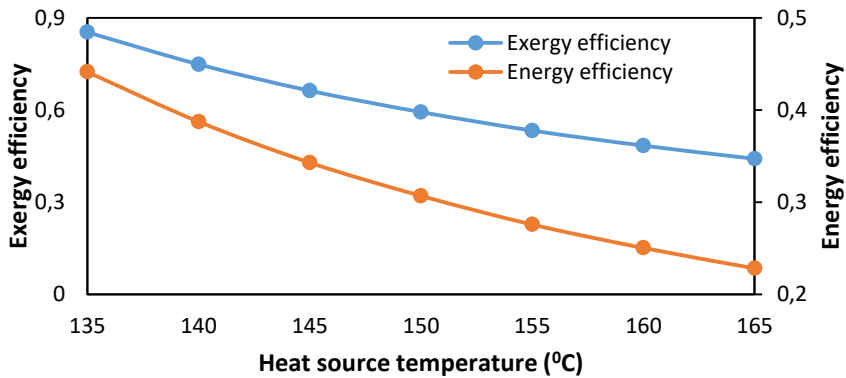


**Fig. 3.** Effect of heat source temperature on thermal efficiency

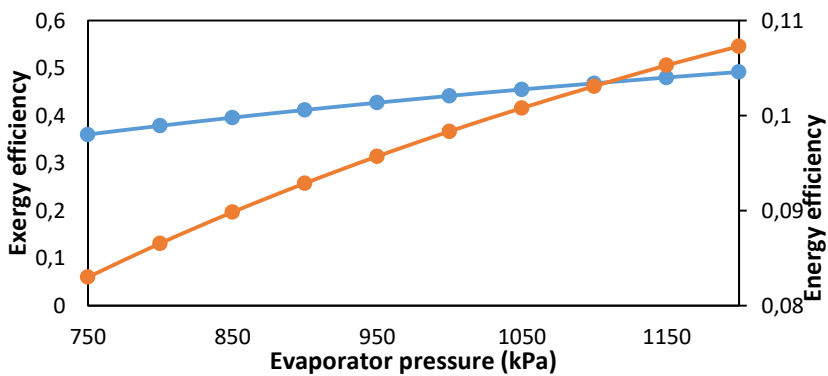


**Fig. 4.** Effect of boiler pressure on energy and exergy efficiency

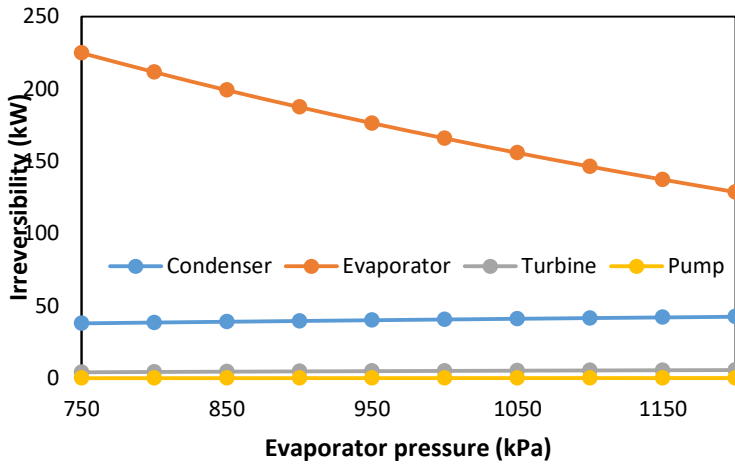


**Fig. 5.** Effect of evaporator pressure on irreversibilities of individual components

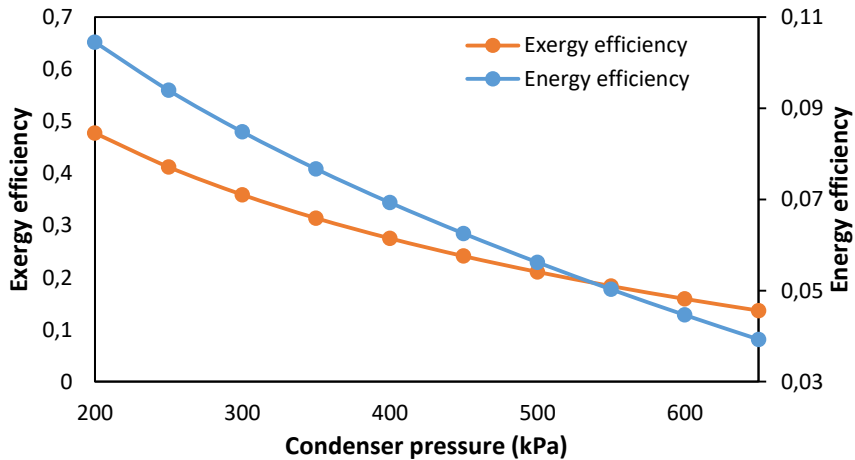


**Fig. 6.** Influence of condenser pressure on energy and exergy efficiency

The irreversibilities in the individual components with the rise in evaporator pressure are shown in Fig. 5. The exergy loss decreases with the rise in evaporator pressure due to increased turbine work. The irreversibilities in other components like turbine, pump and condenser are unaffected with the change in evaporator pressure. The maximum exergy destruction of 225 kW is observed at an evaporator pressure of 750 kPa. The influence of condenser pressure on the energy and exergy efficiency is shown in Fig. 6. Both the energy and exergy efficiency decreases with the rise in condenser pressure. The rise in condenser pressure reduces the new work obtained at the turbine shaft, which is responsible for the reduction in efficiencies. The exergy efficiency reduces from 47.7 % to 13.6% when the condenser pressure increases from 200 kPa to 700 kPa.

## 4. CONCLUSION

The thermodynamic model is built based on the entropy generation for low temperature waste heat recovery system integrated with agricultural engines. The following conclusions have been drawn from the work.

- The net energy and exergy efficiency of the system is 9% & 39%, respectively.
- Energy and exergy efficiency falls with the rise in heat source temperature.
- The rise in evaporator pressure increases the net work output which further enhances the thermodynamic efficiency of the ORC.
- The irreversibilities increase in the evaporator with the rise in pressure.
- The rise in condenser pressure adversely affects the system efficiencies.

The presented results provide a detailed insight into enhancing the exergy efficiency of low-temperature ORC integrated with agricultural, heavy-duty diesel engines.

## NOMENCLATURE

$e$	: Specific exergy flow
$E$	: Exergy rate (kW)
$E_{in}$	: Exergy input (kW)
$I$	: Irreversibility (kW)
$T$	: Temperature (C)
$T_{pp}$	: Pinch point temperature (C)
$W_p$	: Pump work (kW)
$W_t$	: Turbine work (kW)
$\eta$	: Efficiency

## REFERENCES

1. A. Kalinichenko, V. Havrysh, V. Hruban, Heat recovery systems for agricultural vehicles: Utilization ways and their efficiency, Agric. 8 , 2018. doi:10.3390/agriculture8120199
2. Lion, S.; Michos, C.N.; Vlaskos, I.; Taccani, R. A thermodynamic feasibility study of an Organic Rankine Cycle (ORC) for heavy-duty diesel engine waste heat recovery in off-highway applications. Int. J. Energy Environ. Eng. 8, 2017, 81–98
3. Jaber, H.; Khaled, M.; Lemenand, T.; Ramadan, M. Short review on heat recovery from exhaust gas. AIP Conf. Proc. 2016, 1758, 030045
4. A. Uusitalo, J. Honkatukia, T. Turunen-saaresti, Thermodynamic evaluation on the effect of working fluid type and fluids critical

- properties on design and performance of Organic Rankine Cycles, 188 , 2018. doi:10.1016/j.jclepro.2018.03.228.
5. J. Sarkar, Review and future trends of supercritical CO<sub>2</sub> Rankine cycle for low-grade heat conversion, *Renew. Sustain. Energy Rev.* 48, 2015, 434–451. doi:10.1016/j.rser.2015.04.039.
  6. S. Seyedkavoosi, S. Javan, K. Kota, Exergy-based optimization of an organic Rankine cycle (ORC) for waste heat recovery from an internal combustion engine (ICE), *Appl. Therm. Eng.* 126, 2017, 447–457. doi:10.1016/j.applthermaleng.2017.07.124.
  7. X. Yu, Z. Li, Y. Lu, R. Huang, A.P. Roskilly, Investigation of organic Rankine cycle integrated with double latent thermal energy storage for engine waste heat recovery, *Energy.* 170, 2019, 1098–1112. doi:10.1016/j.energy.2018.12.196.
  8. A. Kumar, S.K. Shukla, Analysis and performance of ORC based solar thermal power plant using benzene as a working fluid, 23, 2016, 454–463. doi:10.1016/j.protcy.2016.03.050.
  9. L. Li, Y.T. Ge, X. Luo, S.A. Tassou, Thermodynamic analysis and comparison between CO<sub>2</sub> transcritical power cycles and R245fa organic Rankine cycles for low grade heat to power energy conversion, *Applied Thermal Engineering* 106, 2016, 1290 – 1299. doi:10.1016/j.applthermaleng.2016.06.132.
  10. Ö. Kas, Energy and exergy analysis of an organic Rankine for power generation from waste heat recovery in steel industry, 77, 2014, 108–117. doi:10.1016/j.enconman.2013.09.026.
  11. M. Jankowski, A. Borsukiewicz, K. Szopik-Depczyńska, G. Ioppolo, Determination of an optimal pinch point temperature difference interval in ORC power plant using multi-objective approach, *J. Clean. Prod.* 217, 2019, 798–807. doi:10.1016/j.jclepro.2019.01.250.

### Cite this article

Rupinder Pal Singh and R S Gill, Entropy Generation Analysis of A Low-Temperature Waste Heat Power Generation System Integrated with the Agricultural Machinery, In: Sandip A. Kale editor, *Efficient Engineering Systems: Volume 1*, Pune: Grinrey Publications, 2021, pp. 29-38

# Modelling the Geometry of Wetted Zone in Soil Based Growing Media Under Drip Irrigation

E. Sujitha<sup>a,\*</sup>, G. Thiyagarajan<sup>b</sup>, A. Selvaperumal<sup>c</sup>,  
S. Thangamani<sup>c</sup> and K. Shanmugasundaram<sup>d</sup>

<sup>a</sup>Institute of Agriculture, Tamil Nadu Agricultural University, Kumulur, Trichy, India

<sup>b</sup>Water Technology Centre, Tamil Nadu Agricultural University, Coimbatore, India

<sup>c</sup>Department of Soil and Water Conservation, Agricultural Engineering College and Research Institute, Tamil Nadu Agricultural University, Coimbatore, India

<sup>d</sup>Department of Basic Engineering and Applied Sciences, Agricultural Engineering College and Research Institute, Tamil Nadu Agricultural University, Kumulur, Trichy, India

\*Corresponding author: sujitha047@gmail.com

## ABSTRACT

Water shortage is a serious issue that cripples agricultural production worldwide. One of the most important technologies for the arid and semi-arid regions is drip irrigation. In designing and maintaining the drip irrigation system, knowledge on the depths and widths of the wet soil zone plays a major role. There is a lack of models under soil-based growing media to predict wetting patterns, since the applicability of available models was limited to soil only. Therefore, the objective of this study was to construct a dimensional analysis model to estimate the depth and width of wetting patterns under various growing media. Therefore, a model was developed to determine the geometry of the wetted root area under different growing media using a semi-empirical model and dimension analysis method. The predicted values of wetted zones were compared with those obtained from field experiments performed on the same soil. The experiment included the determination of the maximum wetted zone depths and widths under various growing media. Based on RMSE, ME, and ModEF parameters, model performance was highly valued. It is therefore possible to use established models to predict wetting patterns under soil, soil + sawdust, and soil + coirpith with water source line application. Model developed in this study for different growing media was highly recommended based on ModEF. Therefore, estimated model can be best fitted to desire the emitter spacing in designing of drip irrigation system under soil, soil + sawdust and soil + coirpith. Thus, helps in efficient application irrigation and therefore it will increase in water use efficiency.

**Keywords:** Buckingham Pi Theorem, Drip irrigation, Dimensional analysis, Depth of wetting, Width of wetting

## 1. INTRODUCTION

The demand for water is steadily growing owing to population growth, industrial development and improved living standards. The per capita water allocation has decreased substantially due to population growth, and is perceived to be the limit of water poverty. Water shortages are thus the main issue and a significant limiting factor for implementing the potential economic growth plans of the country. Drip irrigation only helps to increase the efficiency of water use if the system is built to suit the conditions of the soil and plants. The information on the zones of wetting patterns under emitters is a prerequisite for designing and operating system of drip irrigation[1]. This will ensure that the water and fertiliser in the root zone of the crops are uniformly distributed. Among the various inherent problems with drip irrigation, deep percolation water losses and small horizontal wetted width are often considered a issue when applying drip irrigation. Alternative method has been shouted to conserve moisture, such as soilless media, soil based growing media and mulching etc[2]. Now-days artificial growing media getting popularized because of their easy handling, reduced weight, long-lasting moisture storage, easy exchange of media - once the soil born problem arises [11]. [7] A simplified semi-empirical approach has been developed to evaluate the geometry of wetted soil zones in line water sources where the geometry of wet soil (wetting width and depth at the end of irrigation) depends on the form of soil, the discharge of the emitter per unit of lateral length and the content of soil water in the soil. The saturated hydraulic conductivity was represented as the soil type [5]. Only as a function of applied water and basic soil properties such as saturated hydraulic conductivity under surface drip irrigation systems, this model predicts wetting front position [4]. The complexities inherent in computational and analytical approaches for the purpose of design are therefore reduced. For most field conditions, information on the distribution of matric potential or water content within the wet soil zone is not needed[9]. However, knowledge of the depths and widths of the wetted soil region should perform the purpose [3]. There seems to be a lack of model available for estimation of wetting patterns under different soil-based growing media, as the applicability of the above model was restricted to soil-based predictions only. Therefore, there is a necessity to develop a new model to predict wetting patterns under soil-based growing media with a water application line source[10]. The objective of the study was therefore to establish a model of dimensional analysis to predict wetted depth and width under various growing media.

## 2. METHODOLOGY

The investigation was performed on sandy loam soil using pit method and for artificial soil based growing media (soil + sawdust (2:1) and soil + coirpith (2:1)) using flexi glass container. Trench of depth x width x length in 1 x 1 x 1 meter were dug and 0.3 x 0.6 x 0.6 meter flexi glass were used. The flexi glass container had transparent front wall and was filled with the media (soil + sawdust (2:1) and soil + coirpith (2:1)) it was dried by air and passed through a 2 mm sieve. The packing of 5 cm layers of pre-weighed media has ensured standardized bulk density. A dripper test set up consisted a 16 mm OD lateral with a tap valve and end cap. Once the dripper test set up was connected to the water source (from bucket) the dripper discharge rate was measured prior to the start of experiment. To avoid error due to pressure head difference the constant water level was maintained throughout the experiment and it was checked through placing the measuring cylinder below the emitter. Thus, the rate of dripper discharge was regulated accurately by means of measuring cylinder and time before starting the experiment. Therefore, once the dripper discharge was assured to be constant, the lateral tube with dripper was placed on any one side of the pit and the container. Immediately after water flow started dripping on the soil surface, the timer was put ON. The position of wetting depth & width was measured at a fixed time interval until the end of experiment.

### 2.1. Model Development

To estimate the wet geometry of the soil, dimensional analysis is used. Dimensional analysis establishes the relationship between physical variables as one of the methods of establishing numerical models in physics, using the data given by the dimensions of physical variables according to the consistency of dimension theory[6]. More precisely, the  $\pi$ -theorem of Buckingham is used for dimension consistency analysis. The theorem states as “If there are  $n$  variables (dependent and independent ones) in a dimensionally homogeneous equation and if these variables contain  $m$  fundamental dimensions, then the variables are arranged into  $(n-m)$  dimensionless terms and these dimensionless terms are called  $\pi$  terms”. The wetting pattern dimensions depend on the total volume water ( $V$ ), the rate of discharge of the emitter ( $q$ ) and the saturated hydraulic conductivity of the soil ( $K_s$ ) [10]. The two functions can be written as follows: There were two different functional relationships of a wetted soil volume, one for wetted soil depth ( $D$ ) and the other for wetted soil width ( $W$ ).

$$W = f_1(V, q, K_s) \quad (1)$$

$$D = f_2(V, q, Ks) \quad (2)$$

Where  $f_1$  and  $f_2$  are function sign

Three-dimensional independent terms were formed using dimensional analysis that are expressed as the basic dimension of each variable and can be written as follows,

$$W = L, D = L, q = L^3T^{-1}, Ks = LT^{-1}, V = L^3$$

By rule no.1 the number of  $\pi$  terms (free variables) is equal to (n-m).

Whereas,

n = Total no. of variables in the experiment

m = Number of reference dimensions

Free variables = n-m = 5-2 = 3

$$F(\pi_1, \pi_2, \pi_3) = 0 \quad (3)$$

The repeating variables were chosen as q and KS, which include all fundamental dimensions, according to rule no. 3.

### First $\pi$ term

The dimensionless terms were developed by combining one of the free variables with all dependent variables, beginning with free variable W, by incorporating W with dependent variables, so that the first term can be developed by incorporating W with dependent variables as follows,

$$\pi_1 = Ks.q.W \quad (4)$$

Estimating  $a_1$  and  $b_1$  (Combination of  $a_1$  and  $b_1$  is dimensionless)

$$(LT^{-1})^{a_1} \cdot (L^3T^{-1})^{b_1} \cdot L = L^0T^0$$

So:  $a_1 + 3b_1 = -1$  (for L)

$-a_1 - b_1 = 0$  (for T)

Therefore,

$$a_1 = \frac{1}{2} \quad b_1 = -\left(\frac{1}{2}\right)$$

Hence the First  $\pi$  term is

$$\pi_1 = W \left( \frac{Ks}{q} \right)^{\frac{1}{2}} \quad (5)$$

### Second $\pi$ term

The second term can be written as follows by following the previous steps.

$$\pi_2 = Ks.q.D \quad (6)$$

Estimating  $a_1$  and  $b_1$  (Combination of  $a_1$  and  $b_1$  is dimensionless)

$$(LT^{-1})^{a_1} \cdot (L^3T^{-1})^{b_1} \cdot L = L^0T^0$$

So:  $a_1 + 3b_1 = -1$  (for L)

$-a_1 - b_1 = 0$  (for T)

Therefore,

$$a_1 = \frac{1}{2} \quad b_1 = -\left(\frac{1}{2}\right)$$

$$\pi_2 = D \left( \frac{Ks}{q} \right)^{\frac{1}{2}} \quad (7)$$

### Third $\pi$ term

Repeating the preceding steps, the third term can be obtained as follows

$$\pi_3 = Ks.q.V \quad (8)$$

Estimating  $a_1$  and  $b_1$  (Combination of  $a_1$  and  $b_1$  is dimensionless)

$$(LT^{-1})^{a_1} \cdot (L^3T^{-1})^{b_1} \cdot L^3 = L^0T^0$$

So:  $a_1 + 3b_1 = -3$  (for L)

$-a_1 - b_1 = 0$  (for T)

Therefore,

$$a_1 = \frac{3}{2} \quad b_1 = -\left(\frac{3}{2}\right)$$

Hence the third  $\pi$  term is

$$\pi_3 = V \left( \frac{Ks}{q} \right)^{\frac{3}{2}} \quad (9)$$

From eq. 5, 7 and 9 the dimensionless variables are formed as

$$W^* = W \left( \frac{Ks}{q} \right)^{\frac{1}{2}} \quad (10)$$

$$D^* = D \left( \frac{Ks}{q} \right)^{\frac{1}{2}} \quad (11)$$

$$V^* = V \left( \frac{Ks}{q} \right)^{\frac{3}{2}} \quad (12)$$

From graphical representation of the dimensionless variables following power relationship exist between dimensionless parameters.

$$W^* = A_1 (V^*)^{n_1} \quad (13)$$

$$D^* = A_2 (V^*)^{n_2} \quad (14)$$

Where, in above equations  $n_1$  and  $n_2$  are exponents,  $A_1$  and  $A_2$  are constants

Substitute the equation (10) and (12) in Eq. (13) for wetted width,

$$W \left( \frac{Ks}{q} \right)^{\frac{1}{2}} = A_1 \left( V \left( \frac{Ks}{q} \right)^{\frac{3}{2}} \right)^{n_1} \quad (15)$$

$$W = A_1 V^{n_1} \left( \frac{Ks}{q} \right)^{\frac{3n_1-1}{2}}$$

Substitute the equation (11) & (12) in Eq. (14) for wetted depth

$$D \left( \frac{Ks}{q} \right)^{\frac{1}{2}} = A_2 \left( V \left( \frac{Ks}{q} \right)^{\frac{3}{2}} \right)^{n_2} \quad (16)$$

$$D = A_2 V^{n_2} \left( \frac{Ks}{q} \right)^{\frac{3n_2-1}{2}}$$

To estimate the width and depth of the wetted pattern, Eq (15 & 16) can be used and will result in an appropriate range.

---

## 2.2. Performance of the Model

Model output was measured based on a comparison between the statistical parameters of the simulated data and the data observed. Mean error (ME), root mean square error (RMSE) and model efficiency (Mod EF) were the parameters used[5]. The statistical parameter ME is used for the estimation of the accuracy of simulated data in relation to observed data. The positive value of ME is indication of overestimated and the negative value is underestimated. The RMSE magnitude was representative of the model 's efficiency but does not indicate the degree of simulated values being over or underestimated. Another parameter to measure the efficiency of the model was the Mod EF [8].

$$ME = \frac{1}{N} \sum_{i=1}^N (C_{si} - C_{oi}) \quad (17)$$

$$RMSE = \left[ \frac{1}{N} \sum_{i=1}^N (C_{si} - C_{oi})^2 \right]^{1/2} \quad (18)$$

$$Mod_{EF} = 1 - \frac{\sum_{i=1}^N (C_s - C_o)^2}{\sum_{i=1}^N (C_o - C_{om})^2} \quad (19)$$

Where as

N = Total number of data,  $C_s = i^{th}$  Simulated values,  $C_o = i^{th}$  Observed values

$C_{om}$  = Observed mean

## 3. RESULT AND DISCUSSION

The constant discharge rates were applied in the dripper to know the performance of simulation model. The simulation steps for wetted zone (W) and (D) are mentioned in the following outlines for the given q, Ks and t, the W and D values have been observed. The simulation steps for wetted zone (W) and (D) are mentioned in the following outlines for the given q, Ks and t, the W and D values have been observed. During the time intervals (t), the volume of water (V) obtained was determined. Applying eq. 10, 11 and 12 the non-dimensional parameters, W \*, D \*, V \* were computed along with the observed data. The simulation steps for wetted zone (W) and (D) are mentioned in the following outlines for the given q, Ks and t, the W and D values have been observed. During the time intervals (t), the volume of water (V) obtained was determined. Applying eq. 10, 11 and 12 the non-dimensional parameters, W \*, D \* and V \*

were computed along with the observed data. A graphical relationship between dimensionless variables ( $W^*$ ,  $V^*$  and  $D^*$ ,  $V^*$ ) were developed for the growing media soil, soil + sawdust and soil +coirpith and are presented in Fig.1 (a, b, c, d, e and f). Moreover, verifiability of the model for all three growing media is also carried out by plotting observed and simulated values of wetted soil widths and depths for given volume of water and they were illustrated in Fig. 2 (a, b and C) respectively.

The power equations ( $W^*$  &  $D^*$ ) and simulation equation ( $W$  &  $D$ ) were attempted to relate with  $W^*$ ,  $V^*$  and  $D^*$ . The developed relationships were given below for all the three growing media.

### 3.1. For soil as growing media

$$W^* = 2.842(V^*)^{0.250} \quad (20)$$

$$D^* = 1.848(V^*)^{0.546} \quad (21)$$

$$W = 2.842V^{0.250} \left( \frac{Ks}{q} \right)^{-0.125} \quad (22)$$

$$D = 1.8482V^{0.546} \left( \frac{Ks}{q} \right)^{0.319} \quad (23)$$

### 3.2 For soil + sawdust as growing media

$$W^* = 8.459(V^*)^{0.520} \quad (24)$$

$$W = 8.459V^{0.520} \left( \frac{Ks}{q} \right)^{0.28} \quad (25)$$

$$D^* = 0.978(V^*)^{0.371} \quad (26)$$

$$D = 0.978V^{0.371} \left( \frac{Ks}{q} \right)^{0.056} \quad (27)$$

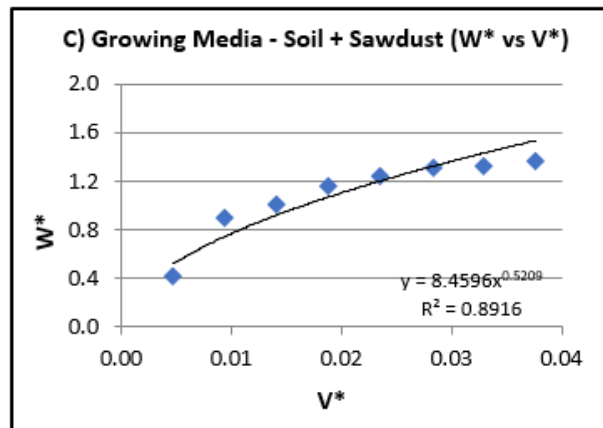
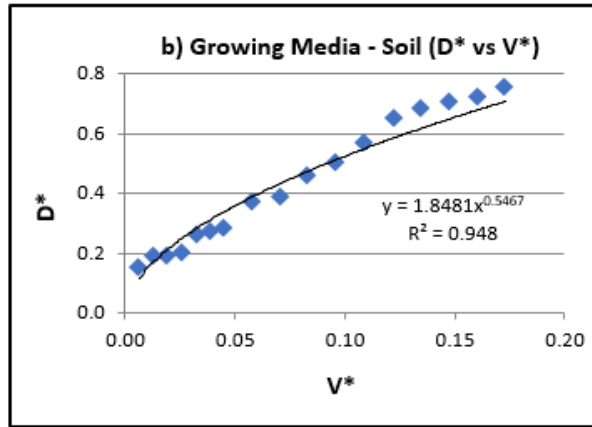
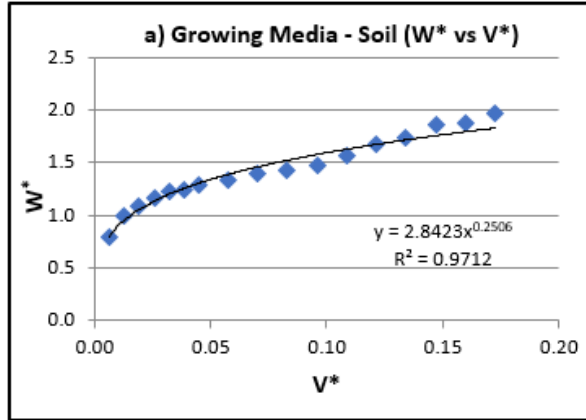
### 3.3 For soil + Coirpith as growing media

$$W^* = 7.398(V^*)^{0.550} \quad (28)$$

$$D^* = 0.905(V^*)^{0.389} \quad (29)$$

$$W = 7.398V^{0.550} \left( \frac{Ks}{q} \right)^{0.325} \quad (30)$$

$$D = 0.905V^{0.389} \left( \frac{Ks}{q} \right)^{0.084} \quad (31)$$



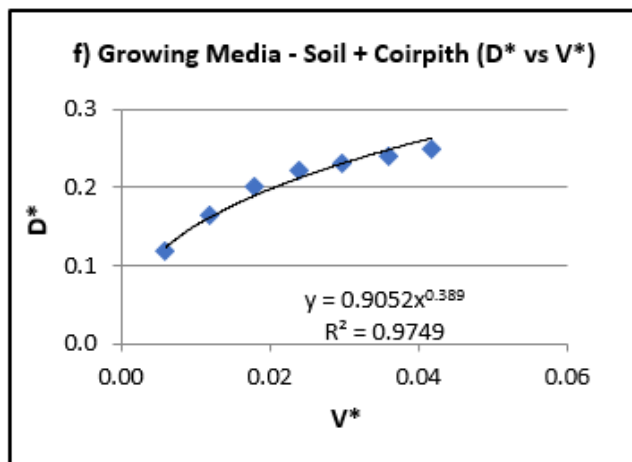
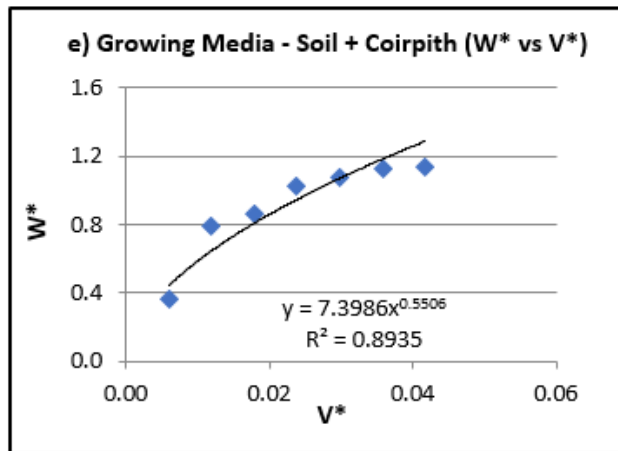
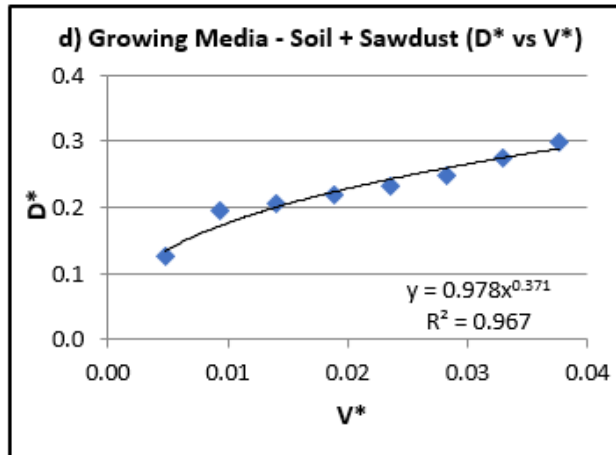


**Fig. 1.** (a, b, c, d, e and f) Relationship between dimensionless variables  $W^*$  vs  $V^*$  and  $D^*$  vs  $V^*$  for the growing media Soil, Soil + Sawdust and Soil + Coirpith

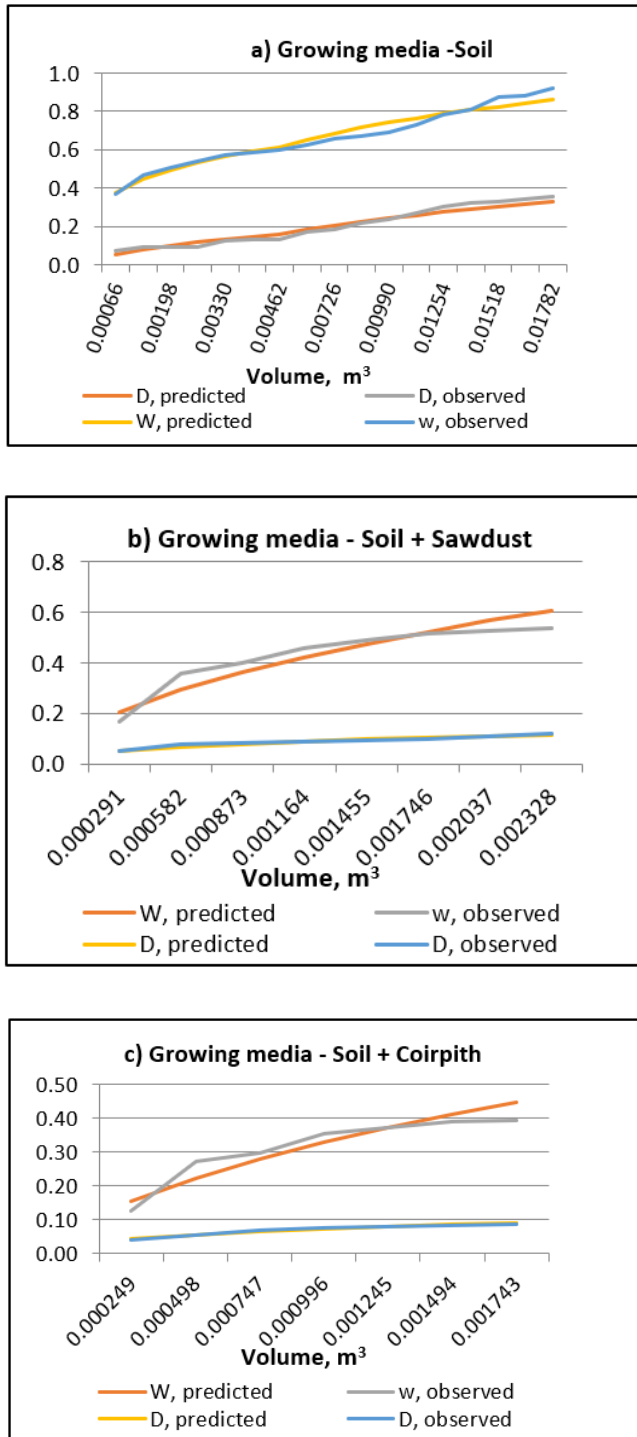


**Fig. 2.** a, b and c - Comparison between volume of water applied versus observed & simulated width and depth for the growing media Soil, Soil + Sawdust and Soil + Coirpith

**Table. 1:** Model performance of wetted zone of growing media

Growing media	ME (Width)	ME (Depth)	RMSE (Width)	RMSE (Depth)	Mod EF (Width)	Mod EF (Depth)
Soil	0.0002	-0.0027	0.0301	0.0192	0.9596	0.9610
Soil + Sawdust	0.0012	0.00003	0.0426	0.0043	0.8654	0.9515
Soil + Coirpith	0.0272	0.0022	0.0327	0.0028	0.8609	0.9662

### 3.4 Performance of model

For the derived model, statistical parameters such as mean error (ME), root mean square error (RMSE) and model efficiency (ModEF) were determined using the formula given in eq. 17, 18 and 19 respectively. The degree of RMSE values was reflective of model efficiency, but there was no degree of over-or under-estimation by the models of the estimated values. The statistical parameter, mean error (ME), was used to compare the precision quantification of calculated and observed soil wetting depth and width values. The positive value of ME is the overestimation indicator and the negative value is the underestimation indicator [12]. The absolute ME value is a measure of model efficiency. The model showed slight under estimation, as presented in Table 1. The performance of the models was found to be strong. The models can also be used to define the depth and width of the water for drip irrigation. [8] Results of the study reported that model predictability of wetted width and depth was estimated as 96.4 and 98.4%, respectively. However, the model efficiency was calculated as 87 percent and 95 percent for soil+sawdust, respectively. At the same time, the model efficiency was measured as 86 percent and 97 percent for soil+coirpith, respectively. This demonstrates that established models (eq. 22, 23, 26, 27, 30 and 31) can be used for the three-growing media with line source of water application to predict wetting pattern.

## 4. CONCLUSION

Experiment was conducted in three different type of growing media. The developed dimensional models were able to predict wetted zones under line source of water application. Model performance evaluated by RMSE and Mod EF. Values predicted were correlated with values observed. Model predictability was expressed for wetted depth and width prediction under soil in terms of model performance, which was calculated to be 96 percent and 96 percent respectively. The model performance, however, was estimated to be 87 percent

and 95 percent respectively for wetted depth and width prediction under soil + sawdust. The model efficiency of wetted depth and width prediction was estimated at 86 percent and 97 percent respectively under soil+coirpith. For efficient design, operation and management of the drip irrigation system, the results of the study would have been helpful.

## NOMENCLATURE

$OD$	:	Outer Diameter
$n$	:	Total number of variables in the experiment
$m$	:	Number of reference dimensions
$V$	:	Total volume water
$q$	:	Rate of discharge of the emitter
$t$	:	Time interval
$K_s$	:	Saturated hydraulic conductivity of the soil
$D$	:	Wetted soil depth
$W$	:	Wetted soil width
$L$	:	Length
$T$	:	Time
$W^*, D^*, V^*$	:	Non-dimensional parameters
$a, b, A, n$	:	Constants
$ME$	:	Mean error
$RMSE$	:	Root Mean Square Error
$Mod\ EF$	:	Model efficiency

## REFERENCES

1. Ainechee. G., Boroomand – Nisab Z., Behzad M., Simulation of soil wetting pattern under point source trickle irrigation. *Journal of applied Science*, 2009, 9 (6), 1170-1174. DOI: 10.3923/jas.2009.1170.1174
2. Aldhfees, B. T., Hegazi, M. M., Abdel-Aziz, A. A., Mathematical model for simulation of the water content from subsurface line source in sandy soil," *Misr. Journal of Agricultural Engineering (MJAE)*, 2007, 24(4), 886-902
3. Al-Ogaidi A.A.M., A. Wayayok, M.K., Rowshon, A.F., Abdullah, Wetting patterns estimation under drip irrigation systems using an enhanced empirical model, *Agric. Water Manage.*, 176 2016, 203–213. DOI: org/10.1016/j.agwat.2016.06.002
4. Liu Z.G., Li P.P., Hu Y.G., Wang J.Z., Modeling the wetting patterns in cultivation substrates under drip irrigation, *J. Coastal Res.*, 2015, 173–176. DOI: 10.5004/dwt.2018.22324

5. Paul, J.C., Mishra J.N., Pradhan P.L. and Panigrahi B., Effect of drip and surface irrigation on yield, water use-efficiency and economics of capsicum (*capsicum annum* l.) grown under mulch and non mulch conditions in eastern coastal India, *European. Journal of Sustainable Development*, 2013, 2(1), 99-108. DOI: 10.14207/ejsd.2013.v2n1p99
6. Samir Ismail, Tarek Zen EL-Abdeen, Abel Aziz, Omara Abdel-Tawab E., Modelling the Soil Wetting Pattern under Pulse and Continuous Drip Irrigation. *American-Eurasian J. Agric. & Environ. Sci.*, 2014, 14 (9), 913-922. DOI: 10.5829/idosi.aejas.2014.14.09.12404
7. Schwatlzman, M., Zur B., Emitter spacing and geometry of wetted soil volume, *Journal of Irrigation and Drainage Engineering*, 1986, 112(3), 242-253. doi.org/10.1061/(ASCE)0733-9437(1986)112:3(242)
8. Singh, D.K., Rajput T.B.S., Singh D.K., Sikarwar H.S., Sahoo R.N., and Ahmad T., Simulation of soil wetting pattern with subsurface drip irrigation from line source. *Agricultural water management*, 2006, 83(1-2), 130 – 134. <https://doi.org/10.1016/j.agwat.2005.11.002>
9. Younis Mohammad Hassan, Ahmed Shihab Ahmed, Sabah AnwerAlmasraf, Simulation of the wetting pattern under groove surface drip irrigation and gravel. *Diyala Journal of Engineering Sciences*, 2016, 9(4): 71-82. DOI: 10.24237/djes.2016.09407
10. Zhigang Liu, Pingping Li, Youguang Hu, Jizhang Wang, Modelling the Wetting Patterns in Cultivation Substrates under Drip Irrigation. *Journal of Coastal Research*, 2015, 73, 173-176. <https://dl.acm.org/doi/abs/10.5555/2781924.2782528>
11. Zhigang Liu, Qinchao Xu, Wetting patterns estimation in cultivation substrates under drip irrigation, *Desalination and Water Treatment*, 2018, 112, 319–324. DOI: 10.5004/dwt.2018.22324
12. ZohrehMosleh, Mohammad Hassan Salehi, AzamJafari, Isa EsfandiarpoorBorujeni, Abdolmohammad Mehnatkesh, The effectiveness of digital soil mapping to predict soil properties over low-relief areas, *Environ Monit Assess*, 2016, 188-195. doi: 10.1007/s10661-016-5204-8. DOI:10.1007/s10661-016-5204-8.

### Cite this article

E. Sujitha, G. Thiyagarajan, A. Selvaperumal, S. Thangamaniand K. Shanmugasundaram, Modelling the Geometry of Wetted Zone Insoil Based Growing Media Under Drip Irrigation, In: Sandip A. Kale editor, *Efficient Engineering Systems: Volume 1*, Pune: Grinrey Publications, 2021, pp. 39-52

# Feasibility of Waste Materials In High Strength Geopolymer Building Blocks

Shamon K. K.<sup>a,\*</sup> and Deepa G. Nair<sup>a</sup>

<sup>a</sup>Division of Civil Engineering, Cochin University of Science and Technology, Kochi, India

\*Corresponding author: kkshamon@gmail.com, deepagnair@cusat.ac.in

## ABSTRACT

Utilization of waste materials in geopolymerization enhances the sustainability of construction. This chapter investigates the feasibility of utilizing waste materials in the production of high strength geopolymer building blocks. Suitability of locally available brick waste as a source material for geopolymer binder and the feasibility of ground granulated blast furnace slag in improving the strength characteristics of geopolymer binder was investigated. After optimizing the influencing parameters of geopolymerization, suitability of the proposed geopolymer binder in high strength concrete building blocks was verified with respect to strength and durability characteristics. Results indicate promising outcomes with respect to strength and durability characteristics and suitability for load bearing construction with high strength requirements.

**Keywords:** Brick waste, geopolymerization, geopolymer concrete blocks, masonry unit

## 1. INTRODUCTION

Production of ordinary Portland cement (OPC) is highly resource intensive and results in the emission of large amounts of carbon dioxide and greenhouse gases. Geopolymers, an ideal alternative to OPC, can be produced by the chemical action of aluminosilicate materials rich in silica and alumina. On interacting with alkaline solution, it produces aluminosilicate gel with binding properties [1][2]. In the past years, many research works have been carried out to investigate the suitability of using waste materials as source materials to produce geopolymer cements [3][4].

Burnt clay bricks are extensively used in construction and its wastes are plenty available during the demolition of old structures and also as unburnt / over burnt wastes near the premises of brick industries. It can be used as a raw material for geopolymer binder. Brick waste contains high levels of silica and alumina which are the essential constituents for geopolymerization process. In brick based geopolymer, geopolymerization process continues in much faster rate with finer fractions of brick. [5][6].

Ground granulated blast-furnace slag (GGBS) is a good aluminosilicate source as it contains high amounts of alumina and silica which are necessary for the geopolymerisation reaction to take place. The geopolymeric binder produced by the alkali activation of GGBS requires reasonably lower alkali activator concentration than flyash and metakaoline based geopolymer [7]. The inclusion of GGBS in the waste fire clay bricks based geopolymer leads to improvement in the physico-mechanical properties of the geopolymer composite [8][9][10].

Since the production of geopolymeric building components consist of low cost raw materials and consumes less energy, development of which give better performance and environmental friendly materials for construction [11]. Geopolymer building blocks possess easy setting and fast drying, achieve considerable compressive strength gain at early ages which makes easy handling of the blocks and hence the geopolymer technology is feasible for use in construction [12][13]. This chapter investigates the suitability of brick waste and GGBS based geopolymer composite in high strength concrete building blocks.

## 2. METHODOLOGY

The concept of Hybrid Dynamic Simulation is that it injects the external signals into the simulation process and it allows interacting with the conventional simulation loops, which interact with the external signals. The Term "Hybrid" refers to sagacity of associating the Real Time Measurements with the Simulation Measurements.

The materials used for this study are brick waste, Ground granulated blast furnace slag (GGBS), sodium silicate solution and sodium hydroxide pellets, M sand (zone II) and coarse aggregate of size 12mm. Brick waste was collected from the dismantled waste of a building near Kothamangalam, Kerala. The brick waste was crushed and powdered manually and sieved through 90 $\mu$ m IS sieve. GGBS used in this study was locally purchased. Table 1 shows the percentage by weight of Silica, Alumina and Calcium in brick powder and GGBS. The properties of the constituent materials used in the study are given in Table 2.

**Table 1.** % by weight of Silica, Alumina and Calcium

Compound	% by weight	
	Brick powder	GGBS
SiO <sub>2</sub>	50.7	13.68
Ca	24.6	23.96
Al <sub>2</sub> O <sub>3</sub>	15	9.63

**Table 2.** Properties of the constituent materials

Material	Property	Value
M sand	Specific Gravity	2.6
	Fineness Modulus	4.05
Coarse aggregate (12mm)	Specific Gravity	2.85
	Fineness Modulus	7.17
Sodium Hydroxide Pellet	Purity	97%
	Grade	Extra pure
Sodium Silicate	Density	1.39g/cm <sup>3</sup>
	pH	11.2

### 2.1. Optimization of influencing parameters for geopolymer binder

The optimization of the influencing parameters i.e. concentration of NaOH, percentage of GGBS, A/B ratio and SS/SH ratio were done by analyzing the compressive strength of geopolymer binder at different ages of curing under ambient and elevated temperature (60<sup>0</sup>C for 24 hours). For this geopolymer mortar cube specimens of size 50mm x 50mm x 50mm were prepared. The specimens were prepared by mixing all the materials in the laboratory at room temperature. As a preliminary study, to optimize the molarity, specimens were cast with brick powder alone by varying the molarity from 8 to 14. In the next step geopolymer mortar cube specimen were prepared by replacing brick powder (BP) with various percentages of GGBS (0%, 20%, 40%, 60%, and 80%). The optimum molarity of NaOH for the geopolymer composite with BP and GGBS was then confirmed. Further, optimization of A/B ratio was done by

investigating the results varying from 0.3 to 0.9. Finally the SS/SH ratio was optimized by conducting experiment with different ratios varying from 1 to 2.5.

## 2.2. Application of geopolymer composite in building blocks

Cement concrete blocks (CCB) and geopolymer concrete blocks (GCB) of size 300mmx200mmx150mm were cast with mix proportion 1:3:6 using a hydraulic block making machine. The mix proportion for producing one building block is shown in Table 3. Figure 1 shows the geopolymer concrete blocks.



**Fig. 1.** Geopolymer concrete blocks

## 2.3. Tests on geopolymer building blocks

The building blocks were tested for strength and durability characteristics in accordance with IS: 2185 (Part I) – 2005 and ASTM C 67 to confirm the suitability as a building material [14],[15].

### 2.3.1 Strength Characteristics

The block density and compressive strength properties of the building blocks were tested (IS: 2185 (Part I) – 2005) and tabulated in Table 4. For block density average of three blocks were considered and for compressive strength, eight blocks were tested and took the average.

**Table 3.** Mix proportion of concrete building blocks

Material	Cement	BP	GGBS	CA	FA	SS	SH	Water
Cement Concrete Building	2.18	0	0	13.08	6.54	0	0	1.09
Geopolymer concrete blocks	0	0.85	1.28	12.78	6.39	0.77	0.17	0.35

**Table 4.** Mechanical properties of Building Blocks

Type of Block	Block Density (Average of 3 blocks in kg/m <sup>3</sup> )	Avg. compressive strength (Average of 8 blocks in N/mm <sup>2</sup> )	
		7 <sup>th</sup> day	28 <sup>th</sup> day
Cement concrete block	2425.5	6.74	9.3
Geopolymer concrete block	2366.11	10.83	15.16

### 2.3.2 Durability Characteristics

Durability characteristics were verified by water absorption test (IS: 2185 (Part I) – 2005) and initial rate of absorption (IRA) test (ASTM C 67). Initial rate of absorption (IRA) is considered as the amount of water absorbed in 1 minute through the bed face of the block. Average test results of three samples were taken for both the tests and the results obtained are tabulated in Table 5.

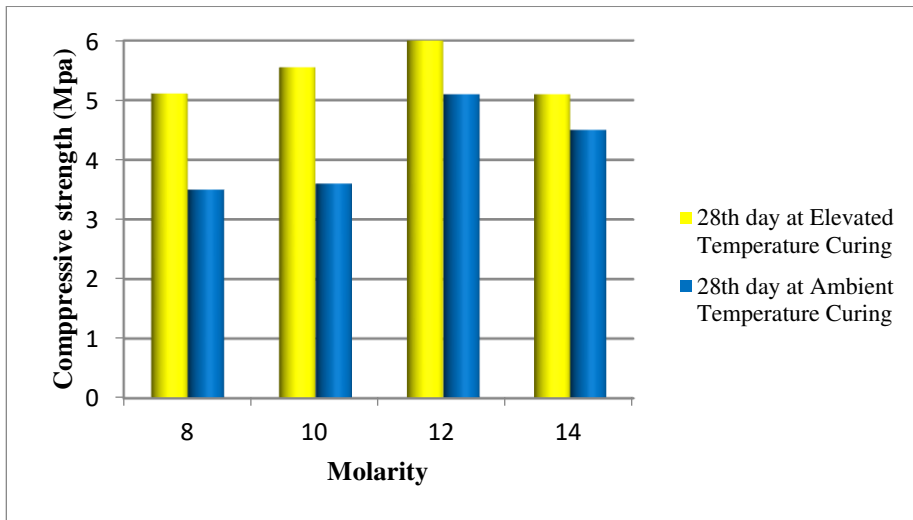
**Table 5.** Durability properties of Building Blocks

Type of Block	% water absorption (Average of 3 blocks)	Initial rate of absorption (Average of 3 blocks in kg/m <sup>2</sup> /min)
Cement concrete block	4.4	1.19
Geopolymer concrete block	3.22	1.02

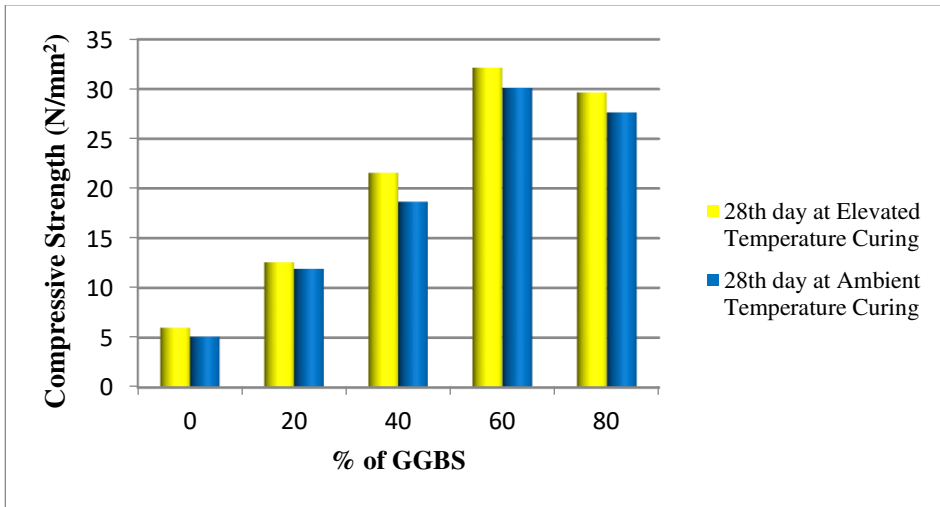
## 3. RESULTS AND DISCUSSIONS

### 3.1. Optimization of influencing parameters

The variation in compressive strength of brick powder based geopolymer specimens for various molarities (8 to 14) cured under both elevated and ambient curing conditions are shown in Figure 2. The compressive strength increases with increase in molarity of NaOH up to 12M and then decreases with further increase in molarity. The maximum compressive strength obtained are 6MPa and 5.1 MPa respectively for elevated and ambient temperature curing. This shows that the compressive strength values obtained are very less.



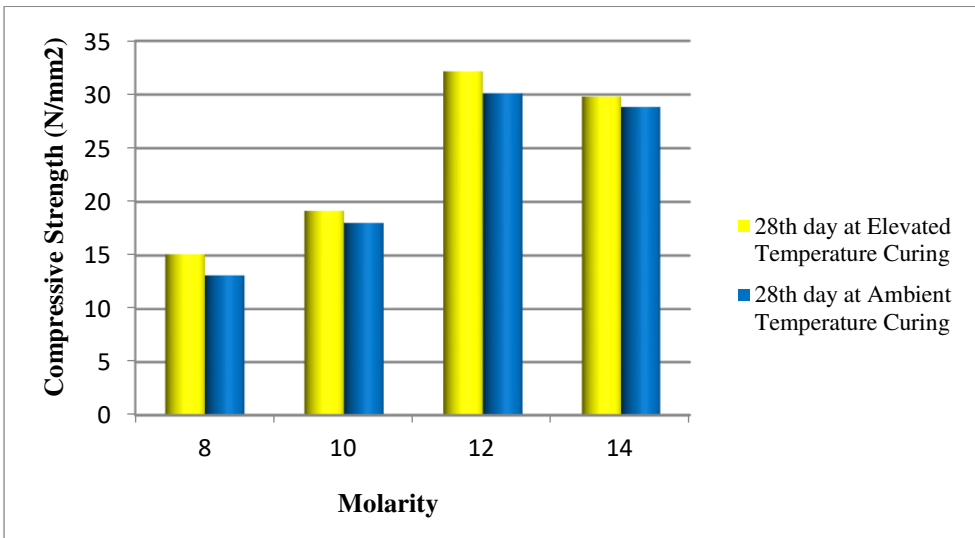
**Fig. 2.** Influence of molarity on geopolymer binder with brick powder alone



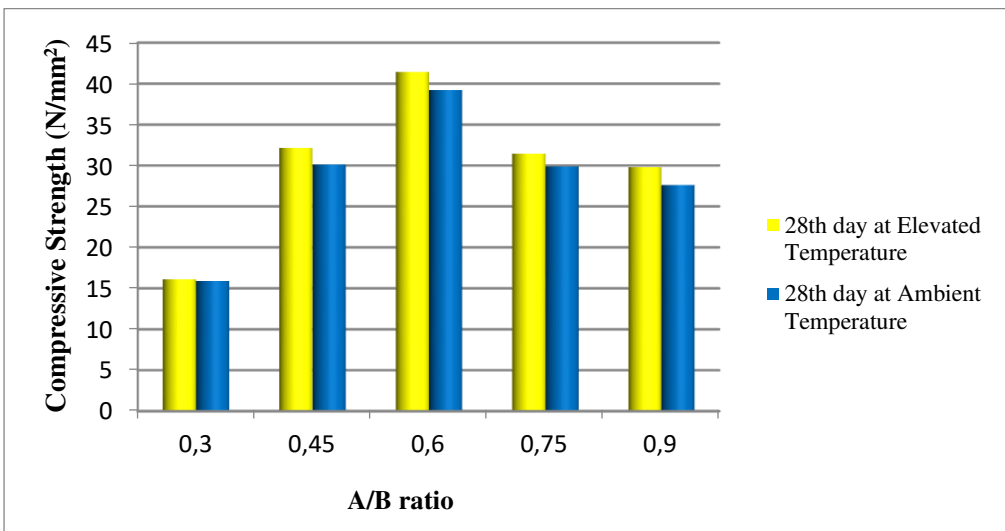
**Fig. 3.** Influence of GGBS percentage

Figure 3 shows the variations in compressive strength of specimens (with optimized molarity) observed on replacing BP with GGBS. Significant increase in compressive strength was observed with a maximum strength at 60% replacement for both ambient curing and elevated curing. These results are in concurrence with the studies conducted by Zawrah et.al [8].

For reconfirming the optimum molarity, tests were again conducted on specimens (BP -40% & GGBS – 60%) with varying molarities from 8 to 14. Results (Figure 4) shows the variations in compressive strength under the ambient curing and elevated curing confirming the molarity (12M). The highest compressive strengths (32.15MPa and 30.12MPa) were obtained at molarity 12 and the values were found decreasing after that.



**Fig. 4.** Confirmation of optimum molarity of geopolymer binder with BP and GGBS



**Fig. 5.** Influence of alkali activator to binder ratio

The influence of activator to binder (A/B) ratio was evaluated by testing samples with varying A/B ratios (0.30, 0.45, 0.60, 0.75 and 0.90). Figure 5 shows the variations. The highest values (41.42MPa and 39.2MPa) were observed with the A/B ratio 0.6 for both the curing conditions.

The influence of sodium silicate to sodium hydroxide (SS/SH) ratio was evaluated with the optimized values of molarity and A/ B ratio by varying SS/SH ratios ( 1, 1.5, 2, and 2.5 ). Compressive strength was (Figure 6) found increasing up to SS/SH ratio of 1.5 and then decreasing in both the curing conditions.

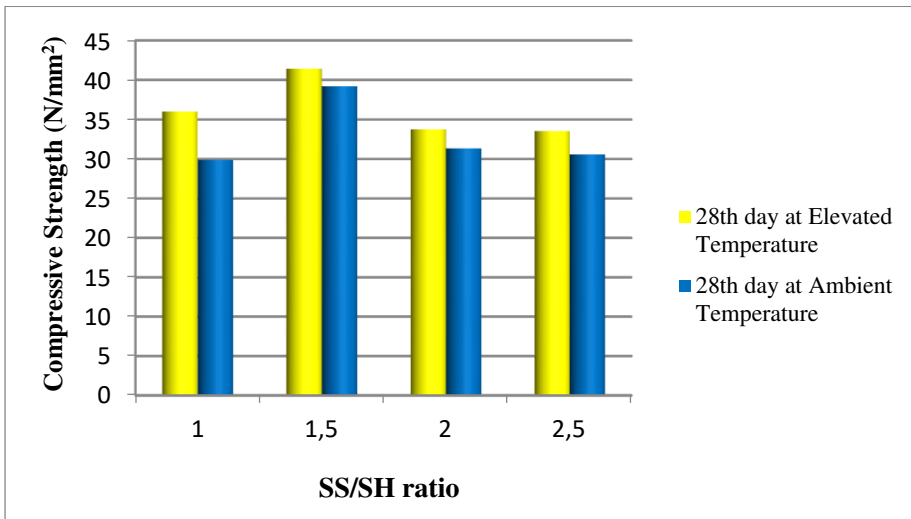


**Fig. 6.** Influence sodium silicate to sodium hydroxide ratio

Even though, higher strength values were obtained for specimens cured at elevated temperature (60<sup>0</sup>C for 24 hours) than that under ambient curing condition, ambient cured samples can be suggested for practical applications as the results are comparable. 28th day strength of the geopolymer composite with ambient curing was even better (39.2MPa) than that of OPC 33 grade cement.

### 3.2. Application of geopolymer composite in building blocks

#### 3.2.1. Strength and Durability

Figure 7 shows the comparison of compressive strength results for cement concentrate blocks and geopolymer blocks. Higher compressive strength of the proposed geopolymer blocks (15.16MPa) indicate its suitability for load bearing masonry with high strength requirements over cement concrete blocks (9.3 MPa). Early strength of proposed geopolymer blocks (7th day compressive strength - 10.83MPa) can be considered as a positive feature in practical applications

Block density of geopolymer blocks (2366.11 kg/m<sup>3</sup>) and cement concrete blocks (2425.5 kg/m<sup>3</sup>) were found satisfying the IS code requirements. Comparing the block densities, geopolymer blocks were lighter than the corresponding cement concrete block.

The durability properties of geopolymer blocks and cement concrete blocks with respect to water absorption and initial rate of absorption were found satisfying the standards and verifying the better performance of proposed geopolymer blocks.

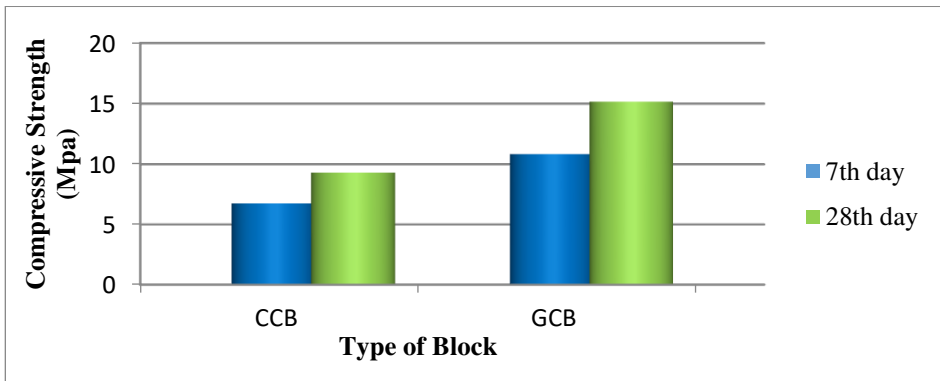


**Fig. 7.** Compressive Strength of Building Blocks

#### 4. CONCLUSION

This research has confirmed the potential of using a combination of brick waste and GGBS (40 :60) in high strength geopolymer building blocks. The optimized condition for this combination was arrived as, molarity of NaOH - 12M, alkali activator to binder ratio - 0.60, sodium silicate to sodium hydroxide solution ratio - 1.5, curing condition- ambient temperature. The proposed geopolymer blocks exhibited superior strength and durability over cement concrete blocks and proved its suitability for load bearing masonry with high strength requirements. Utilization of waste brick powder and GGBS as source materials in geopolymer building blocks also established the environmental sustainability of the proposed blocks. Comparatively lower block density, better dimensional qualities and surface finishes over cement concrete blocks add to its sustainability characteristics.

#### REFERENCES

1. Zivica A.V, Martin T.P and Martin K., Geopolymer cement and their properties: a review. *Building Research Journal*, 2014, 61(2), 85-100.
2. Davidovits, J., Geopolymer Cement: a review. *Geopolymer Science and Technics*, 2013, 21, 1-13.
3. Allaverdi, A and NajafiKani, E, Construction waste as raw materials for geopolymer binders. *International Journal of Civil Engineering*, 2009, 7(3), 154-160.
4. Ouda, A.S and Gharieb, M, Development of the properties of brick geopolymer pastes using concrete waste incorporating dolomite aggregate. *Journal of Building Engineering*, 2020, 27, 1-13.
5. Komnitsas, K, Zaharaki, D, Vlachou, A, Bartzas, G and Galetakis, M, Effect of synthesis parameters on the quality of construction and demolition wastes (CDW) geopolymers. *Advanced Powder Technology*,

- 2014, 26(2), 368–376.
6. Reig L, Tashima M. M., Borrachero M.V., Monzo J, Cheeseman C.R., and J. Paya, Properties and microstructure of alkali activated red clay brick waste. *Construction and Building Materials*, 2013, 43, 98-106.
  7. Rakhimova, N and Rakhimova, R, Alkali-activated cements and mortars based on blast furnace slag and red clay brick waste. *Materials and Design*, 2015, 85, 324–331.
  8. Zawrah, M.F, Gado, R.A, Feltin, N., Ducourtieux, S. and Devollie, L., Recycling and utilization assessment of waste fired clay bricks (Grog) with granulated blast-furnace slag for geopolymer production. *Process Safety and Environmental Protection*, 2016, 1(6),237–251.
  9. Adanagouda and Murthy, B, Strength and durability properties of geopolymer concrete made with GGBS. *International Journal of Creative Research Thoughts*, 2017, 5(4), 2540-2548.
  10. Kumar, S, Gautam, P.D and Kumar, B.S.C, Effect of Alkali Activator Ratio on Mechanical Properties of GGBS based Geopolymer Concrete. *International Journal of Innovative Technology and Exploring Engineering*, 2019, 8(12), 947-952.
  11. Petrillo, Antonella, Cioffi, Raffaele, Claudio Ferone, Francesco Colangelo and Claudia Borrellia, Eco-sustainable Geopolymerconcrete blocks production process. *Agriculture and Agricultural Science Procedia*, 2016, 8, 408-418.
  12. Venugopal, K., Radhakrishna, Vinod, M. and Sasalatti, Development of alkali activated solid and hollow geopolymer masonry blocks. *IOP Conference Series: Material Science and Engineering*, 2016, 149, 1-12
  13. Khater, H.M., Abdeen, M.E.N. and Ezzat, M, Optimization of alkali activated grog/ceramic wastes geopolymer bricks. *International Journal of Innovative Research in Science, Engineering and Technology*, 2016, 5(1), 37-46.
  14. IS 2185-1 (2005): Concrete masonry units, Part 1: Hollow and solid concrete blocks.
  15. ASTM. (2013a), “Standard test methods for sampling and testing brick and structural clay tile”, ASTM C67-13, ASTM International, USA.

---

### Cite this article

Shamon K K and Deepa G Nair, Feasibility of Waste Materials In High Strength Geopolymer Building Blocks, In: Sandip A. Kale editor, Efficient Engineering Systems: Volume 1, Pune: Grinrey Publications, 2021, pp. 53-62

---

# Pyrolysis of Tyre Waste: A Sustainable Waste Management Approach

A. Sudharshan Reddy <sup>a,\*</sup> and Abhilash T. Nair <sup>a</sup>

<sup>a</sup>Department of Applied Sciences and Humanities,  
National Institute of Foundry and Forge Technology, Ranchi,  
Jharkhand, India

\*Corresponding author: : nairabhisht@gmail.com

## ABSTRACT

Tyre waste is produced in large amounts and demands proper management as its disposal is associated with concern for the environment and public health. Proper management of tyre waste can result in material recovery, energy recovery and other value added products. This chapter discusses about the problems associated with waste tyre disposal, waste tyre pyrolysis products and application of pyrolysis products in circular economy. Pyrolysis of the tyre can be considered one of the most suitable due to the possibility of maximum benefits regarding economy circulation, environment, and sustainability. Through waste tyre pyrolysis, we can produce quality products such as oil, char, steel, and gas that have high commercial demand in industrial applications and have societal impact. With this, it is possible to circulate economy and there are almost negligible waste products by ultimately ending the life of tyre with a positive impact on the environment and society. Therefore, the end life of waste tyre through pyrolysis resulting in sustainable waste tyre management with minimum environmental impacts and maximum economic benefits.

**Keywords:** Waste tyre, pyrolysis, value-added products

## 1. INTRODUCTION

Dumping of the waste tyre has been a serious concern globally due to its aesthetic, environmental and health issues. Almost 1.6 billion new tyres per year are produced, and at the same time, 1.5 billion scrap tyres per year are generated [1]. Because of non-biodegradability, the scrap tyre can persist in the environment for many years and can potentially impact the environment and human health. Accidental fire hazards, toxicants leaching, vector breeding and associated epidemics and wastage of land, are the common problems associated with waste tyre disposal. Therefore, for environment and human health safety, disposal of scrap tyre should be replaced with other alternative routes to mitigate these issues. Different methods have been adopted to manage the scrap tyre, including reducing or reuse, recycling (civil engineering applications and thermochemical treatments (combustion, gasification and pyrolysis)) and landfilling.

According to waste tyre management global statistics- 2011, 77% of the waste goes to dump sites illegally, 7% for recycling and 11% treated for fuel production. But the above statistics are drastically changing due to rigid environmental policies and standards and also innovations in the technologies even though all these methods (reduce, reuse and recycling) have some economic and non-economic barriers. Majority (25-60%) of the waste tyre is utilised for energy recovery, 5-23% is reused, 3-15% is recycled and 20-30% goes to landfills [2]. Recycling is the most recommended feasible way of waste tyre management, which mainly include recovery of materials (for civil engineering applications), energy (by thermochemical treatments) and value-added products (through pyrolysis) in a sustainable way. In this economy-oriented world, among these options again, the most appropriate route for obtaining the maximum benefits concerning circular economy, environment and sustainability from the waste tyre is the recovery of the value-added products. These products have high commercial demand in various industrial and societal applications. This main objective of this chapter is to discuss about problems associated with waste tyre disposal, application of pyrolysis process for management of tyre waste and the uses of waste tyre pyrolytic products.

## 2. SCHARACTERISATION OF WASTE TYRE

Before using any process for managing scrap tyre, it is crucial to understand the composition and characteristics of the tyre. The material composition of tyre mainly contain natural rubber (NR), synthetic rubber (SR) (BR: butadiene rubber and SBR: styrene-butadiene rubber), carbon black, additives like sulphur

and zinc oxide, steel, textiles and fillers. This composition varies depending upon the type of tyre and ranges in between 14-48% of NR, 10-27% of SR, 11-28% of carbon black, 14-25% of steel, and 12-17% of fabric, fillers and accelerators [3]. Various materials are added to the tyre to enhance its properties. For example use of natural rubber improves the cracking resistance, synthetic rubber improves the rolling resistance, carbon black increases tire resistance against abrasion and improves the strength, steel improves wear performance and tire handling and sulphur and zinc oxide are used for rubber vulcanisation [4, 5]. According to elemental composition, the tyre contains carbon, hydrogen, nitrogen, sulphur, oxygen and other metals, and this composition also varies depending on the type of tyre [4, 5].

### **3. PROBLEMS ASSOCIATED WITH WASTE TYRE DISPOSAL**

Due to non-biodegradability, longer life span and chemical composition of the waste tyre, disposal is associated with various serious problems such as fire hazards, leaching, vector-borne diseases and large space requirements creating negative impacts on both environment as well as public health.

#### **3.1. Fire Hazards**

Many studies have revealed that tyre fires are the most dangerous than any other problems associated with tyre waste as the tyre fires can pollute the environment at every stage in tyre fire dynamics [6].

##### **3.1.1 Air pollution**

Tyre fires release more toxic air pollutants that include particulates, carbon monoxide (CO), sulfur oxides (SO<sub>x</sub>), oxides of nitrogen (NO<sub>x</sub>), and volatile organic compounds (VOCs); hazardous air pollutants (HAPs), such as polycyclic aromatic hydrocarbons (PAHs), dioxins, hydrogen chloride, benzene, polychlorinated biphenyls (PCBs); and metals such as arsenic, cadmium, nickel, zinc, mercury, chromium, and vanadium into the environment [7, 8]. The potential health impacts can be short term or long term and include cancer, asthma, lung and heart diseases, respiratory effects, and irritation to skin, eye, nose and throat [7, 6].

##### **3.1.2 Water pollution**

During tyre combustion, high internal temperature of around 2000<sup>o</sup>C can lead to oil runoff into surface water and other areas depending upon the location of the tyre fire [7]. Various combustion residues like zinc, cadmium and lead can also be carried into the water.

##### **3.1.3 Soil pollution**

Tyre fires can lead to soil pollution in two ways. The oil from the tyre fire may penetrate into the soil and the ash left after the tyre fire can enter into the soil through rainfall or any other means [9].

### **3.2. Leachate**

Another most prominent problem with tyre waste is the leaching of chemicals and heavy metals into the ground. The leachate from the scrap tyre contains both organic and inorganic compounds and contaminates the groundwater and the soil. The organic compounds from the tyre leachate include polycyclic aromatic hydrocarbons (PAH), nitrogen and sulphur containing organic compounds, aromatic compounds (ketones) and volatile organics (benzene, toluene, carbon disulphide and methyl ethyl ketone), whereas the inorganic compounds (like metals) include arsenic, barium, cadmium, calcium, chromium, iron, lead, manganese, selenium and zinc. These toxicants can get transported to other locations that can potentially harm the animals and human health when they contact these toxicants through various means [10]. The quality (contaminants) and quantity (concentration) of the tyre leachate in the soil and water (ground and surface) depends upon various factors, which include the type of tyre (based on size: scrap or whole tyre; based on composition: low vehicle, medium vehicle or heavy vehicle tyre), chemical conditions (acidic or basic: under acidic environment leaching of metals is quick whereas in alkaline environment leaching of organic compounds is faster), soil characteristics (like soil permeability), and horizontal distance from tyre storage site to the downstream direction and vertical distance to groundwater table [9].

### **3.3. Vector breeding**

The whole tyre can hold the rain water inside the tyre space and can retain the temperature for a longer period that provides a better environment for mosquitoes to breed [11]. In addition to this, the leaves filled in the tyre provide energy for mosquitoes. These mosquitoes can easily spread the diseases, such as malaria, Zika virus, West Nile virus, and Encephalitis [12].

### **3.4. Large space requirement**

For any waste to be disposed, compaction is a crucial factor to be considered due to land scarcity. Scrap tyre are difficult to compact and therefore its disposal demands larger space requirement. On the other hand, its size reduction for disposal is not cost-effective. Another concern about storing waste tyres in large quantity can cause injury to workers or even death.

#### 4. WASTE TYRE PYROLYSIS

The term pyrolysis defines the thermal degradation of carbonaceous waste material under certain operating conditions, mainly in the absence of oxygen by heating resulting in the conversion of waste material into liquid, solid and gaseous phases. Although, the pyrolysis process seems to be a straightforward phenomenon, but involves several complex, simultaneous on-going reactions. Initially, moisture present in the waste material is evaporate and then de-volatilisation takes place. The non-volatile fraction will be left as a solid residue. Further, the volatiles convert into lighter molecules depending upon the residence time. These volatiles further condense into liquid and the non-condensed volatiles leave the system as gases.

The product distribution in terms of quality and the quantity will mainly depend on temperature, residence time (RT) and reactor pressure. Also, feed material composition, size of feed material, heating rate (HR) and gas flow rate influence the product distribution. The variation of the optimum yield of tyre pyrolytic products with the various operating conditions are listed in Table 1. For example, in case of waste tyre pyrolysis, depending upon type of tyre products, distribution varies for the same operating conditions. Smaller particle size leads to faster heat transfer inside the material, resulting in more gas yield whereas for larger particles yield of char is more because of slower heat transfer. For higher heating rate accelerates the process and produce more volatile fraction than less heating rates. The higher temperature inside the reactor leads to a higher gaseous fraction, and less char than the lower temperature. If the pressure inside the reactor is vacuum condition, then the yield of liquid fraction is more and requires less pyrolysis temperature than the atmospheric pressure inside the reactor. If the residence time for volatiles inside the reactor is large, more gaseous products are produced due to further disintegration of volatiles into lighter molecules whereas less volatile residence time results in more liquid yield. Also, the flow rate of carrier gas influences the residence time for volatiles which in turn influence the yield distribution.

Different types of reactors and various technologies in pyrolysis process have shown significant variation in the distribution of the product. Fixed bed reactor, fluidised bed reactor, moving bed reactor, conical spouted bed reactor, rotary kiln reactor, and microwave reactor are the different reactors used in the waste tyre pyrolysis process. Thermal pyrolysis, catalytic pyrolysis, microwave pyrolysis and vacuum pyrolysis are the different type of pyrolysis technologies used for the waste tyre pyrolysis process. Each of these reactor types and technologies targeted to improve the process for optimum quality and quantity

of the products. All the three products (oil, char and gas) resulting from the waste tyre pyrolysis can be utilised for various applications as shown in Figure 1, which indicates that pyrolysis process is nearly zero waste products discharge. Based on the quality of the product the process can be commercialised, and multiple uses of these products are detailed below. Also, pyrolysis process can provide employment opportunities for plant operation and maintenance.

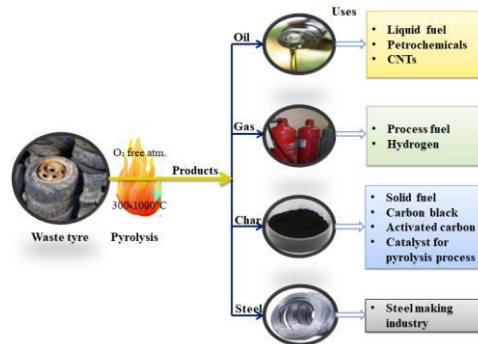


**Fig. 1.** Uses of products obtained from pyrolysis of waste tyre

#### 4.1. Tyre pyrolytic oil

The tyre derived pyrolytic oil contains both lighter and heavier fractions known as gasoline-like fuels and diesel-like fuels, respectively [22]. These have properties (density, viscosity, calorific value, carbon and hydrogen content) almost similar to standard commercial fuels such as diesel and petrol [13, 14]. Therefore it is suitable to blend this oil with conventional diesel [24] or may be used as alternative fuel [14]. But more than 50% blending is not recommended for direct use in a diesel engine as it releases more CO, HC, SO<sub>2</sub> and smoke emissions [25]. The presence of sulphur restricts the direct use as diesel fuel or oil for direct combustion in standard engines without changes in engine configuration, but this can be possible after its quality improvement [13, 15]. The use of suitable catalysts can reduce the sulphur and ash content in the oil fraction [17, 18]. Tyre pyrolytic oil is a complex mixture of compounds largely aromatics and aliphatic and small amounts of nitrogenated and benzothiazol [27]. The high aromatics content in pyrolytic oil makes it suitable for industrial purposes [20, 21]. Improvements in technology, mainly catalytic pyrolysis, can improve the oil quality by increasing the lighter hydrocarbons content due to catalytic activity [29]. Benzene, toluene, xylene, ethylbenzene and styrene which are mostly used in the production of petrochemicals and plastics and in chemical industries can also be extracted from high quality pyrolysis oil [23, 24]. Tyre pyrolytic oil can also be suitable for the production of quality Carbon Nano Tubes CNTs [32].

**Table 1.** Optimum yield production by varying operating conditions in tyre pyrolysis

Sr. No.	Sample	Feed size	Amount	Reactor type	HR (°C/Min)	RT	Temp. (°C)	Optimum yield (wt%)			Ref.	
								liquid	gas	solid		
1	Passenger car, truck, airplane & motor cycle tyre	5-20 mm	7.51 kg	Rotary kiln	20 & 60	10 min	450-600	43.0	21.5	35.5	[13]	
2	Bicycle tyre	1cm <sup>2</sup>	20 g/run	Semi batch	20	N/A	450-700	49.6	12.5	44.5	[14]	
3	Tyres from dump sites	2-10 mm	10g/batch	Fixed Bed	15	30 min.	375-750	34.4 ± 2	38.85	59.58 ± 7	[15]	
4	Motorcycle tyre	2-12 cm <sup>3</sup>	750 ± 2 g	Fixed bed	10-60	50 min	375-575	49 ± 1.3	N/A	41 ± 1.5	[16]	
5	Tyres from recycling plants	4 mm	5g/10 min	Pilot plant	N/A	N/A	450	37.8	N/A	35.2	[17]	
							750	10.87	N/A	37		
6	Used tyre	20×20 mm	300g	Batch reactor	12	gas: 1-1.5 min	1000	<0.01	N/A	37.7		
							400-700	30.0-	2.4-	64.0-	[18]	
7	Car & truck tyres	1-3 cm <sup>2</sup>	15g	Batch reactor	16.5, 9 & 7.5	N/A	450	42.6	11.1	46.3	[5]	
							570	50	9.3	40.7		
8	Passenger car tyres	1×1×1 & 6×5×1 cm <sup>3</sup>	1500g	Fixed bed	1.81	30 min	500	40.51	N/A	N/A	N/A	[19]
								53.49	N/A	N/A	N/A	
								50.86	N/A	N/A	N/A	
9	Waste tyre	1-4 mm	10g	Fixed bed	5.0- 35.0	1 hr	350-600	38.8	33.8	35.1	[20]	
10	Passenger car tyre	3cm×1.5cm	3Kg	Batch	5	90 min	450-600	58.2	8.9	38.3	[21]	

## 4.2. Tyre pyrolytic solid residue

The solid residue in the tyre pyrolysis products comprises steel and char. The recovered steel can be used by steel industries for metal recycling. Char has fixed carbon, ash, sulphur and other impurities. Because of high fixed carbon content this char can be used as a raw material for category-A briquettes production [33]. The char can also be used to manufacture various rubber items (footwear, conveyor belts, dock fenders etc.), which requires even low-quality carbon black [27]. Because of the reasonable amount of energy content, it is suitable to use as a solid fuel. It may also be used in the manufacturing of new tyre [34]. The produced char with the high surface area can be comparable with commercially available activated carbons. With further treatments, the char can be used as an activated carbon catalyst for wastewater treatment [28, 18]. It can also be used as a pigment in printing inks [33]. The pyrolytic tyre char can also be suitable as a catalyst in the tyre pyrolysis process to produce petrochemicals [36].

## 4.3. Tyre pyrolytic gas

The tyre pyrolysis gas consists of CO, CO<sub>2</sub>, hydrocarbons (HC), H<sub>2</sub>, and sulphur and nitrogen compounds [37]. Because of its high energy content it can be used as fuel in the pyrolysis plant processes [19, 31] and also suitable as liquefied petroleum gas (LPG) [34]. The pyrolysis gas has high energy content but its utilisation as a fuel requires equipment to control SO<sub>x</sub> and other emissions [39]. Selection of optimum process conditions and suitable catalyst to minimize sulphur content in the gas phase can result in less polluting flue gas emissions. Using of suitable catalyst can result in more H<sub>2</sub> production [25, 33]. Higher temperature can result in higher gas yield but can affect the economy of the pyrolysis process [37]. Therefore, to recover maximum energy at viable conditions, it is recommended to target more than one product type [41].

## 5. CONCLUSION

Literatures suggest that pyrolysis of the waste tyre can significantly reduce the mass and volume of the waste and recover energy and value-added products. Energy production through waste tyre pyrolysis can decrease energy demand from fossil fuels. End of life of tyre can be possible through the pyrolysis process to completely eliminate the problems associated with waste tyre. The pyrolysis process emits less pollutant than burning and the gas obtained in the process can be used as fuel to fulfil the energy demand. Among all three tyre pyrolytic products, oil and solid products have significant advantages. Oil recovered in the process has several applications mainly as a liquid fuel because of its high calorific value after adequate purifications. Also, tyre pyrolytic oil

comprises chemicals used for synthesis of petrochemicals and plastics and even carbon nano tubes. Solid residue from the tyre pyrolysis can be used as a solid fuel, and the carbon present in the soot can be converted into activated carbon. Hence all these products have high commercial applications. Pyrolysis process itself demand the human resources for plant operation and maintenance, which ensures new employment opportunities. Therefore, from the literatures it can be concluded that waste tyre pyrolysis can be considered a sustainable approach for circular economy for waste tyres. However, an in-depth research is still required to optimise the process to produce maximum benefits.

## REFERENCES

1. A. Mohajerani *et al.*, “Recycling waste rubber tyres in construction materials and associated environmental considerations: A review,” *Resour. Conserv. Recycl.*, vol. 155, no. December 2019, p. 104679, 2020, doi: 10.1016/j.resconrec.2020.104679.
2. S. S. Narani, M. Abbaspour, S. M. Mir Mohammad Hosseini, E. Aflaki, and F. Moghadas Nejad, *Sustainable reuse of Waste Tire Textile Fibers (WTFs) as reinforcement materials for expansive soils: With a special focus on landfill liners/covers*, *Journal of Cleaner Production*, Volume 247, 20 February 2020, 119151
3. R. Kumar Singh *et al.*, “Pyrolysis of three different categories of automotive tyre wastes: Product yield analysis and characterization,” *J. Anal. Appl. Pyrolysis*, vol. 135, pp. 379–389, 2018, doi: 10.1016/j.jaap.2018.08.011.
4. P. T. Williams, S. Besler, and D. T. Taylor, “The pyrolysis of scrap automotive tyres. The influence of temperature and heating rate on product composition,” *Fuel*, vol. 69, no. 12, pp. 1474–1482, 1990, doi: 10.1016/0016-2361(90)90193
5. M. Bajus and N. Olahová, “Thermal conversion of scrap tyres,” *Pet. Coal*, vol. 53, no. 2, pp. 98–105, 2011.
6. T. F. Dynamics, P. Oil, F. S. Strategies, and E. Impacts, “Westley Tire Fire Case Study.”
7. USFA, “Special Report : Scrap and Shredded Tire Fires,” *Tech. Rep. Ser.*, no. USFA-TR-093, 1998.
8. J. Downard *et al.*, “Uncontrolled combustion of shredded tires in a landfill - Part 1: Characterization of gaseous and particulate emissions,” *Atmos. Environ.*, vol. 104, pp. 195–204, 2015, doi: 10.1016/j.atmosenv.2014.12.059.
9. K. Norqay, “End-of-Life Tyre Management : Storage Options,” *Rev. Lit. Arts Am.*, no. July, 2004.
10. J. J. Evans, “Rubber tire leachates in the aquatic environment.,” *Rev. Environ. Contam. Toxicol.*, vol. 151, pp. 67–115, 1997, doi: 10.1007/978-1-4612-1958-3\_3.
11. A. Rubio, M. V. Cardo, and D. Vezzani, “Tire-breeding mosquitoes of public health importance along an urbanisation gradient in Buenos Aires, Argentina,” *Mem. Inst. Oswaldo Cruz*, vol. 106, no. 6, pp. 678–684, 2011, doi: 10.1590/S0074-02762011000600006.

12. D. A. Adebote, E. Kogi, S. J. Oniye, and F. Akoje, "Epidemiological significance of the breeding of mosquitoes in discarded automobile tyres in Zaria, Northern Nigeria," *J. Commun. Dis.*, vol. 43, no. 3, pp. 183–192, 2011.
13. A. Zabaniotou, N. Antoniou, and G. Bruton, "Analysis of good practices, barriers and drivers for ELTs pyrolysis industrial application," *Waste Manag.*, vol. 34, no. 11, pp. 2335–2346, 2014, doi: 10.1016/j.wasman.2014.08.002.
14. D. Pradhan and R. K. Singh, "Thermal Pyrolysis of Bicycle Waste Tyre Using Batch Reactor," *Int. J. Chem. Eng. Appl.*, vol. 2, no. 5, pp. 332–336, 2011, doi: 10.7763/ijcea.2011.v2.129.
15. J. I. Osayi, S. Iyuke, M. O. Daramola, P. Osifo, I. J. Van Der Walt, and S. E. Ogbeide, "Evaluation of pyrolytic oil from used tires and natural rubber (*Hevea brasiliensis*)," *Chem. Eng. Commun.*, vol. 205, no. 6, pp. 805–821, 2018, doi: 10.1080/00986445.2017.1422493.
16. M. Rofiqul Islam, H. Haniu, and M. Rafiqul Alam Beg, "Liquid fuels and chemicals from pyrolysis of motorcycle tire waste: Product yields, compositions and related properties," *Fuel*, vol. 87, no. 13–14, pp. 3112–3122, 2008, doi: 10.1016/j.fuel.2008.04.036.
17. J. A. Conesa, I. Martín-Gullón, R. Font, and J. Jauhiainen, "Complete study of the pyrolysis and gasification of scrap tires in a pilot plant reactor," *Environ. Sci. Technol.*, vol. 38, no. 11, pp. 3189–3194, 2004, doi: 10.1021/es034608u.
18. C. Berrueco, E. Esperanza, F. J. Mastral, J. Ceamanos, and P. García-Bacaicoa, "Pyrolysis of waste tyres in an atmospheric static-bed batch reactor: Analysis of the gases obtained," *J. Anal. Appl. Pyrolysis*, vol. 74, no. 1–2, pp. 245–253, 2005, doi: 10.1016/j.jaap.2004.10.007.
19. R. Alkhatib, K. Loubar, S. Awad, E. Mounif, and M. Tazerout, "Effect of heating power on the scrap tires pyrolysis derived oil," *J. Anal. Appl. Pyrolysis*, vol. 116, pp. 10–17, 2015, doi: 10.1016/j.jaap.2015.10.014.
20. M. Banar, V. Akyildiz, A. Özkan, Z. Çokaygil, and Ö. Onay, "Characterization of pyrolytic oil obtained from pyrolysis of TDF (Tire Derived Fuel)," *Energy Convers. Manag.*, vol. 62, pp. 22–30, 2012, doi: 10.1016/j.enconman.2012.03.019.
21. A. M. Cunliffe and P. T. Williams, "Composition of oils derived from the batch pyrolysis of tyres," *J. Anal. Appl. Pyrolysis*, vol. 44, no. 2, pp. 131–152, 1998, doi: 10.1016/S0165-2370(97)00085-5.
22. A. Ayanoğlu and R. Yumrutaş, "Production of gasoline and diesel like fuels from waste tire oil by using catalytic pyrolysis," *Energy*, vol. 103, pp. 456–468, 2016, doi: 10.1016/j.energy.2016.02.155.
23. R. Miandad, M. A. Barakat, M. Rehan, A. S. Aburiazaiza, J. Gardy, and A. S. Nizami, "Effect of advanced catalysts on tire waste pyrolysis oil," *Process Saf. Environ. Prot.*, vol. 116, pp. 542–552, 2018, doi: 10.1016/j.psep.2018.03.024.
24. R. Idris, C. T. Chong, and F. N. Ani, "Microwave-induced pyrolysis of waste truck tyres with carbonaceous susceptor for the production of diesel-like fuel," *J. Energy Inst.*, vol. 92, no. 6, pp. 1831–1841, 2019, doi: 10.1016/j.joei.2018.11.009.
25. C. Ilkiliç and H. Aydin, "Fuel production from waste vehicle tires by catalytic

- pyrolysis and its application in a diesel engine,” *Fuel Process. Technol.*, vol. 92, no. 5, pp. 1129–1135, 2011, doi: 10.1016/j.fuproc.2011.01.009.
26. N. Zandi-Atashbar, A. A. Ensafi, and A. H. Ahoor, “Magnetic Fe<sub>2</sub>CuO<sub>4</sub>/rGO nanocomposite as an efficient recyclable catalyst to convert discard tire into diesel fuel and as an effective mercury adsorbent from wastewater,” *J. Clean. Prod.*, vol. 172, pp. 68–80, 2018, doi: 10.1016/j.jclepro.2017.10.146.
27. I. De Marco Rodriguez, M. F. Laresgoiti, M. A. Cabrero, A. Torres, M. J. Chomón, and B. Caballero, “Pyrolysis of scrap tyres,” *Fuel Process. Technol.*, vol. 72, no. 1, pp. 9–22, 2001, doi: 10.1016/S0378-3820(01)00174-6.
28. J. I. Osayi and P. Osifo, “Utilisation of Synthesised Zeolite for Improved Properties of Pyrolytic Oil Derived from Used Tire,” *Int. J. Chem. Eng.*, vol. 2019, 2019, doi: 10.1155/2019/6149189.
29. A. Hijazi, A. H. Al-Muhtaseb, S. Aouad, M. N. Ahmad, and J. Zeaiter, “Pyrolysis of waste rubber tires with palladium doped zeolite,” *J. Environ. Chem. Eng.*, vol. 7, no. 6, p. 103451, 2019, doi: 10.1016/j.jece.2019.103451.
30. R. Yuwapornpanit and S. Jitkarnka, “Cu-doped catalysts and their impacts on tire-derived oil and sulfur removal,” *J. Anal. Appl. Pyrolysis*, vol. 111, pp. 200–208, 2015, doi: 10.1016/j.jaap.2014.11.009.
31. S. Muenpol, R. Yuwapornpanit, and S. Jitkarnka, “Valuable petrochemicals, petroleum fractions, and sulfur compounds in oils derived from waste tyre pyrolysis using five commercial zeolites as catalysts: Impact of zeolite properties,” *Clean Technol. Environ. Policy*, vol. 17, no. 5, pp. 1149–1159, 2015, doi: 10.1007/s10098-015-0935-8.
32. W. Li *et al.*, “Catalysts evaluation for production of hydrogen gas and carbon nanotubes from the pyrolysis-catalysis of waste tyres,” *Int. J. Hydrogen Energy*, vol. 44, no. 36, pp. 19563–19572, 2019, doi: 10.1016/j.ijhydene.2019.05.204.
33. J. F. González, J. M. Encinar, J. L. Canito, and J. J. Rodríguez, “Pyrolysis of automobile tyre waste. Influence of operating variables and kinetics study,” *J. Anal. Appl. Pyrolysis*, vol. 58, no. 59, pp. 667–683, 2001, doi: 10.1016/S0165-2370(00)00201-1.
34. A. Undri, S. Meini, L. Rosi, M. Frediani, and P. Frediani, “Microwave pyrolysis of polymeric materials: Waste tires treatment and scharacterisation of the value-added products,” *J. Anal. Appl. Pyrolysis*, vol. 103, no. x, pp. 149–158, 2013, doi: 10.1016/j.jaap.2012.11.011.
35. A. Lucchesi and G. Maschio, “Semi-active carbon and aromatics produced by pyrolysis of scrap tires,” *Conserv. Recycl.*, vol. 6, no. 3, pp. 85–90, 1983, doi: 10.1016/0361-3658(83)90033-4.
36. S. Seng-eiad and S. Jitkarnka, “Untreated and HNO<sub>3</sub>-treated pyrolysis char as catalysts for pyrolysis of waste tire: In-depth analysis of tire-derived products and char characterisation,” *J. Anal. Appl. Pyrolysis*, vol. 122, pp. 151–159, 2016, doi: 10.1016/j.jaap.2016.10.004.
37. D. Czajczyńska, R. Krzyżyńska, H. Jouhara, and N. Spencer, “Use of pyrolytic gas from waste tire as a fuel: A review,” *Energy*, vol. 134, pp. 1121–1131, 2017, doi: 10.1016/j.energy.2017.05.042.
38. M. F. Laresgoiti, I. De Marco, A. Torres, B. Caballero, M. A. Cabrero, and M.

- J. Chomón, “Chromatographic analysis of the gases obtained in tyre pyrolysis,” *J. Anal. Appl. Pyrolysis*, vol. 55, no. 1, pp. 43–54, 2000, doi: 10.1016/S0165-2370(99)00073-X.
39. D. Susa and J. Haydary, “Sulphur distribution in the products of waste tire pyrolysis,” *Chem. Pap.*, vol. 67, no. 12, pp. 1521–1526, 2013, doi: 10.2478/s11696-012-0294-4.
40. S. Kordoghli, B. Khiari, M. Paraschiv, F. Zagrouba, and M. Tazerout, “Production of hydrogen and hydrogen-rich syngas during thermal catalytic supported cracking of waste tyres in a bench-scale fixed bed reactor,” *Int. J. Hydrogen Energy*, pp. 11289–11302, 2019, doi: 10.1016/j.ijhydene.2018.09.102.
41. D. Y. C. Leung, X. L. Yin, Z. L. Zhao, B. Y. Xu, and Y. Chen, “Pyrolysis of tire powder: Influence of operation variables on the composition and yields of gaseous product,” *Fuel Process. Technol.*, vol. 79, no. 2, pp. 141–155, 2002, doi: 10.1016/S0378-3820(02)00109-1.

### Cite this article

---

A. Sudharshan Reddy and Abhilash T. Nair, Pyrolysis of Tyre Waste: A Sustainable Waste Management Approach, In: Sandip A. Kale editor, Efficient Engineering Systems: Volume 1, Pune: Grinrey Publications, 2021, pp. 63-74.

# Analysis of Strengthened Industrial Structure under Seismic Loading

Varsha Gokak<sup>a,\*</sup>, Swati Bekkeri<sup>b</sup>, Tejas Doshi<sup>a</sup> and R. V. Raikar<sup>a</sup>

<sup>a</sup>Department of Civil Engineering, KLE DR.M. S. Sheshgiri College of Engineering and Technology, Belagavi, India

<sup>b</sup>Engineer, D. L. Kulkarni, Belagavi, India

\*Corresponding author: varsha.gokak87@gmail.com

## ABSTRACT

Industrial structures are used in power, petrochemical, agriculture and manufacturing sectors. The function of industrial structures is to encounter the extreme variations in loads that are likely to occur during manufacturing and finishing process of any industry such as temperature variation, variation in internal pressure and exposure to highly toxic and corrosive materials. Hence, it is important to have detailed information regarding the industrial processes and their effects, as this may guide to compute the loads in order to design a stable industrial structure. In the present work an existing industrial building subjected to different loading and having two strengthening methods: provision of secondary beams normal to the primary beams and providing knee bracings. The analysis has been performed using STAAD Pro V8i. Time history analysis is carried out for machine loading. For earthquake loading, both linear static and linear dynamic methods are used. The results indicate that the fundamental time period reduces with strengthening techniques and overall stiffness of the structure increases. The resonance frequency can be eliminated. Further, the provision of secondary beams normal to the primary beams gives better results.

**Keywords:** Bracings, Dynamic Loads, Industrial Structures, STAAD PRO, Steel Structures

## 1. INTRODUCTION

Industrial structures are different from general buildings as depicted through their forms and functions. They are well suited for power, petrochemical, agriculture and other manufacturing sectors. These structures encounter the extreme variations in loads, that is likely to occur during various processes in any industry. The loads include those due to temperature variation, variation in internal pressure and exposure to highly toxic and corrosive materials in addition to external loads. Because of the dynamic nature of the loads, the design of industrial structure is complex and challenging. Therefore, it is important to have detailed information regarding the various specific industrial processes and their effects, as this may become guide in planning and structural framing operations as well as in computing the loads for the stable design. Further, it is important that the plan shall be flexible as the service conditions diverge usually in these structures and provision shall be available for future extension without altering the present manufacturing layout [1].

The flooring systems commonly used in any industrial structure are composite steel deck concrete floor and steel chequered plate floor. Chequered plate is rolled steel plate with non-slippery patterns. The thickness of the plate varies from 3mm to 12mm (approximately weighing 287 to 990 N/m<sup>2</sup>). The patterns project approximately 1.5 mm above the plain plate. Fig.1 shows the typical chequered plate. Composite deck slab consists of reinforced concrete slab on top of steel sheeting and are connected by shear connectors. The deck slab is supported by secondary beams at the bottom forming the composite slab as illustrated in Fig. 2.

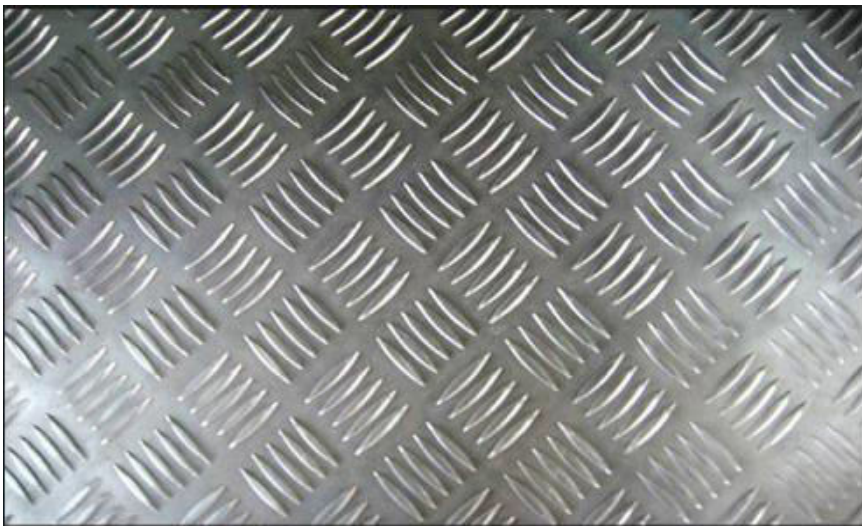


**Fig. 1.** Chequered plate

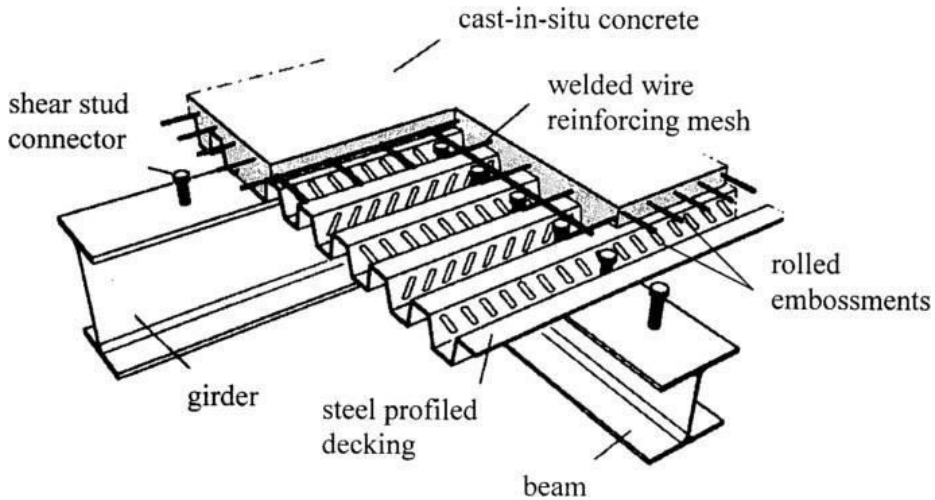


**Fig. 2.** Composite Deck Slab

In addition, an efficient bracing system provided in both transverse and longitudinal direction facilitate in preventing the deformations of the industrial structure caused due to the actions of wind, seismic loads and machine loads [2]. Iervolino *et al.* [3] presented natural procedure for seismic vulnerability assessment of industrial construction considering the large range of structural type. They related fragility curves with parameters in the design domain of structural design using regression method. Subramanian [4] has detailed several methods of analysis that accurately determine the forces and moments in various elements of steel structures along with behavior of the structure when bracings are provided in longitudinal and transverse direction.

Richard *et al.* [5] studied the seismic behavior of a heavy industrial building with highly irregular geometry, mass and stiffness distribution using STAAD Pro software. The building considered was braced with low ductility concentrically braced steel frames. They concluded that response spectrum analysis provides appropriate prediction of the seismic response of the industrial building. They further analysed seismic response of regular mill type crane supporting steel structures and irregular heavy industrial building using elastic time-history dynamic analyses and validated through equivalent static force procedure and the response spectrum analysis method [6].

Liberatore *et al.* [7] compared the damages observed at Emilia Region of Northern Italy during May 2012 earthquake with that of L'Aquila (central Italy), earthquake of 2009. The area affected by earthquake was highly dense with

industrial buildings. They considered seven main types of damage related to: column base, short column failure, column top, shed beam, roof element, cladding/infill panel, and steel stand. The results of the analyses highlight the directionality of damage, the relevance of the vertical component of earthquake excitation, along with the significant inelastic rotation induced in the columns.

Hong Hao [8] presented the predictions of structural response under dynamic loads with different loading rates. He discussed the basic concepts of structural dynamics, differences in influence by low-rate dynamic and high-rate blast loadings the structures. The single-degree-of-freedom analysis is proved to be more accurate in structural response analysis to blast loadings. Ramesh and Vinothkumar [9] used SAP to numerically analyze an industrial structure subjected to wind, earthquake and blast load. They reported that the provision of shear walls reduce the stress under dynamic loading. In addition to columns, the structure shall be modified with shear walls. Adin *et al.* [10] adopted X-bracing, eccentric bracing, diagonal bracing alongwith dampers in their analysis to find the most suitable lateral supporting system for an industrial building subjected to seismic loading. They found that the x bracing and damper with mass ratio 2% are suitable to improve the performance of the building under earthquake load and wind load.

Muhsina et al. [11] used STAAD Pro software to find out the ideal property of the machine foundation that can be placed at each story of an industrial building to safely resist the loads transmitted by machines. They employed response spectrum method for seismic analysis to analyze nuclear power plant (G+2) building. The machines were placed on different floor levels and the response of the machinery on each floor were obtained. Floor response spectrum is generated to study the overall response of the industrial building. Michael Angelides [12] presented the design consideration for industrial structures such as chimneys, bunkers, silos, cooling towers and ducts. He used American (ACI), German ((CICIND) and Belgium (CEN) code of practices for the study. Fabrizio [13] evaluated the intensity of non-structural damage in single-storeyed industrial steel buildings using different levels of cladding panels. Ravali and Poluraju [14] employed SAP 2000 and ETABS to carry out response spectrum analysis of 3D pre-engineered industrial structures. They used X-bracings and dampers as the lateral supporting system. They reported that X-bracings are more suitable than dampers as they are effective in reducing the seismic effect as well as economical, while dampers require regular maintenance.

Brunet et al. [15] performed nonlinear response history analyses to examine and compare the seismic response using seismic provisions of Canadian standards.

The suggested the modifications to mobilize higher brace inelastic response, mitigate storey drift concentrations, along with ensuring that the columns can safely resist the seismic induced axial and flexural demands.

The present study attempts to obtain the response of an existing industrial building substantiated with different strengthening methods that are used to withstand heavy loads. The analysis has been performed using STAAD Pro V8i. Time history analysis is carried out for machine loading. For earthquake loading, both linear static and linear dynamic methods are used.

## 2. STRUCTURAL MODELLING

The G+3 storey steel building is considered in the present analysis. The building consists of composite steel deck floor system on which different machine setups are resting. The column spacing is 5 m in both the directions. The plan, elevation and three dimensional views are shown in the Figs. 3 to 5. Table 1 furnishes details of the building.

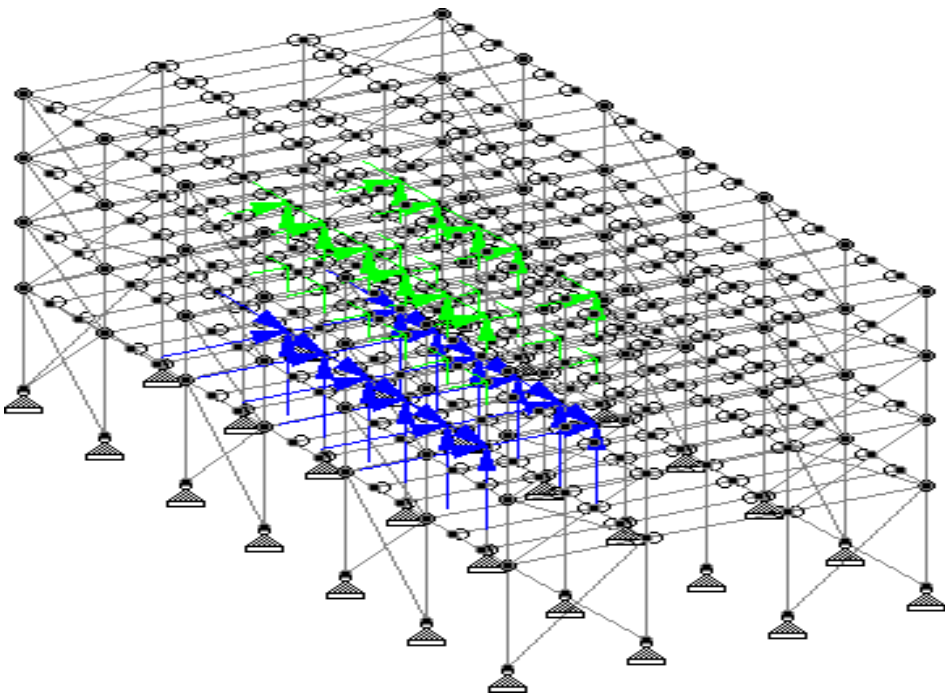


**Fig. 3.** Machine Loading Points

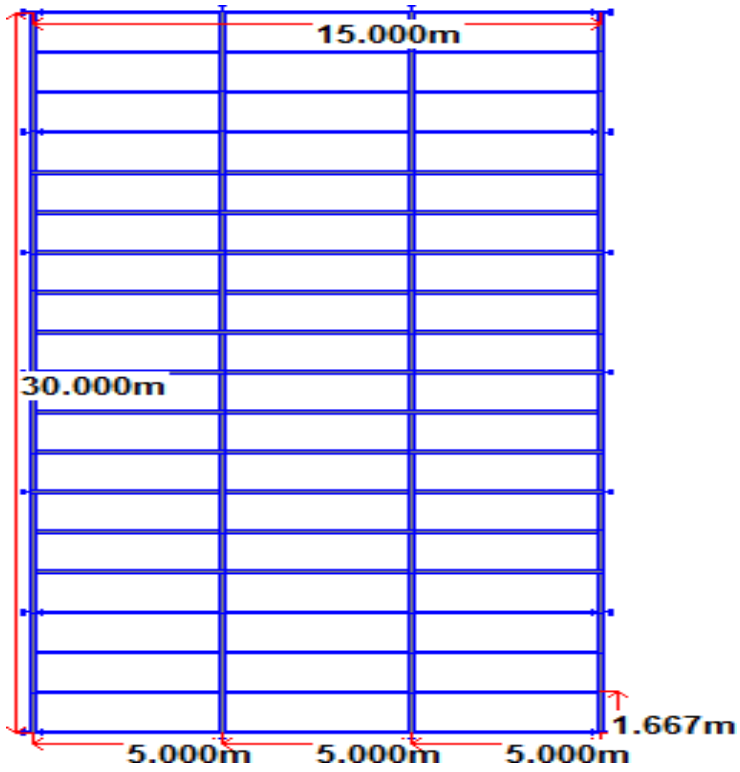


Fig. 4. Plan of the building

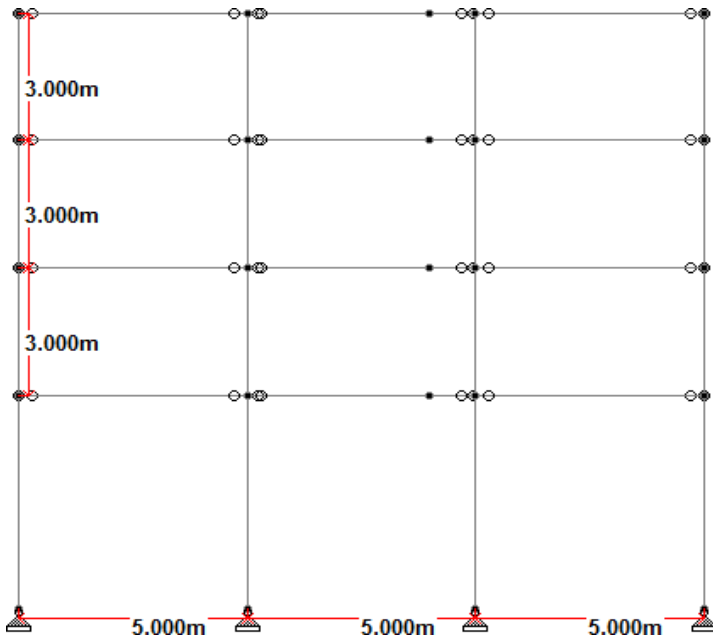
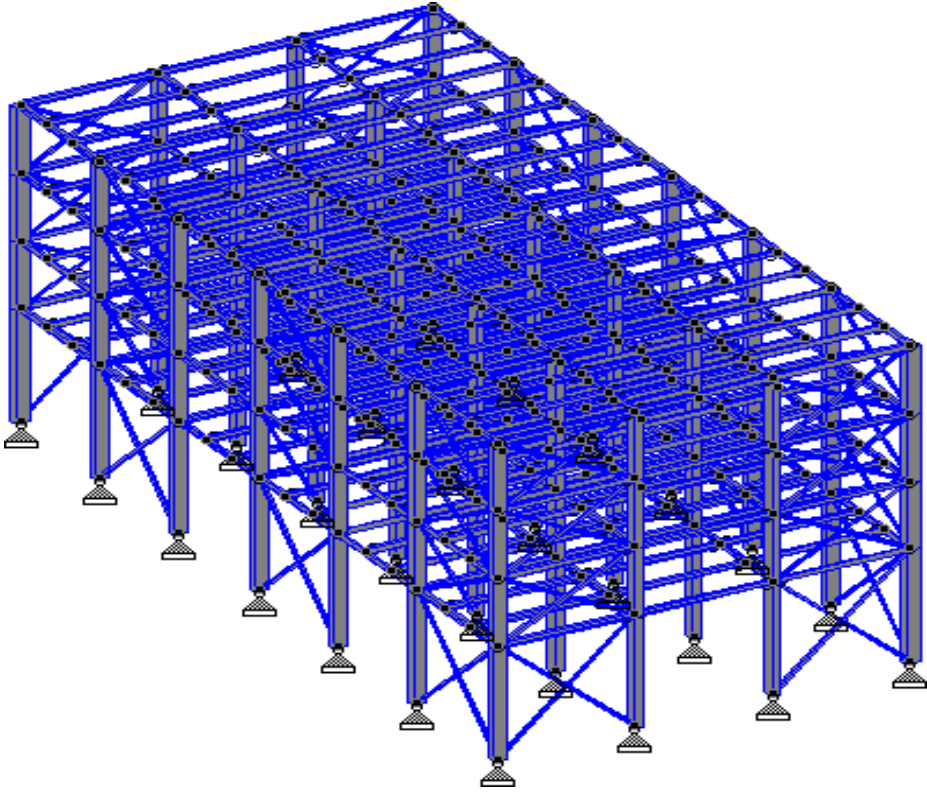
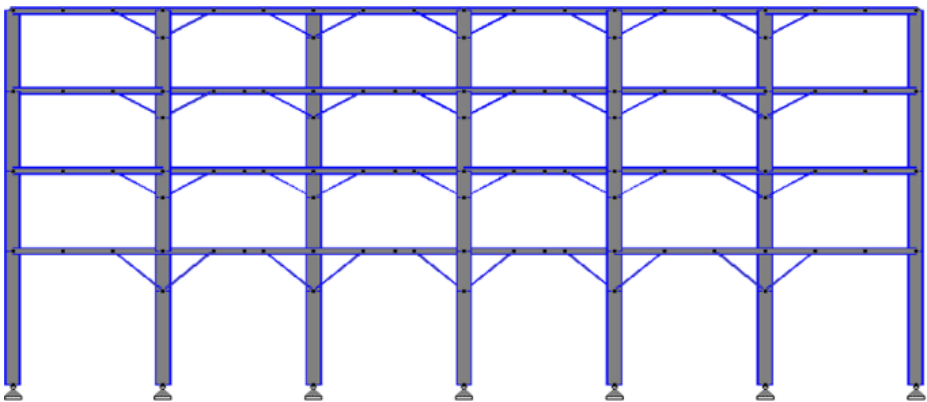


Fig. 5. Elevation of the Building



**Fig. 6.** Model 1 for Industrial Structure under Seismic Loading



**Fig. 7.** Model 2 for Industrial Structure under Seismic Loading

**Table 1.** Building Data

Particulars	Details
Type of structure	Steel
No. of floors	G+3
Floor Height	3 m
Plan dimension	15m x 30m
Column	ISMB 500
Beam	ISMB 250
Bracings	ISA 75x75x6
Type of flooring system	Composite steel deck
Thickness of profiled steel sheeting	10 mm
Profile height	75 mm
Thickness of concrete slab	100 mm
Spacing of secondary beams	1.6 m

## 2.1. Machine Data

Table 2 gives the details of the machines considered for the present study.

**Table 2.** Loading details of Machine Type-1 (Forces at points of support in kgf)

Static	Dynamic			
	In operating condition		During start & end	
	Vertical	Horizontal	Vertical	Horizontal
F1 = 3500	F1=± 135	F1=± 112	F1= ± 3825	F1= ± 220
F2 = 3500	F2=± 135	F2=± 112	F2= ± 3825	F2= ± 220
Frequency = 29.84 Hz      No of load cycles = 30				
Maximum allowable displacement = 0.08 mm				

## 2.2. Developed Model

The analysis is performed on an existing industrial building on which heavy machine setups are planned to be placed at different stories such as Ist, IInd and IIIrd floor. The machines that are going to be used in the industry are Rotating machines. On all floor levels three machines are operating with different loads and frequency. To resist these heavy loads, different types of strengthening methods are employed. To study the response of the building when different strengthening methods are used, 2 models were analysed and their behavior is observed. Model 1 is with the secondary beams normal to the primary beams having the section of ISMC 100 while Model 2 is with provision of knee bracing of section ISA 50 × 50 × 6.

### 3. ANALYSIS AND RESULTS

The industrial structure taken up for the present work is subjected to varying combinations of static and dynamic loads. The results analyzed using STAAD Pro v8i are used to compare the response the structure when different strengthening techniques that are employed. The results obtained are presented in the following sub-sections.

#### 3.1. Results of Model 1 – Provision of Secondary Beams Normal to Primary Beams

In this study, secondary beams having section of ISMC 100 are provided perpendicular to the primary beams to control the displacement and avoid the failure of certain columns and beams. The exterior columns are provided with bracings. Results for this model are as follows:

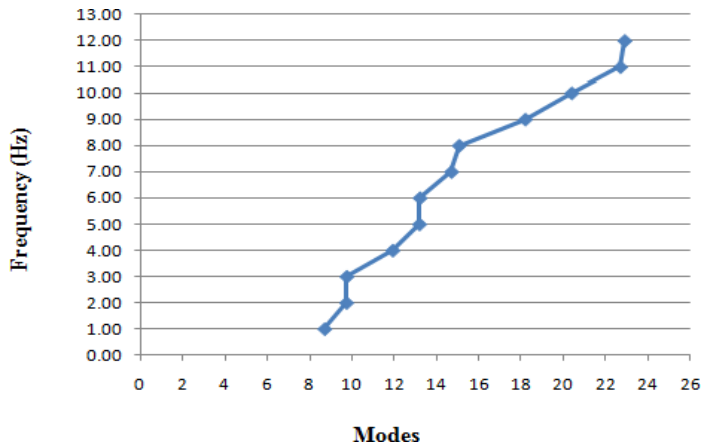


**Fig. 8.** Variation of frequency with modes

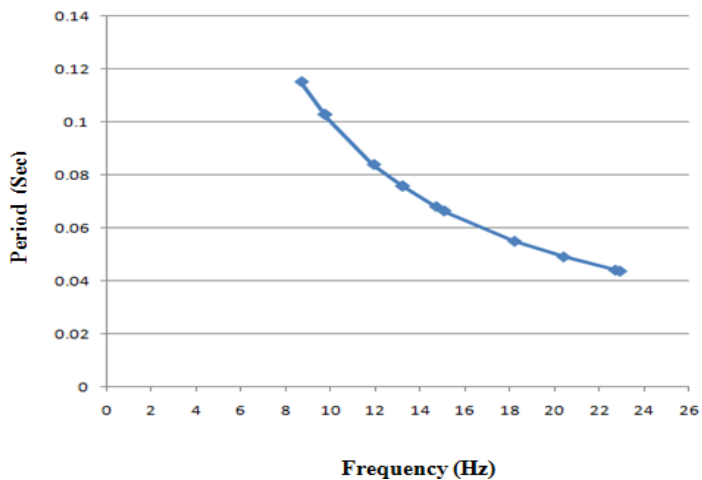


**Fig. 9.** Variation of frequency with Period

Figure 8 presents the increase trend in frequency with an increase in modes. However, the frequency-period variation is given in Figure 9. Further, Figures presented in Table 3 illustrate the displacements in x-, y-, and z-direction of stories I to III. The maximum value of storey displacement in z-direction occurs in floor III and is 3.376 mm. This maximum value is for the load case EQX (Earthquake in x-direction). The maximum values for joint displacements are 0.052 mm, 0.12 mm and 0.15 mm (in Z – direction) for first, second and third floor respectively. The permissible joint displacements are 0.008 mm, 0.2 mm and 0.2 mm for first, second and third floor respectively. The joint displacements are within the permissible limits. For third storey the value is 0.646 mm (in Z- direction). But the permissible limit is 0.2 mm. These results indicate that the building is resisting the applied loads efficiently and the displacements are within the limits.

**Table 3.** Displacements due to Model 1

Floor	Direction	Displacement plot
I	X-direction	<p>X-Disp.(E-3 mm) - Node: 47</p> <p>Time - Displacement</p>
	Y-direction	<p>Y-Disp.(mm) - Node: 47</p> <p>Time - Displacement</p>
	Z-direction	<p>Z-Disp.(mm) - Node: 47</p> <p>Time - Displacement</p>

II	X-direction	<p>X-Disp.(E-3 mm) - Node: 75</p> <p>Time - Displacement</p>
	Y-direction	<p>Y-Disp.(E-3 mm) - Node: 75</p> <p>Time - Displacement</p>
	Z-direction	<p>Z-Disp.(mm) - Node: 75</p> <p>Time - Displacement</p>
III	X-direction	<p>X-Disp.(E-3 mm) - Node: 103</p> <p>Time - Displacement</p>
	Y-direction	<p>Y-Disp.(E-3 mm) - Node: 103</p> <p>Time - Displacement</p>
	Z-direction	<p>Z-Disp.(mm) - Node: 103</p> <p>Time - Displacement</p>

### 3.2. Results of Model 2 – Provision of Knee Bracing

In this model, knee bracings of section ISA 50x50x6 are used and the exterior columns are provided with bracings. Results for this model are as given below:

Figure 10 presents the increase trend in frequency with an increase in modes. However, the frequency-period variation is given in Figure 11. Further, Figures listed in Table 4 illustrate the displacements in x-, y-, and z-direction of stories I to III. The maximum value of story displacement is 3.67 mm. This maximum value is for the load case EQX. The maximum values for joint displacements are 0.092 mm, 0.218 mm and 0.295 mm (in Z – direction) for first, second and third floor respectively. The permissible joint displacements are 0.008 mm, 0.2 mm and 0.2 mm for first, second and third floor respectively. The joint displacements are slightly exceeding the permissible limits. From the analysis results, we can say that the building is resisting the applied loads efficiently and the displacements are also within the limits.

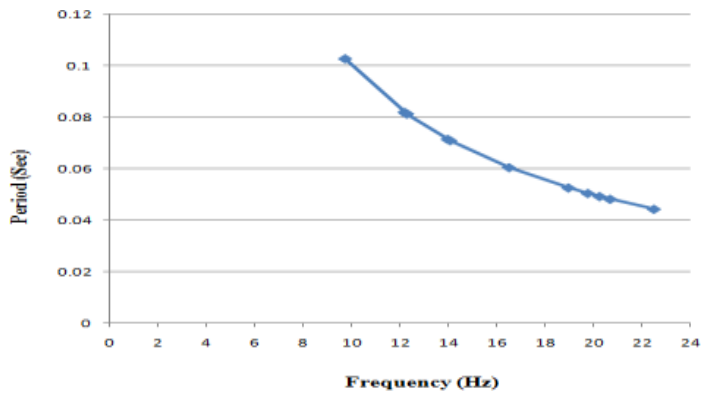


Fig. 10. Variation of frequency with modes

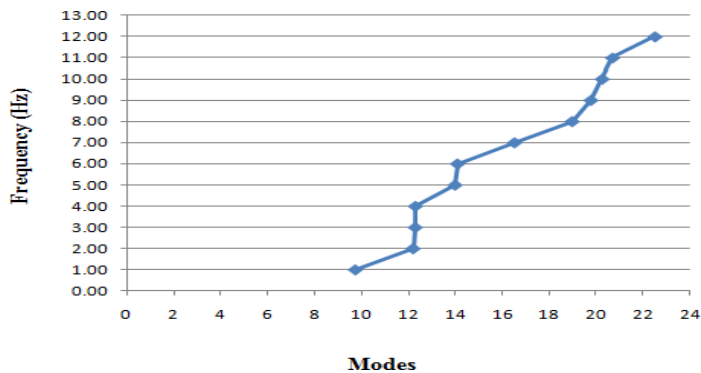
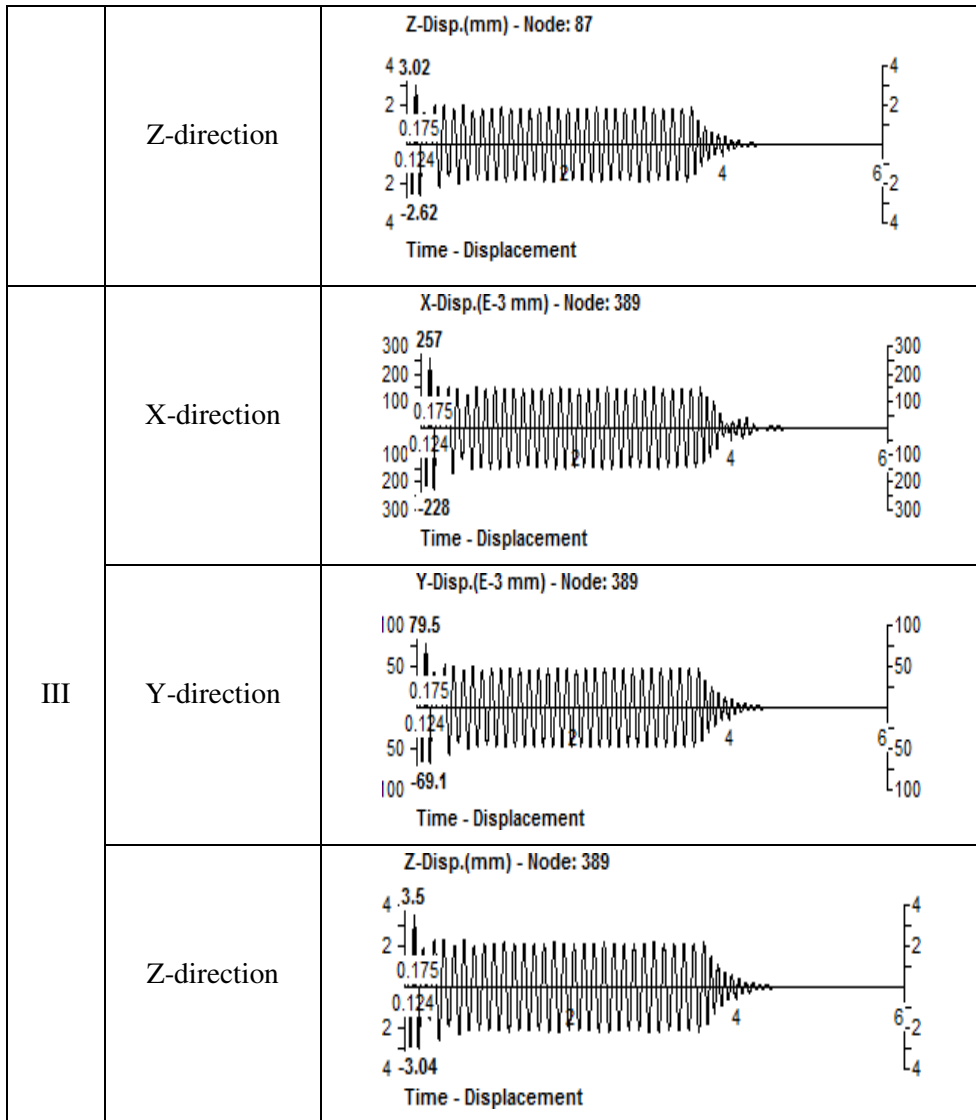


Fig. 11. Variation of frequency with Period

**Table 4.** Displacements due to Model 2

Floor	Direction	Displacement plot
I	X-direction	<p>X-Disp.(E-3 mm) - Node: 197</p> <p>Time - Displacement</p>
	Y-direction	<p>Y-Disp.(E-3 mm) - Node: 197</p> <p>Time - Displacement</p>
	Z-direction	<p>Z-Disp.(mm) - Node: 197</p> <p>Time - Displacement</p>
II	X-direction	<p>X-Disp.(E-3 mm) - Node: 87</p> <p>Time - Displacement</p>
	Y-direction	<p>Y-Disp.(E-3 mm) - Node: 87</p> <p>Time - Displacement</p>



#### 4. CONCLUSION

In the present work, the study is done on an existing industrial structure with machines under dynamic loads. To resist the applied loads efficiently different strengthening methods are adopted and their behavior is studied. The results of the present study lead to the following conclusions:

1. Base shear and axial force which are the values of response parameters increases with strengthening methods.
2. The fundamental time period reduces with the adoption of strengthening techniques and the value is least by providing bracings to the exterior

columns and strengthening of existing columns by adding T section to the web of the column.

3. The overall stiffness of the building increases by providing strengthening methods and thus the natural period decreases.
4. Accept in case of bracings provided to the exterior columns the joint displacement values are reduced to permissible limits than the allowable joint displacement.
5. The occurrence of resonance is avoided as the natural frequency of the structure is away from the operating frequency of the machines by at least 20%.
6. Both the models with strengthening methods are resisting the applied loads such as gravity loads, machine loads and seismic loads effectively. The displacements obtained are also within the allowable limits (slightly higher for model-2). Model-1 is the most suitable strengthening option.

## REFERENCES

1. Ramachandra and Virendra Gehlot, Design of steel structures, Laxmi Publications, New Delhi, Fourth Edition, 1984.
2. K. G. Bhatia, Foundations for industrial machines, Handbook for Practicing Engineers, First edition, 2011.
3. Iunio Iervolino, Giovanni Fabbrocino, Gaetano Manfredi, Fragility of standard industrial structures by a response surface based method, *Journal of Earthquake Engineering*, Vol. 8, Issue 6, 2004, 927-945.
4. K.V. Subramanian, Evolution of seismic design of structures, systems and components of nuclear power plants, *Journal of Earthquake Technology*, Paper No. 512, Vol. 47, No. 2-4, June-Dec.2010, pp. 87-108.
5. Julien Richard, Sanda Koboevic, Robert Tremblay, Seismic design and response of heavy industrial steel building, *3<sup>rd</sup> ECCOMAS Thematic Conference on Computational Methods in Structural Dynamics and Earthquake Engineering*, 25-28 May 2011.
6. Julien Richard, Sanda Koboevic, Robert Tremblay, Seismic design and response of crane supporting and heavy industrial steel structures, *Engineering Journal*, Vol. 48(3), 2011, 205-224.
7. Laura Liberatore, Luigi Sorrentino, Domenico Liberatore, Luis D. Decanini, Failure of industrial structures induced by the Emilia (Italy)

- 2012 earthquakes, *Engineering Failure Analysis*, Vol. 34, 2013, 629-647.
8. Hong Hao, Predictions of structural response to dynamic loads of different loading rates, *International Journal of Protective Structures*, Vol. 6, No. 4, 2015, 585-605.
  9. S. Ramesh, V, Vinoth Kumar, Parametric study on an industrial structure for various dynamic load, *International Journal of Research in Engineering and Technology*, Vol. 4, Issue 2, 2015, 134-143.
  10. C. B. Adin, Praveen, J. V., Raveesh, R. M., Dynamic analysis of industrial steel structure by using bracings and dampers under wind load and earthquake load, *International Journal of Engineering Research and Technology*, Vol. 5, Issue 7, 2016, 87-92.
  11. Muhsina, C. K, Jaisal, A. K, Romy Mohan, Study on industrial building with heavy machinery under dynamic Loading using floor response spectrum method, *International Journal of Engineering Research and Technology*, 2016, Vol. 5, Issue 9, pp. 344-348.
  12. Michael Angelides, Seismic design considerations for industrial structures, 15<sup>th</sup> European Conference on Earthquake Engineering, 2018, Thessaloniki.
  13. Fabrizio Scozzesea, Giusy Terraccianob, Alessandro Zonaa, Gaetano Della Corteb, Andrea Dall’Astaa, Raffaele Landolfo, Analysis of seismic non-structural damage in single-storey industrial steel buildings, *Soil Dynamics and Earthquake Engineering*, Vol. 114, 2018, 505-519.
  14. Ravali, B., Poluraju, P. Seismic analysis of industrial structure using bracings and dampers, *International Journal of Recent Technology and Engineering*, Vol. 7, Issue 6C2, 2019, 22-26.
  15. Frédéric Brunet, Robert Tremblay, Julien Richard, Mark Lasby, Improved Canadian seismic provisions for steel braced frames in heavy industrial structures, *Journal of Constructional Steel Structures*, Vol. 153, 2019, 638-653.

---

### Cite this article

Varsha Gokak, Swati Bekkeri, Tejas Doshi and R. V. Raikar, Analysis of Strengthened Industrial Structure under Seismic Loading, In: Sandip A. Kale editor, Efficient Engineering Systems: Volume 1, Pune: Grinrey Publications, 2021, pp. 75-90

---

# Strategies for the Distribution of Uses, Occupation and Allocation of Land: Explained with a Case Study of Paseo De Los Cañarís in the City of Cuenca

Carla Sigüencia<sup>a,\*</sup>, Marco Avila<sup>b,\*</sup> and Yonimiler Castillo<sup>a</sup>

<sup>a</sup>Master in local development mention planning, development and land use planning, University Catholic of Cuenca, Cuenca, Ecuador

<sup>b</sup>School of Architecture, University Catholic of Cuenca, Cuenca, Ecuador

\*Corresponding author: soledad\_376@yahoo.com,  
mavila@ucacue.edu.ec

## ABSTRACT

The present research aims to generate strategies for the distribution of uses and allocation of land occupation characteristics, supported by geostatistical analyzes in the search to generate an interaction more adjusted to reality, to understand the dynamics of urban spaces, the forms occupation of space by the population (relationships between human beings and the physical space of their habitat), as well as the dynamics generated by certain elements and the impact on their immediate context.

**Keywords:** Geostatistics, occupation characteristics, geographic information systems, spatial autocorrelation, corema, diversity index

## 1. INTRODUCTION

The uses of the land, and their physical expression, constitute the main element of modification of the landscape, being the socioeconomic structures those that determine the direction and tendencies of land uses that transform the natural environment.[1]– [5].

From the socioeconomic point of view, the land uses of a territory make up the landscape where the secular and current relationships of man with the environment are expressed in a characteristic way [6][7]–[10], on the other hand, the land use patterns derived from the influence of the Human activities, in certain cases constitute a series of threats to natural and productive systems, due to environmental degradation [11], [12].

Factors such as: subdivision (morphology of land occupation), urbanization (construction of urban infrastructure) and building (construction of buildings according to typologies and in response to the activities carried out in it).

They can be analyzed in consolidated areas that experience dynamism such as city occupation, transformation of urban space and its growth and consolidation; in such a way that the city itself becomes a space on which it is possible to carry out several analyzes that support future actions [13]– [16].

The research proposes generate strategies for the distribution of uses and allocation of land occupation characteristics, as specific objectives we seek:

- Identify and characterize the relevant urban elements of the study area.
- Analyze and identify the spatial patterns of land use and occupation in the study area.
- Prepare a synthesis based on the relationship between behavior patterns and relevant urban element.

New form of analysis of land uses, which, although the same results are obtained from traditional analyzes, as an advantage, the deduction that many of the times is obtained empirically, from the application of tools, has been rigorously proven. Geostatistics available in the ArcGIS [17], [18] geographic information system, whose calculation basis is the distance variable, which is different according to the location of one use versus another.

The study area has an area of 150 Ha, around Av. Paseo de los Cañaris, which is an area made up of important road axes such as Av. Huayna Cápac, Max Uhle, Av. Pumapungo and Av. González Suárez, which due to its dynamics allows us to analyze the impact of the use and occupation of land around them. In order to have quality data, the property census of the study area was carried out, using a

form applied to all the properties of the study area to collect information on both land use and occupation characteristics per building, to From the survey, the database is prepared, which contains all the information collected in the field.

The content of the information is presented in four sections, first theoretical references and research related to the subject, then the relevant urban elements of the study area are identified and analyzed, in the third section an analysis of the distribution of the groups of uses is presented. of soil present in the study area and the evaluation of current regulations. Subsequently, the spatial analysis of land use I thus determining the concentration, trend, and existing patterns through the application of methods such as Kriging, the Moran index and LISA. Finally, strategic objectives are established for the balanced development of the area according to the predominant factor that influenced its conformation.

## **2. METHODOLOGY**

This research is of a mixed type that has a qualitative and quantitative, exploitative, descriptive and documentary space. Territorial planning is developed in three stages: diagnosis, territorial planning, and management of the plan. The geographical spaces must be studied to understand the functioning of the territorial system to design adequate plans for the conditions of each region. This work indicates the procedures used to determine the urban land management categories as a territorial planning mechanism. In the study the following methodology is used, composed of four phases, in the first one a data collection is carried out, in phase two characterization of the relevant elements, in phase three selection of the geostatistical tool and we end with phase 4 that includes the proposed study and system. The methodology that was carried out in the investigation is described through Figure 1.

The main source of information was the in-situ survey of land uses at the farm level in the city of Cuenca. The study is carried out in an area consisting of 150 Ha located to the Southeast of the city of Cuenca, around Av. Paseo de los Cañaris, which is an area made up of major road axes such as Av. Huayna Cápac, Av. Max Uhle, Av. Pumapungo and Av. González Suárez, which due to their dynamics will allow to analyze the impact of the use and occupation of the land around them, in addition this area is characterized by having a homogeneous topography.

Being part of the urban area of the city of Cuenca, the occupation process has been completed almost entirely, presenting particularities in terms of the diversity of land use and occupation. For the delimitation, the following aspects were considered:

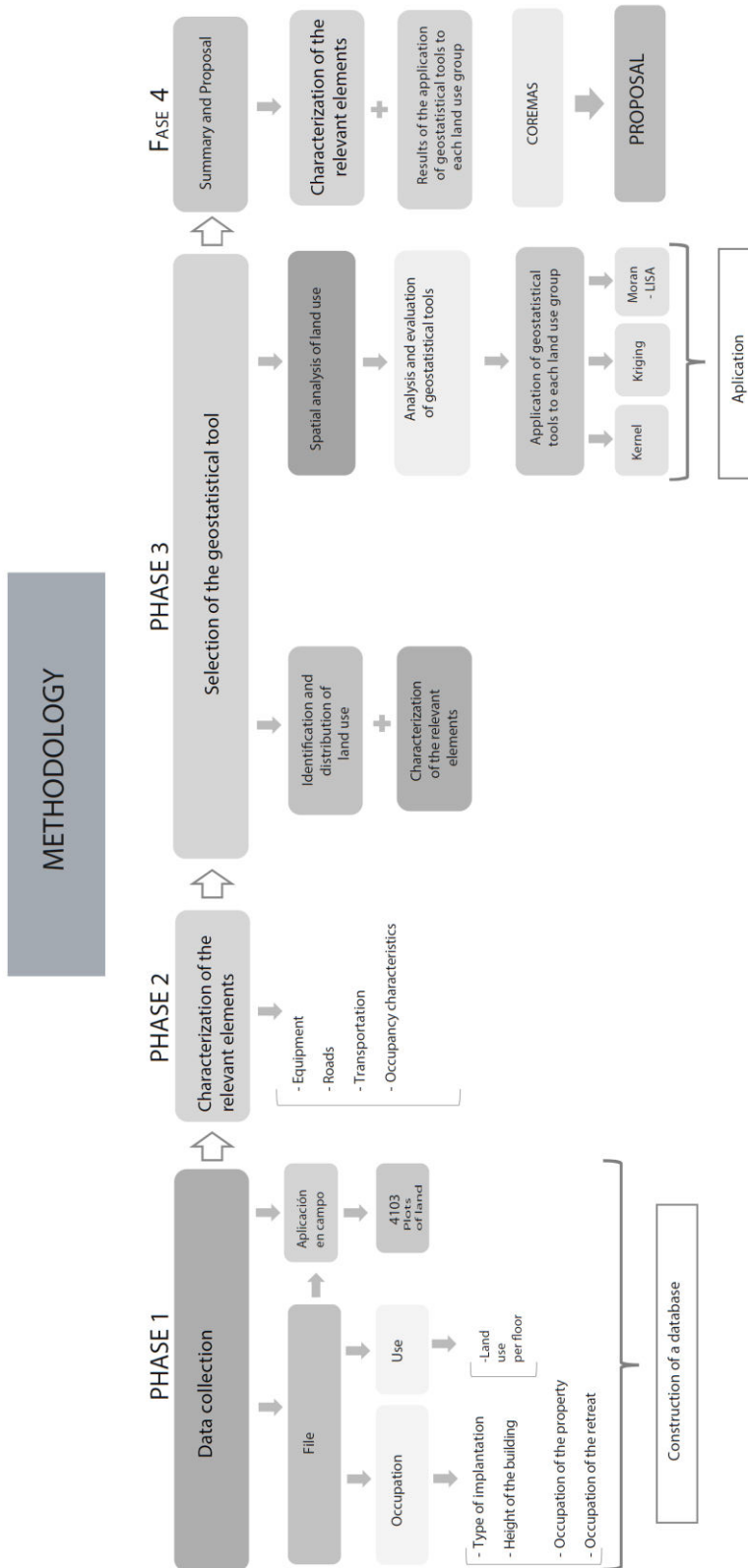


Fig. 1. Research methodological framework

- Incorporate the area of influence of the Paseo de los Cañaris.
- Incorporate the road axes, Av. Huayna Cápac, Av. Max Uhle, Av. Pumapungo and Av. González Suárez.

After defining the limit of the study area, the sectorization of the same is carried out under criteria and conditions of land use, topographic characteristics and road axes, obtaining as a result 6 sectors distributed as follows.

## 2.1. Facilities

In the study area, 151 facilities were identified distributed throughout the study area, the most numerous being those considered in the classification figure 2: administration and management (51), followed by health facilities (39), social welfare facilities, religious, education, security and supply.

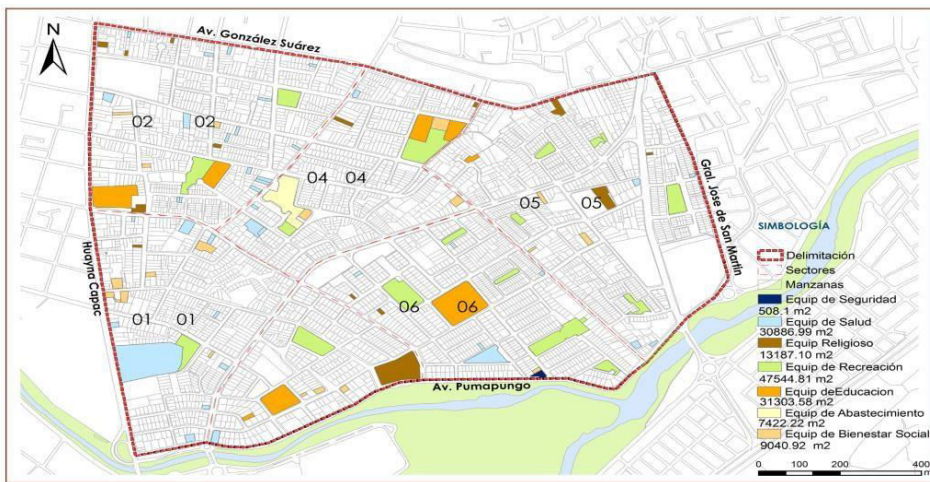


**Fig. 2.** Equipment of the study area. Prepared by the authors with data from the Property Census, 2015

### 2.2.1 Education Equipment

This type of equipment is legally governed by the Ministry of Education through the Zonal Directorate 6 of Education of Azuay. For the analysis of the educational facilities located in the study area, the buildings in which the different levels of education work established by the Ministry of Education with regard to the Initial, Basic and Baccalaureate levels and by the SENESCYT were identified as regards the Superior level, figure 3.

### 2.2.2 Health Equipment

They are mostly for public use and make up the comprehensive public health network, whose policies are attributed to the Ministries of Health. For the

classification of health facilities, the one carried out in the diagnosis phase of the Cuenca Urban Planning Plan (2015) 6 has been considered, where the “typology to standardize Health establishments by levels of National System Care has been taken of Health”, corresponding to agreement N ° 001203 of the corresponding Ministry. The study area has both public and private health facilities that are framed within the different levels of care provided by the Ministry of Health.



**Fig. 3.** Location of educational facilities in the study area. Prepared by the authors with data from the Property Census, 2015

### 2.2.3 Provisioning

The supply equipment is understood as the adequate buildings and infrastructures to promote exchange, where the suppliers (producers or sellers) and demanders (consumers or buyers) enter into a close commercial relationship in order to carry out abundant commercial transactions of perishable products and not perishable. In addition, this facility has free parking and security guards. Likewise, it has a Comprehensive Development Center (CDI), so that all children (children of merchants) can do their homework supported by professionals.

### 2.2.4 Social Welfare Facilities

Governed by the Ministry of Social Welfare or by local governments, in charge of formulating, directing and executing state policies regarding the protection of the most vulnerable sectors of society (minors, youth, older adults, people with disabilities, indigenous people and peasants) with in order to promote good living. Considering the classification defined by the Ministry of Social Inclusion (2010) [8] in the study area, 18 social welfare facilities have been identified, of

which 16 correspond to nurseries, 1 nursing home and 1 Social reintegration centers.

### **2.2.5 Safety Equipment**

Buildings whose objective is to contribute to citizen security and public order. The study area has a Community Police Unit (UPC), located to the south between Av. Pumapungo and José de la Cuadra street. This facility has police on permanent duty, 24 hours a day in 8-hour shifts. Recreation equipment: urban spaces, equipped, preserved and mainly animated for leisure and recreation, which has social importance since they are places of meeting and coexistence.

Based on the information collected in the field, the parks, which are mostly neighborhood and children's parks (17) and the fields (2), have been considered as green areas. Cult equipment: eIn the study area, 13 religious facilities have been identified, which preach various types of religions.

## **2.2. Roads**

After the field review of the road hierarchy carried out by the Municipal GAD of the Cuenca [6] canton, adjustments have been considered, since the hierarchical level does not respond to the reality of the operation of the road system in the study area. Taking into account the above, the road network has been classified as follows:

- Arterial roads: their main characteristic is to carry traffic between different areas of the city, they support a high traffic flow.
- Collector roads: with the function of absorbing the traffic of the local roads, taking the vehicular flows towards the main system. In the study area there are 12 collector routes,
- Local roads: constituted by those roads that give access to adjacent properties, also facilitate local traffic. They are directly connected to the collector and / or arterial routes. These pathways are the most quantity in the study area.

## **2.3. Transport**

The Public Transport Network forms a mesh of transport channels, which allows the flow of users between their places of origin and destination, in an efficient, comfortable and safe way. The proper functioning of the components of this network guarantees the fulfillment of its objective [9]. According to the information available in the Municipal Transit Office (DMT) [10]; The study area has the service of 13 bus lines, which move users to other sectors of the city.

## 2.4. Spatial Analysis of Land Use

The classification and identification of the land uses that are presented in the study area, was carried out based on the table of land uses existing in the Reform, Update, Complementation and Codification of the Ordinance that sanctions the Land Use Plan of the Cuenca canton [7]. The results are found in Table 1.

**Table 1.** Land uses according to the codification of the Ordinance that sanctions the Territorial Ordinance Plan of the Canton Cuenca

Code	Code Description
100	Occasional trade in retail housing supply products
200	Artisanal production and manufacture of goods compatible with housing
310	Security services
320	Financial services
340	Transport and communications service
350	Tourism and recreation services
360	Food services
380	Professional services
400	Personal and housing-related services
500	Daily trade of food and non-food supply products for housing
520	Retail trade in inputs for agricultural and forestry production
540	Retail trade in inputs for agricultural and forestry production
540	Trade Of Light Machinery And Equipment In General And Spare Parts And Accessories And Vehicles And Machinery
570	Trade in construction materials and accessory elements
600	Community and neighborhood equipment
700	living place
900	Special uses
1000	Management and administration

Ordinance that sanctions the Territorial Ordinance Plan of the Cuenca Canton, 2011.7

## 2.5. Analysis and Evaluation of Geostatistical Tools

For the evaluation of the geostatistical tools, the occasional trade land use group is used, since it has a similar amount of data to the other land use groups and above all it exceeds the minimum data required by the tools to be executed.[19]

As a first measure, a preliminary analysis of the data to be studied is carried out, this process is of vital importance since a good result depends on this. For this, different existing tools in ArcGIS are used and compared, such as Kernel and Kriging. Finally, the two tools were analyzed: Kernel Density and Kriging[20] [21][20]

The Kriging method is chosen because this method relies on mathematical and statistical models that include probability. That is, when the prediction is made, it is associated with a probability and the prediction error is calculated. Furthermore, this method allows spatially assessing the trend and concentration of land uses in the study area. Additionally, it was important to study the behavior of the land uses present in the study area, to understand the dynamics they generate. Although it is possible to have a general idea of the dynamics that land uses generate through cartographic representation or simply with data from the field survey, such analysis continues to be subjective, while statistical calculation allows to mathematically determine the behavior of land uses floor.

## **2.6. Tools used**

### **2.6.1 Kriging tool**

This analysis tool allows us to know: • Trend analysis, • Concentration Analysis, •Pattern[22]–[24] The figure 4 below shows the procedure carried out for the evaluation and application of this tool.

### **2.6.2 Global Moran Index (spatial autocorrelation)**

It makes it possible to know if the distribution of land uses in the different categories is shaping patterns of grouped, dispersed or random spatial distribution. Spatial autocorrelation allows a simultaneous analysis of the distance between the location of the uses and the values of the sum of the number of land uses per block. It can be interpreted as a standardized measurement ranging from -1.0 to +1.0.[25]–[28]

Types of patterns that land use groups may be generating shown in Figure 5:

- LISA test (Local Indicators of Spatial Association)

It varies between -1 and +1, representing the degree of correlation. As a result, the index identifies disaggregated territorial units, where high or low analysis values are spatially grouped.

- Evaluation and Application of the LISA Test.
- Land use occasional trade in retail housing supply products.

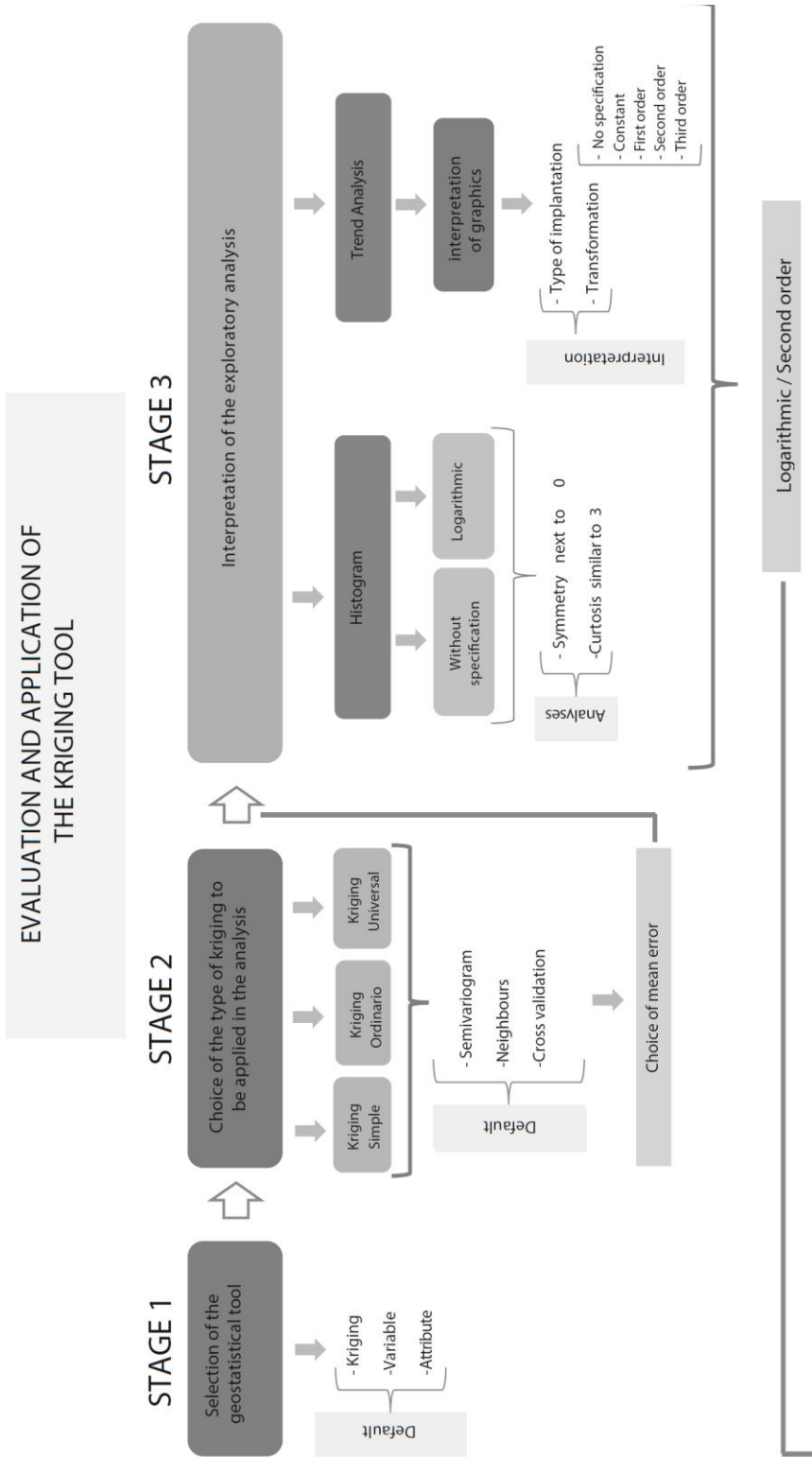


Fig. 4. Calculate Kriging (Stages 1-3)

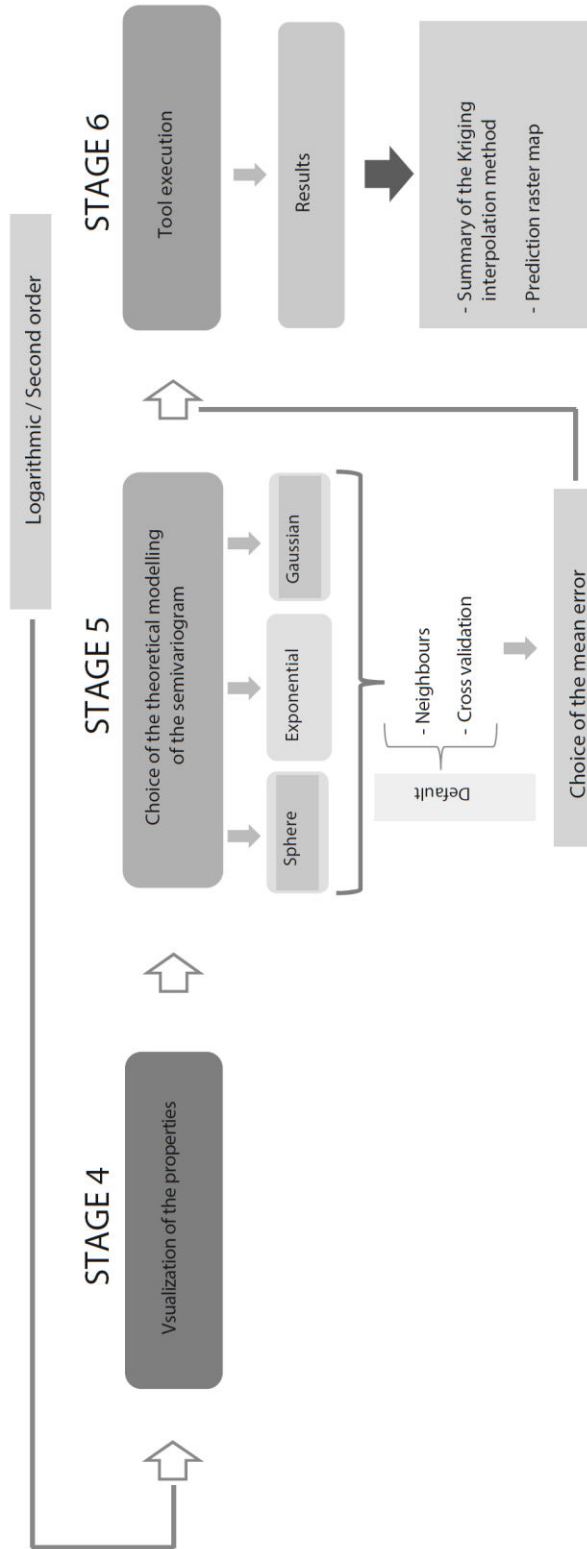


Fig. 4. Calculate Kriging (Stages 4-6)

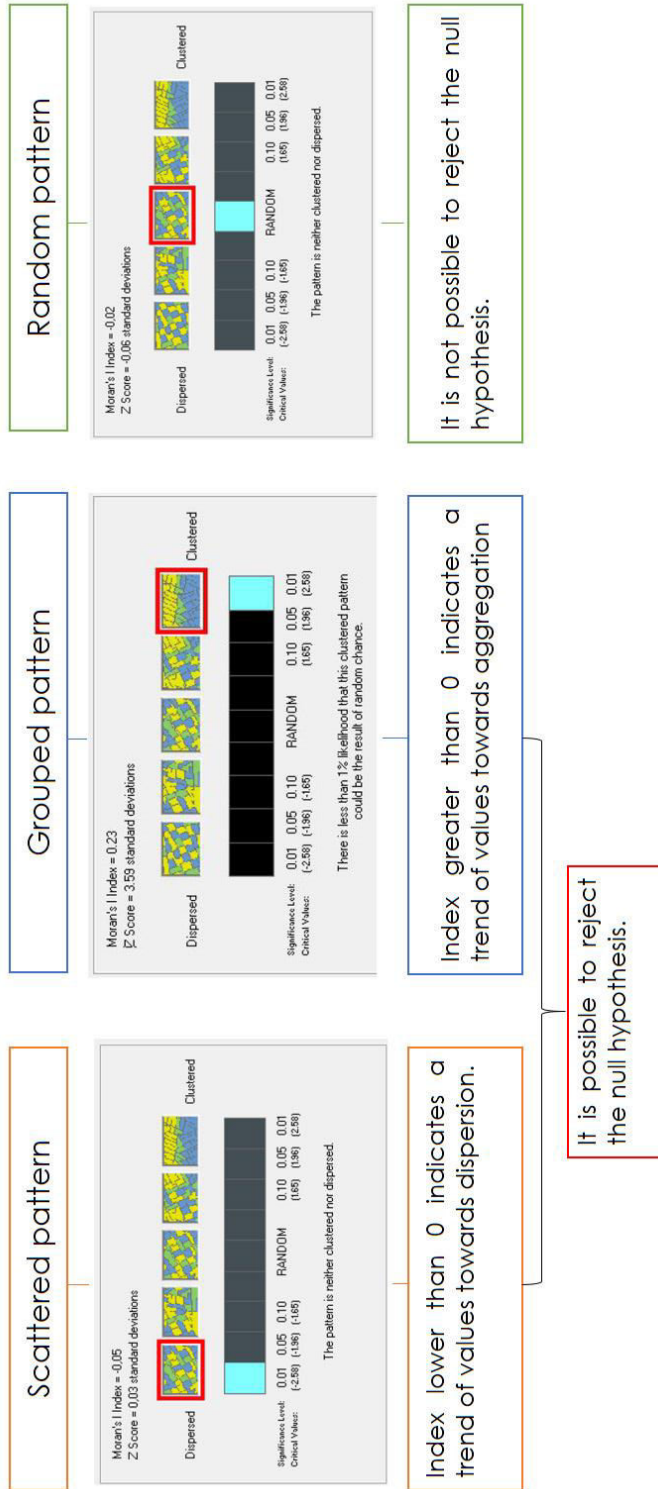
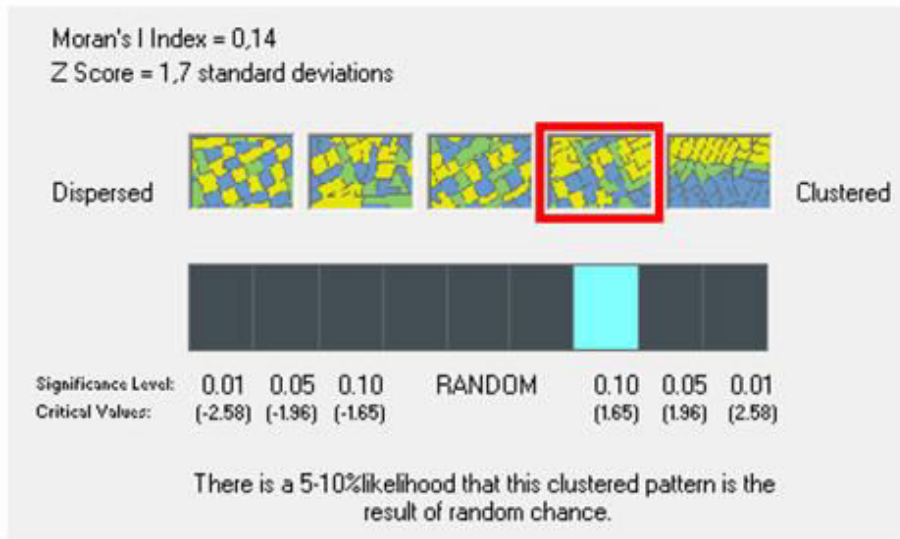


Fig. 5. Calculate global Moran Index

The figure 6 shows Moran's Spatial Autocorrelation Test I of the use of occasional trade in supply products to retail housing. [25], [27]– [29]



Global Moran's I Summary	
Moran's Index:	0,136633
Expected Index:	-0,013333
Variance:	0,007782
Z Score:	1,699977
p-value:	0,089135

Fig. 6. Moran's Spatial Autocorrelation Test I

### 3. RESULTS

The research generated strategies for the distribution of uses and allocation of land occupation characteristics.

- The relevant elements of the study area that have a direct impact on the behavior of land use and occupation were identified and characterized through diagnoses based on the data obtained from the field survey.
- Land use patterns were analyzed and identified through the application of geostatistical tools such as Kriging, Moran-Lisa, which allowed obtaining results of trend, concentration and distribution of land use patterns based on mathematical bases that make this rigorous. study.

- The synthesis was made from relating the results obtained from the spatial analysis of land use and the relevant urban elements, through the crossing of variables obtaining information on the current situation of the study area in relation to land use and characteristics Of occupation.
- A model was generated based on the graphical application (corema), explicit in the work, which can be complemented with the Shannon diversity index.

Concluding that, the presence of strong urban elements with important road equipment or axis for the city, generate intense dynamics in terms of variety of land uses and in turn these uses maintain a close relationship with certain patterns in terms of occupancy characteristics even above what is established by the regulations; situation that can be made visible from a model resulting from the application of geostatistical analysis with the support of Geographic Information Systems.

Based on the results obtained from the different analyzes carried out to study the behavior of land use and occupation characteristics, the following strategies have been established to generate favorable land use dynamics in the study area:

- Adequate distribution of land uses related to housing, so that the uses of service, commerce, and equipment compatible with housing are diversified and in turn enhance the dynamics that are generated between them. Avoiding in this way reaching an extreme specialization of uses, which increases displacements due to the need for supply. A spatial behavior like that of the study area should be sought, since there is a supply from points of concentration of different land uses or by areas with medium and high diversity indices, which allow the resident to acquire goods and services on foot.
- Maintain the purpose of retreats in a building, through proper use of these spaces, without altering the type of implantation assigned. Thus, avoiding sudden changes in the reading of the urban landscape
- Strategic location of influential facilities in the study area to promote areas with a high diversity of land uses. Similar to what happens, for example, around the supply equipment of the study area, the same that directly influences the concentration, diversification and probable trends in the location of land uses related to each other and to the home, thus avoiding cause incompatibilities.

#### 4. DISCUSSION

Make use of the study of trends in the location of commercial and service land uses to plan a parking system that does not affect the operation of the road system. That is, to identify the roads that host or will host a high number of these types of uses through the Kriging tool that provides information on the likelihood of location of groups of land uses and thus provide parking systems on roads that require it, strategy that could be applied in already occupied areas.

- Promote commercial road axes that have a variety of land uses related to commerce and the provision of services, which supplies an area, without chaotizing vehicular traffic, or altering the characteristics of the road. This strategy is feasible to apply both in occupied areas and in the process of occupation, after carrying out a study of both concentration, location trend and diversity of land uses in their immediate context.
- Locate supply equipment in strategic areas that require diversity of uses related to housing. As a strategy to energize areas where residential use is high and uses need to be diversified. Strategy that was verified in the present study, since as observed in the commerce and service coremas, around the supply equipment, high diversity and dynamics are generated between land uses, without causing incompatibilities.
- Prevent commercial and service uses from replacing the main housing use, since they must be distributed in a balanced way and complement each other, to avoid dispersion, a phenomenon that on a larger scale translates into an unnecessary growth of the cities. Hence the importance of having statistical data that verify the concentration, trend and the conformation of behavior patterns of land uses to take the necessary measures.
- Enhance the dynamism of land use, in areas where densification is required. Because the diversification of land uses increases the population that resides in the surroundings, causing the area to densify, regardless of the height of the building. This could be verified through the coremas of service, commerce, and housing, where in an area with high concentration, conformation of patterns and probability of location of land uses, are causally related to non-compliance with the rules established by the Autonomous Decentralized Municipal Government.

It is necessary to develop the concept of allocation, in a more precise and forceful way, with the social and economic reality of the population without distorting the criteria for the control of impacts, involving concepts of

accessibility, functionality, habitability, security, relation public space, space private, demand, among others.

- Faced with the limitations that exist in certain land uses at the time of applying the Kriging 11 tool, it is recommended to perform the analysis by means of graphs that contain the count of the uses present in the study area, thus, in this way It solved this inconvenience, bearing in mind that this procedure approximates an empirical way, since it is visually determined where they are concentrated and where there is a trend of these land uses.

Finally, it would be important to extend the analysis to the rest of the city, taking different areas of different growth moments and in this way see the changes that have occurred over time, measure the effect of commercial and service concentration on the demand for public and private transport (vehicle flow). Validate if the behavior of land uses is more regular, while they are closer to the city center. Finally, to promote the use of geostatistical tools in studies of land use and occupation, to obtain objective results supported by mathematical relationships, which contribute to the planning of a city and study the relationship of land uses with other factors such as frequencies. of trips, displacements, areas of occupation, among others.

## **5. CONCLUSIONS**

The objective of the research is aimed at transcending the diagnosis of land use and occupation beyond the basic mapping of the characteristics of land occupation, buildability, forms and number of uses, which are usually carried out, for later based on observations and subjective analysis, make decisions to organize the use and occupation of the territory.

This research is a first link towards the search for a methodology that allows studying the behavior of land use and occupation through geostatistical tools that allow to mathematically support the concentrations, dispersions, behavior patterns, occupation trends that support decision-making in matter of policies of ordering, control, and regulation of the ordering of the use and occupation of land.

It could be said that since the use and occupation of land are expressions of human activities in the territory, these actions are changing and complex, so it is necessary to expand the studies looking for methodologies that allow being precise in the diagnosis of the dynamics that are generated in their immediate surroundings to promote or regulate the activities that are concentrated or dispersed in the study area.

It is important that the results of the application of geostatistical tools in the study of land use and occupation are compared with variables of the relevant elements such as equipment, roads, physical environment that complement the diagnoses for land use plans. In addition, initiatives focused on creating ordinances must be rigorous and consistent with the economic, social, and environmental reality of the territory, involving concepts of accessibility, functionality, habitability, security, relationship between public and private space, cultural, among others.

## **ACKNOWLEDGEMENT**

The Catholic University of Cuenca, and especially the teachers of the Master in local development mention planning, development, and land use planning, as well as the municipality of the Cuenca - Ecuador for providing the facilities to carry out this study.

## **REFERENCES**

1. A. V. Banerjee, "Land Reforms: Prospects and Strategies," *SSRN Electron. J.*, no. October, 2005.
2. O. Mertz, R. L. Wadley, and A. E. Christensen, "Local land use strategies in a globalizing world: Subsistence farming, cash crops and income diversification," *Agric. Syst.*, vol. 85, no. 3 SPEC. ISS., pp. 209–215, 2005.
3. J. U. Jepsen, C. J. Topping, P. Odderskær, and P. N. Andersen, "Evaluating consequences of land-use strategies on wildlife populations using multiple-species predictive scenarios," *Agric. Ecosyst. Environ.*, vol. 105, no. 4, pp. 581–594, 2005.
4. K. T. Geurs and B. van Wee, "Accessibility evaluation of land-use and transport strategies: Review and research directions," *J. Transp. Geogr.*, vol. 12, no. 2, pp. 127–140, 2004.
5. K. Geurs, B. Zondag, G. de Jong, and M. de Bok, "Accessibility appraisal of land- use/transport policy strategies: More than just adding up travel-time savings," *Transp. Res. Part D Transp. Environ.*, vol. 15, no. 7, pp. 382–393, 2010.
6. A. Gutiérrez, "Movilidad, transporte y acceso: una renovación aplicada al ordenamiento territorial," *Rev. electrónica Geogr. y ciencias Soc.*, vol. XIV, no. 331 (86), pp. 1–17, 2010.

7. R. Jordán and D. Simioni, *Gestión urbana para el desarrollo sostenible en América Latina y el Caribe*. 2003.
8. A. Beuf, “Concepción de centralidades urbanas y planeación del crecimiento urbano en la Bogotá de s XX,” *XII Coloq. Int. Geocrítica*, no. September, pp. 1–21, 2007.
9. M. Pérez, “El desarrollo local sostenible,” *Econ. Desarro.*, vol. 140, no. 2, pp. 60–71, 2006.
10. A. Romeo, C. Menta, E. A. Vázquez, and O. Madoery, “Aspectos Estrategicos Del Desarrollo Local,” *Transform. Glob. Inst. y políticas Desarro. local.*, pp. 1–20, 2001.
11. Naciones Unidas, *Indicadores ambientales y de desarrollo sostenible: avances y perspectivas para América Latina y el Caribe manuales 55 Santiago de Chile, diciembre de 2007*. 2007.
12. A. E. GUERRA TANA, “Plan de uso y ocupación del suelo del área urbana de la ciudad de San Gabriel provincia del Carchi al año 2031,” no. 593, pp. 1–29, 2017.
13. A. M. Cabeza, “Ordenamiento territorial: experiencias internacionales y desarrollos conceptuales y legales realizados en Colombia,” *Perspect. Geográfica*, vol. 4, *Ordenamiento territorial, Colombia*, pp. 7–70, 1999.
14. D.P.D.E. León, “Su desarrollo local sostenible the determining of indicators for evaluating the urban use in the town of san josé de las lajas in the development of local sustainable functions,” pp. 39–48.
15. H. Romero, A. Vázquez, and F. Ordenes, “Ordenamiento territorial y desarrollo sustentable a escala regional, ciudad de Santiago y ciudades intermedias en Chile,” *Glob. y Biodivers. oportunidades y desafíos para la Soc. Chil.*, no. January, pp. 167–224, 2003.
16. J. Soto Cortés, “El crecimiento urbano de las ciudades: enfoques desarrollista, autoritario, neoliberal y sustentable,” *Paradig. económico*, vol. 7, no. 1, pp. 127–149, 2015.
17. O. Vázquez, “La gestión urbana sostenible: conceptos, rol del gobierno local y vinculación con el marketing urbano,” *Provincia*, no. 31, pp. 147–171, 2014.
18. A. Monterrubio, “Estado actual del régimen de planeación y ordenamiento territorial metropolitano en México,” *Espac. Públicos*, vol. 151, no. 0718–0241, pp. 91–118, 2013.

19. M. C. Nicholson and T. N. Mather, "Methods for Evaluating Lyme Disease Risks Using Geographic Information Systems and Geospatial Analysis," *J. Med. Entomol.*, vol. 33, no. 5, pp. 711–720, 1996.
20. W. J. Fu, P. K. Jiang, G. M. Zhou, and K. L. Zhao, "Using Moran's  $i$  and GIS to study the spatial pattern of forest litter carbon density in a subtropical region of southeastern China," *Biogeosciences*, vol. 11, no. 8, pp. 2401–2409, 2014.
21. F. Moral García, F. Carranza Romero, F. Honorio Guisado, J. Rodríguez Bernabé, and J. Cruz Blanco, "Técnicas geoestadísticas aplicadas al análisis de la distribución de capturas de *Helicoverpa armigera* (Hübner) (Lepidoptera: Noctuidae) mediante trampas conferomonas sexuales en una plantación de tomate.," *Boletín Sanid. Veg. Plagas*, vol. 30, no. 4, pp. 733–744, 2004.
22. J. Martínez-Frutos and P. Martí, "Diseño óptimo robusto utilizando modelos Kriging: Aplicación al diseño óptimo robusto de estructuras articuladas," *Rev. Int. Metod. Numer. para Calc. y Disen. en Ing.*, vol. 30, no. 2, pp. 97–105, 2014.
23. U. D. C. Rica, U. D. C. Rica, S. José, C. Rica, and D. E. L. I. Kriging, "Disponible en: <http://www.redalyc.org/articulo.oa?id=43629206>," 2005.
24. M. D. E. Las, V. D. E. La, S. U. Mineralizaci, L. A. Autores, S. B. Martell, and A. M. Romero, "Instituto superior minero metalúrgico," 2001.
25. C. Guilmoto, "Spatial correlation and demography . To cite this version ;," 2010.
26. J. L. Ping, C. J. Green, R. E. Zartman, and K. F. Bronson, "Exploring spatial dependence of cotton yield using global and local autocorrelation statistics," *F. Crop. Res.*, vol. 89, no. 2–3, pp. 219–236, 2004.
27. B. Flahaut, M. Mouchart, E. S. Martin, and I. Thomas, "The local spatial autocorrelation and the kernel method for identifying black zones: A comparative approach," *Accid. Anal. Prev.*, vol. 35, no. 6, pp. 991–1004, 2003.
28. A. Soltani and S. Askari, "Exploring spatial autocorrelation of traffic crashes based on severity," *Injury*, vol. 48, no. 3, pp. 637–647, 2017.

29. N. Cressie and L. B. Collins, “Patterns in spatial point locations: Local indicators of spatial association in a minefield with clutter,” *Nav. Res. Logist.*, vol. 48, no. 5, pp. 333–347, 2001.

---

**Cite this article**

Carla Siguencia, Marco Avila and Yonimiler Castillo, Strategies for the Distribution of Uses, Occupation and Allocation of Land: Explained with a Case Study of Paseo De Los Cañarís in the City of Cuenca, In: Sandip A. Kale editor, *Efficient Engineering Systems: Volume 1*, Pune: Grinrey Publications, 2021, pp. 91-110.



## Book Series by Grinrey Publications

- Research Transcripts in Energy
- Engineering Research Transcripts
- Research Transcripts in Materials
- Research Transcripts in Computer, Electrical and Electronics Engineering



[www.grinrey.com](http://www.grinrey.com)

**GRINREY**

ISBN 978-81-948951-8-3



9 788194 895183